6. RESULTS AND DISCUSSION

6.1 Experimental Investigation

The experimental runs were carried out on the experimental set-up described in Chapter 5. The flow rate studied covered the range of collector flow rates recommended in solar collector array for solar water heating systems [Soin(1982),Klein etal(1979) and Beckman(1977)]. In the present experimental study the flow rates studied were 0.0095,0.0167,0.0239 and 0.0312 $kgs^{-1}m^{-2}$.

The DC potential used for the measurement of the polarisation current was 0.80 volts, since the polarising current was achieved for the complete flow range obtainable with the experimental set-up. The details of the experimental procedure has been described in Chapter 5. The runs were taken both for symmetric and asymmetric flow configuration.

The electrolyte properties (0.50 NaOH) used has been taken from Rao(1962) and the temperature corrections for the density is taken from Perry(1963). The same as a function of temperature are reproduced below.

Temperature	Density	Viscosity
°C	kg m^{-3}	N sm^{-2} x 1000
30.0	1020.7	0.8975
31.0	1020.3	0.8787
32.0	1020.0	0.8589
33.0	1019.7	0.8429
34.0	1019.3	0.8254

6.1.1 Experimental Results

The results of the experiments are given in Tables 6.1 to 6.8. The polarisation currents for all the ten risers are presented as minimum, maximum and mean values. The experimental riser flow rates (of the electrolyte) are that of the mean value of polarisation currents. The values given in the tables are based on three sets of readings to ensure repeatibility.

Table 6.1 Flow Profile for Experimental Collector, Asymmetric Flow

Q_{in} = 76.4388 E-6 m^3s^{-1}, T = 32° C.

Riser No.	Polarisation Current			Riser flow rate, $m^3s^{-1}x10^6$	
	Max, mA	Min, mA	Mean, mA	Expt	Theo
1	0.5184	0.4981	0.5083	5.8571	6.6746
2	0.5403	0.5216	0.5310	6.0987	6.8040
3	0.5613	0.5372	0.5493	6.2935	6.9610
4	0.5761	0.5527	0.5644	6.4547	7.1478
5	0.6130	0.5798	0.5964	6.7952	7.3671
6	0.6508	0.6069	0.6289	7.1406	7.6217
7	0.6685	0.6430	0.6558	7.4268	7.9151
8	0.7166	0.6751	0.6959	7.8536	8.2508
9	0.7612	0.7083	0.7348	8.2675	8.6325
10	0.8197	0.7542	0.7870	8.8231	9.0639
			Total	71.0108	76.4385

Table 6.2 Flow Profile for Experimental Collector, Asymmetric Flow

Q_{in} = 58.7388 E-6 m^3s^{-1}, T = 32° C.

Riser No.	Polarisation Current			Riser flow rate, $m^3s^{-1}x10^6$	
	Max, mA	Min, mA	Mean, mA	Expt	Theo
1	0.4106	0.3960	0.4033	4.7402	5.1112
2	0.4361	0.4032	0.4197	4.9142	5.2021
3	0.4383	0.4170	0.4277	4.9993	5.3183
4	0.4535	0.4319	0.4277	5.1595	5.4616
5	0.4689	0.4421	0.4555	5.2957	5.6343
6	0.4958	0.4625	0.4792	5.5471	5.8392
7	0.5191	0.4786	0.4989	5.7571	6.0796
8	0.5364	0.4977	0.5171	5.9507	6.3590
9	0.5749	0.5236	0.5493	6.2934	6.6815
10	0.6052	0.5613	0.5833	6.6552	7.0518
			Total	55.3127	58.7386

Table 6.3 Flow Profile for Experimental Collector, Asymmetric Flow

Q_{in} = 41.039 E-6 m^3s^{-1}, T = 32° C.

Riser No.	Polarisation Current			Riser flow rate, $m^3s^{-1}x10^6$	
	Max, mA	Min, mA	Mean, mA	Expt	Theo
1	0.3035	0.2889	0.2962	3.6004	3.7235
2	0.3029	0.2916	0.2973	3.6116	3.7632
3	0.3172	0.2954	0.3063	3.7079	3.8178
4	0.3195	0.3007	0.3101	3.7483	3.8881
5	0.3231	0.3028	0.3130	3.7787	3.9751
6	0.3350	0.3183	0.3267	3.9245	4.0803
7	0.3463	0.3270	0.3367	4.0309	4.2050
8	0.3529	0.3384	0.3457	4.1267	4.3510
9	0.3857	0.3472	0.3665	4.3808	4.5201
10	0.4096	0.3644	0.3870	4.5667	4.7144
			Total	39.4765	41.0385

Table 6.4 Flow Profile for Experimental Collector, Asymmetric Flow

Q_{in} = 23.339 E-6 m^3s^{-1}, T = 32° C.

Riser No.	Polarisation Current			Riser flow rate, $m^3s^{-1}x10^6$	
	Max, mA	Min, mA	Mean, mA	Expt	Theo
1	0.1563	0.1508	0.1536	2.0823	2.2167
2	0.1578	0.1525	0.1552	2.0993	2.2230
3	0.1599	0.1527	0.1563	2.116	2.2361
4	0.1605	0.1532	0.1569	2.1174	2.2562
5	0.1660	0.1578	0.1619	2.1712	2.2837
6	0.1685	0.1596	0.1641	2.1941	2.3190
7	0.1736	0.1623	0.1682	2.2382	2.3626
8	0.1853	0.1665	0.1759	2.3202	2.4151
9	0.1870	0.1689	0.1780	2.3420	2.4771
10	0.1962	0.1709	0.1836	2.4016	2.5491
			Total	22.0779	23.3386

Table 6.5 Flow Profile for Experimental Collector,Symmetric Flow

Q_{in} = 76.4388 E-6 m^3s^{-1}, T = 32° C.

Riser No.	Polarisation Current			Riser flow rate, $m^3s^{-1}x10^6$	
	Max, mA	Min, mA	Mean, mA	Expt	Theo
1	0.7580	0.6893	0.7327	8.1494	8.5480
2	0.7266	0.6724	0.6995	7.8924	8.2282
3	0.7078	0.6511	0.6795	7.6790	7.5992
4	0.6784	0.6225	0.6505	7.3704	7.7368
5	0.6672	0.6116	0.6394	7.2528	7.5577
6	0.6531	0.6069	0.6300	7.1528	7.4185
7	0.6354	0.5927	0.6141	6.9830	7.3164
8	0.6312	0.5793	0.6053	6.8894	7.2490
9	0.6298	0.5786	0.6042	6.8782	7.2142
10	0.6281	0.5772	0.6027	6.8617	7.2105
			Total	73.1091	76.4385

Table 6.6 Flow Profile for Experimental Collector, Symmetric Flow

Q_{in} = 58.7388 E-6 m^3s^{-1}, T = 32° C.

Riser No.	Polarisation Current			Riser flow rate, $m^3s^{-1}x10^6$	
	Max, mA	Min, mA	Mean, mA	Expt	Theo
1	0.5561	0.5084	0.5323	6.1125	6.5018
2	0.5286	0.4835	0.5061	5.8337	6.2816
3	0.5198	0.4793	0.4996	5.7645	6.0955
4	0.4924	0.4736	0.4830	5.5884	5.9412
5	0.5016	0.4582	0.4799	5.5554	5.8162
6	0.4863	0.4359	0.4611	5.3553	5.7185
7	0.4812	0.4296	0.4554	5.2947	5.6463
8	0.4785	0.4297	0.4541	5.2808	5.5979
9	0.4772	0.4261	0.4571	5.2547	5.5720
10	0.4756	0.4245	0.4501	5.2377	5.5675
			Total	55.2777	58.7385

Table 6.7 Flow Profile for Experimental Collector, Symmetric Flow

Q_{in} = 41.039 E-6 m^3s^{-1}, T = 32° C.

Riser No.	Polarisation Current			Riser flow rate, $m^3s^{-1}x10^6$	
	Max, mA	Min, mA	Mean, mA	Expt	Theo
1	0.3671	0.3394	0.3533	4.2076	4.4902
2	0.3567	0.3329	0.3448	4.1176	4.3562
3	0.3490	0.3168	0.3329	3.9910	4.2424
4	0.3362	0.3153	0.3258	3.9149	4.1474
5	0.3298	0.3016	0.3157	3.8079	4.0701
6	0.3286	0.2971	0.3129	3.7776	4.0093
7	0.3228	0.2946	0.3087	3.7334	3.9638
8	0.3198	0.2933	0.3066	3.7106	3.9327
9	0.3177	0.2925	0.3051	3.6591	3.9154
10	0.3166	0.2966	0.3038	3.6813	3.9111
			Total	38.6370	41.0386

Table 6.8 Flow Profile for Experimental Collector, Symmetric Flow

Q_{in} = 23.339 E-6 m^3s^{-1}, T = 32° C.

Riser No.	Polarisation Current			Riser flow rate, $m^3s^{-1}x10^6$	
	Max, mA	Min, mA	Mean, mA	Expt	Theo
1	0.1897	0.1762	0.1830	2.3952	2.5201
2	0.1835	0.1728	0.1782	2.3441	2.4564
3	0.1783	0.1672	0.1728	2.2866	2.4020
4	0.1751	0.1613	0.1682	2.2382	2.3563
5	0.1730	0.1624	0.1677	2.2329	2.3188
6	0.1704	0.1577	0.1641	2.1941	2.2889
7	0.1679	0.1586	0.1633	2.1855	2.2663
8	0.1658	0.1577	0.1618	2.1696	2.2505
9	0.1640	0.1568	0.1604	2.1552	2.2412
10	0.1638	0.1559	0.1599	2.1494	2.2380
			Total	22.3508	23.3385

6.1.2 Comparison with theory

Theoretical values were obtained for the experimental module described in Chapter 5 with the mathematical model proposed in Chapter 3 and are presented in Tables 6.1 to 6.8. The same information is presented graphically in Figs. 6.1 to 6.8.

The theoretical runs were obtained by using the actual electrolyte properties given above at 32° C. The collector flow rate, G is computed based on the experimental collector module area of 2.50154 m^2 for the selected inlet flow rate, Q_{in}.

From Figs. 6.1 to 6.8 it is observed that the experimental values are very close to the theoretical ones, both for symmetric and asymmetric and for all the flow rates studied.

At the bottom of the each table the total flow rates are given for the experimental and theoretical ones. It is observed that the total of the experimental riser flow rates is less than the inlet flow rate, Q_{in}. The ratio of the theoretical total to that of experimental one given indicates that the difference between the two is 4.5 to 7.5 %.

The small variations between the experimental and predicted flow rates could be due to errors during the experimentation and the assumptions made in the model. The experimental errors could be due to error in the measurements of flow rate, fluctuations in the

polarising current and minor variations in the temperature during the experimental runs. The contribution of various experimental errors has been estimated and is found to be less than 2 %.

Considering the extent of difference of 4.5 -7.5 % the agreement between the theoretical and experimental results is excellent.

Further, it is observed that the tee loss coefficients for the turbulent range can be used without any corrections. Thus the assumtions made in Chapter 3 were valid.

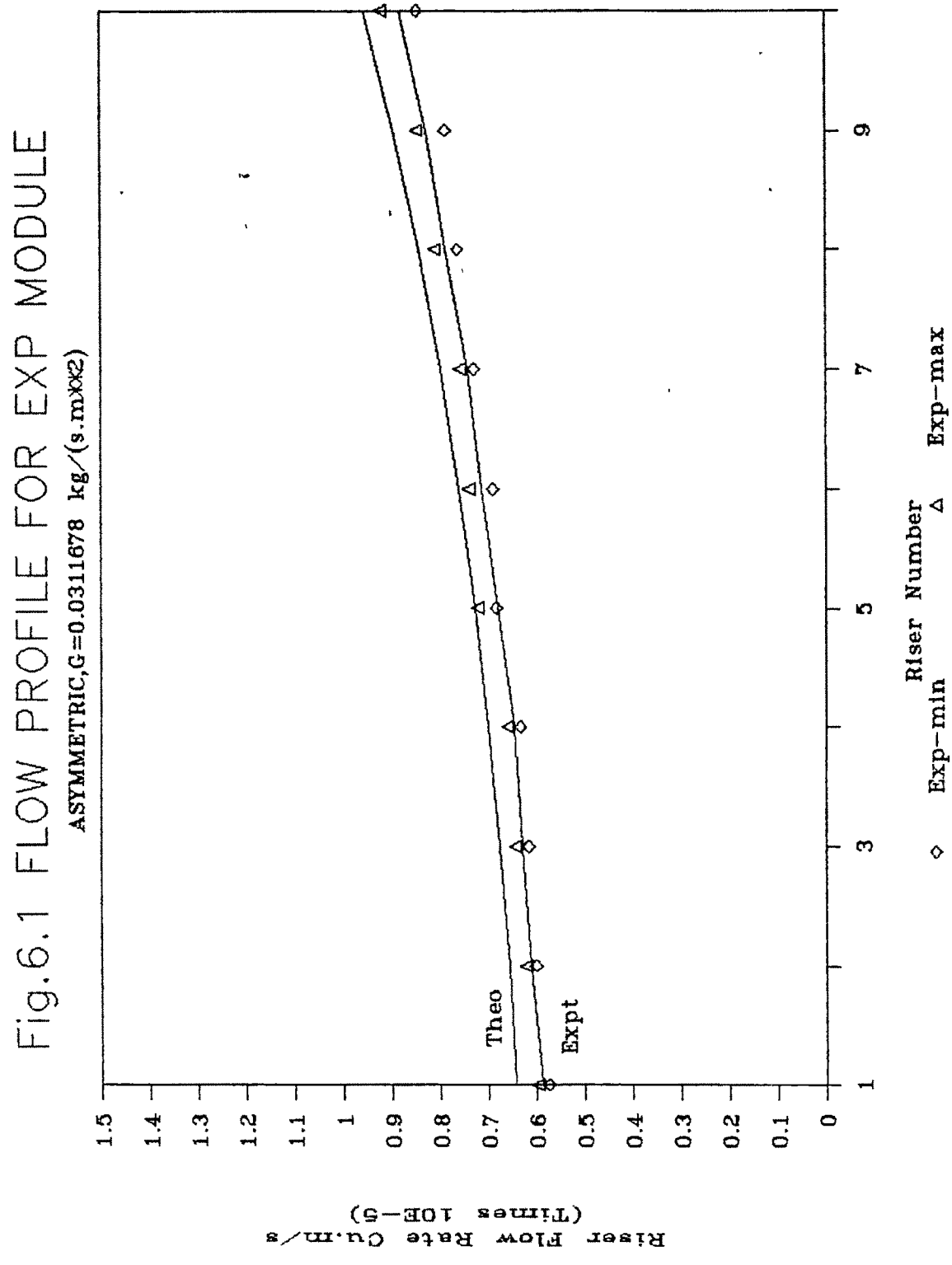
Fig.6.1 FLOW PROFILE FOR EXP MODULE
ASYMMETRIC,G=0.0311678 kg/(s.mxx2)
Riser Flow Rate Cu.m/s
(Times 10E-5)
1.5
1.4
1.3
1.2
1.1
1
0.9
0.8
0.7
0.6
0.5
0.4
0.3
0.2
0.1
0
Theo
Expt
1
3
5
7
9
Riser Number
◇ Exp-min △ Exp-max

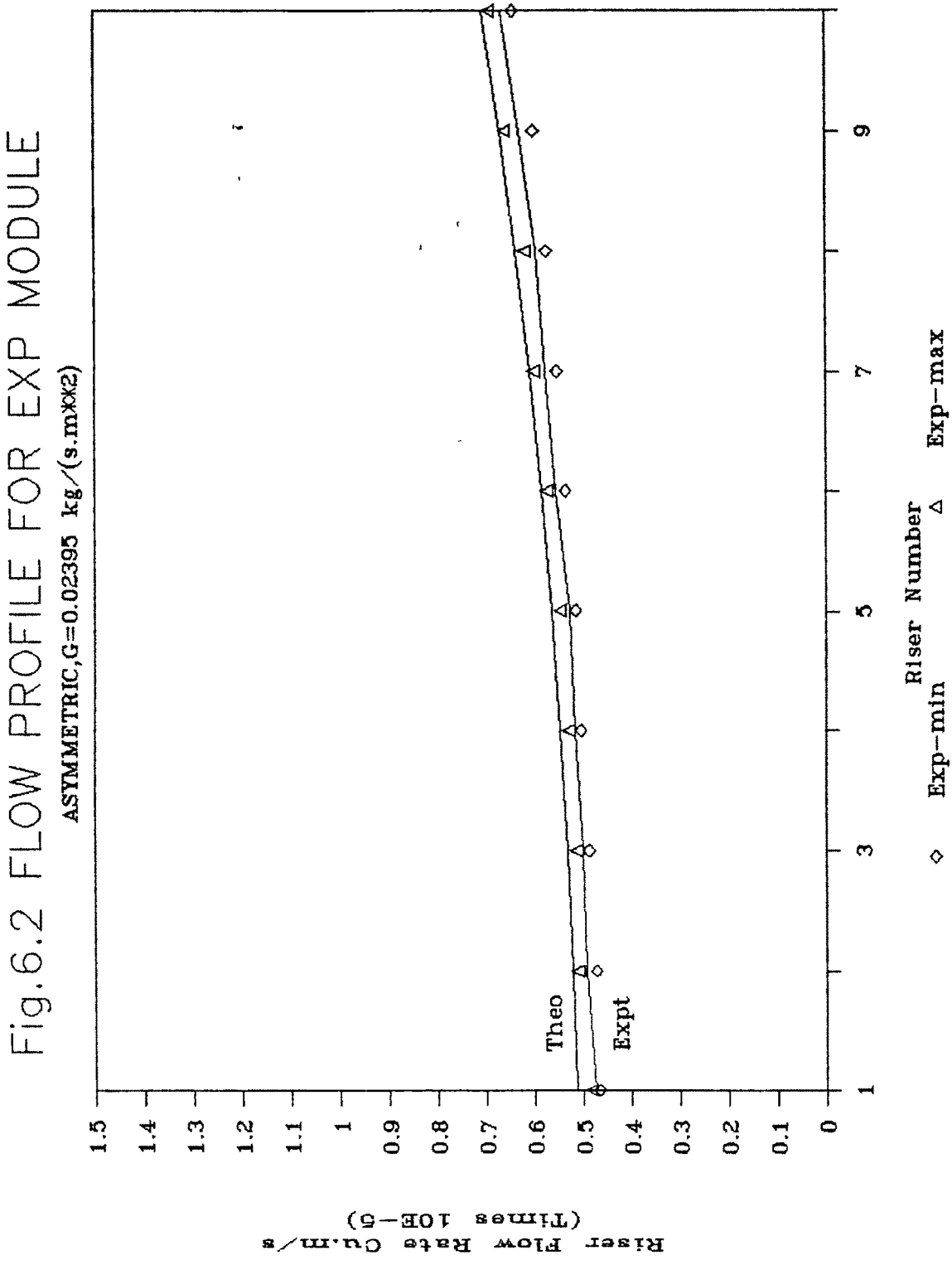
Fig.6.2 FLOW PROFILE FOR EXP MODULE
ASYMMETRIC,G=0.02395 kg/(s.m**2)
Riser Flow Rate Cu.m/s
(Timas 10E-5)
1.5
1.4
1.3
1.2
1.1
1
0.9
0.8
0.7
0.6
0.5
0.4
0.3
0.2
0.1
0
1
3
5
7
9
Riser Number
Theo
Expt
Exp-min
Exp-max

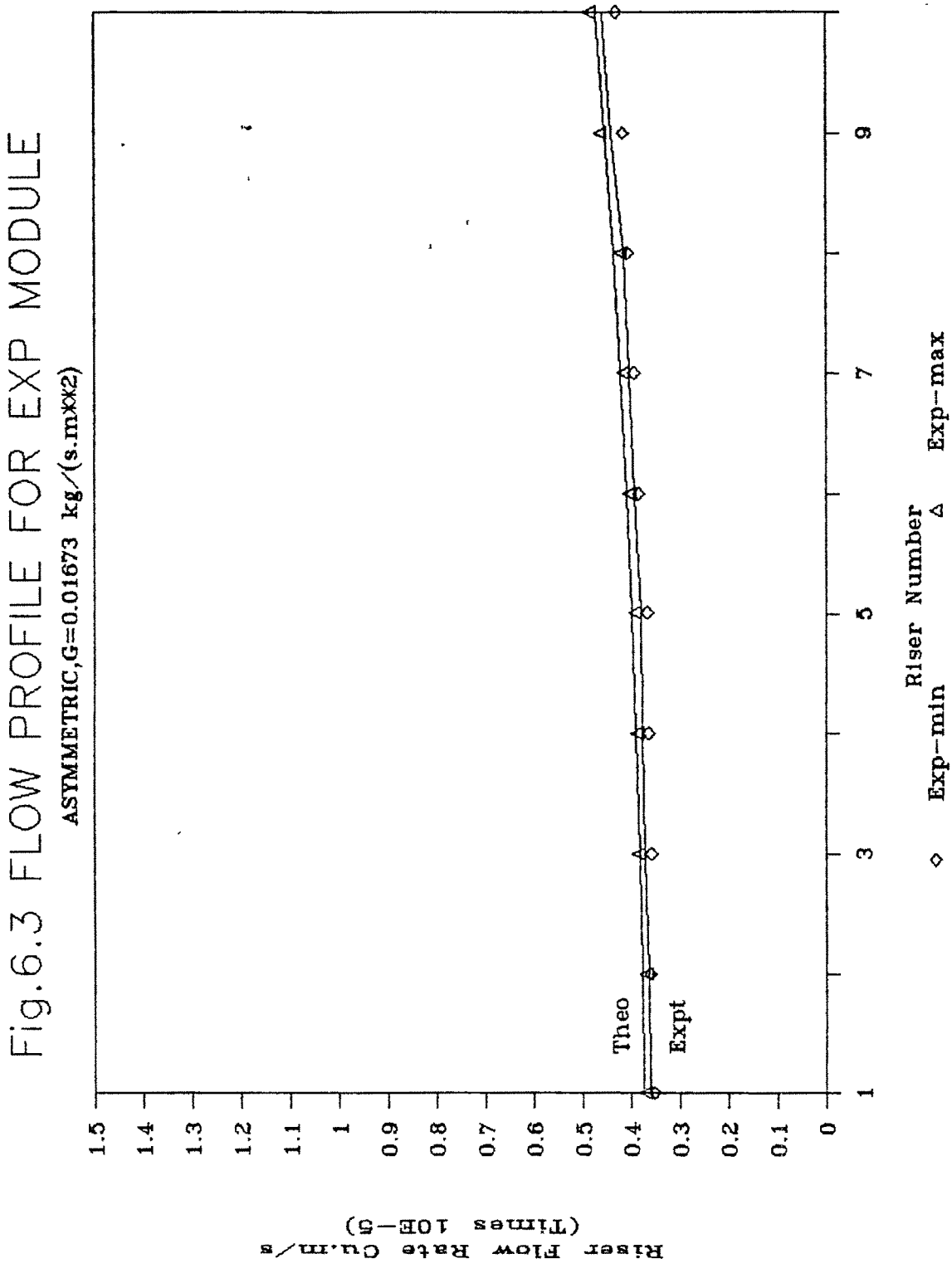
Fig.6.3 FLOW PROFILE FOR EXP MODULE
ASYMMETRIC,G=0.01673 kg/(s.mXX2)
Riser Flow Rate Cu.m/s
(Times 10E-5)
1.5
1.4
1.3
1.2
1.1
1
0.9
0.8
0.7
0.6
0.5
0.4
0.3
0.2
0.1
0
Theo
Expt
1
3
5
7
9
Riser Number
Exp-min
Exp-max

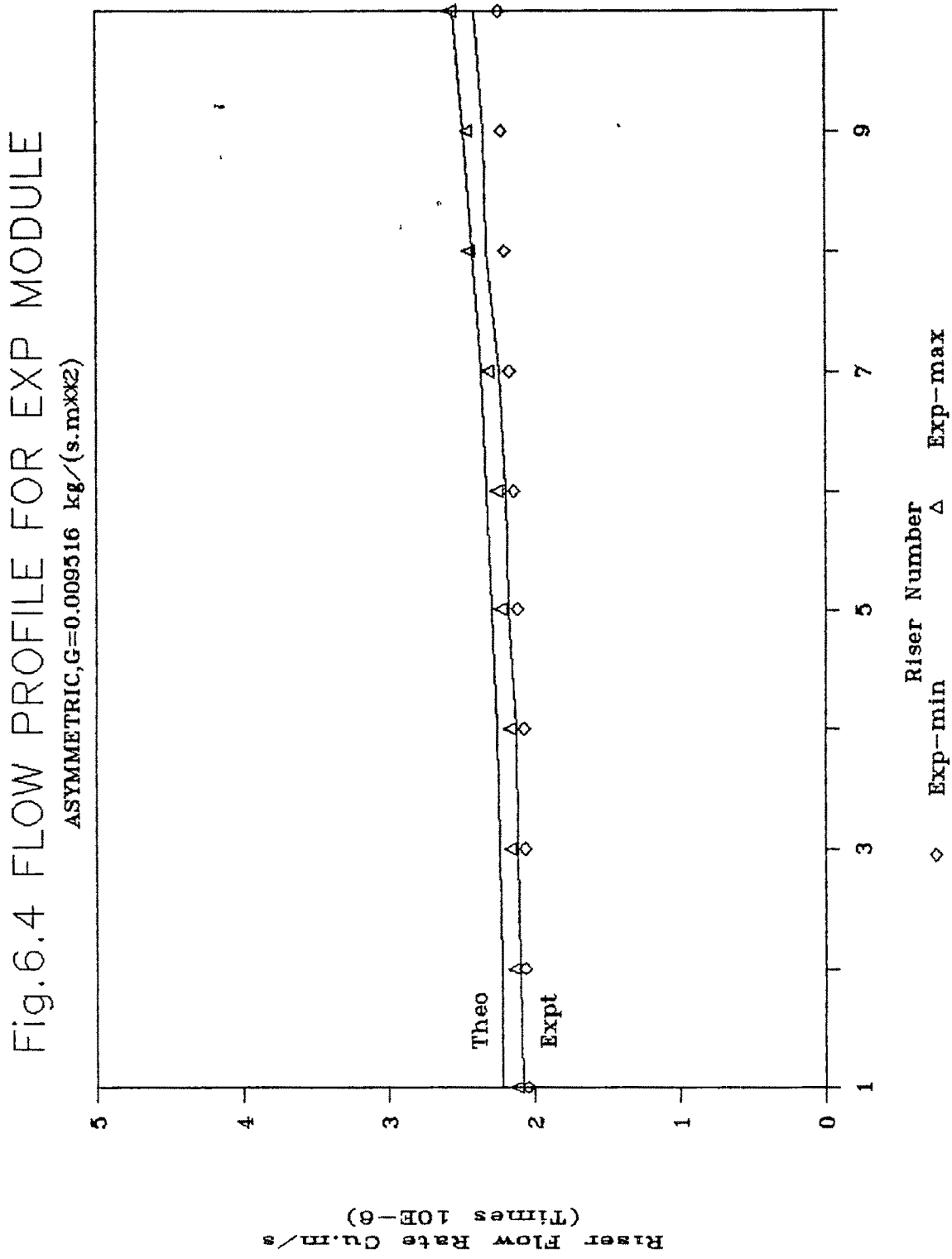
Fig.6.4 FLOW PROFILE FOR EXP MODULE
ASYMMETRIC,G=0.009516 kg/(s.m**2)
Riser Flow Rate Cu.m/s
(Times 10E-6)
5
4
3
2
1
0
Theo
Expt
1
3
5
7
9
Riser Number
◇ Exp-min
△ Exp-max

Fig.6.4a COMPARATIVE FLOW FOR EXP MODULE

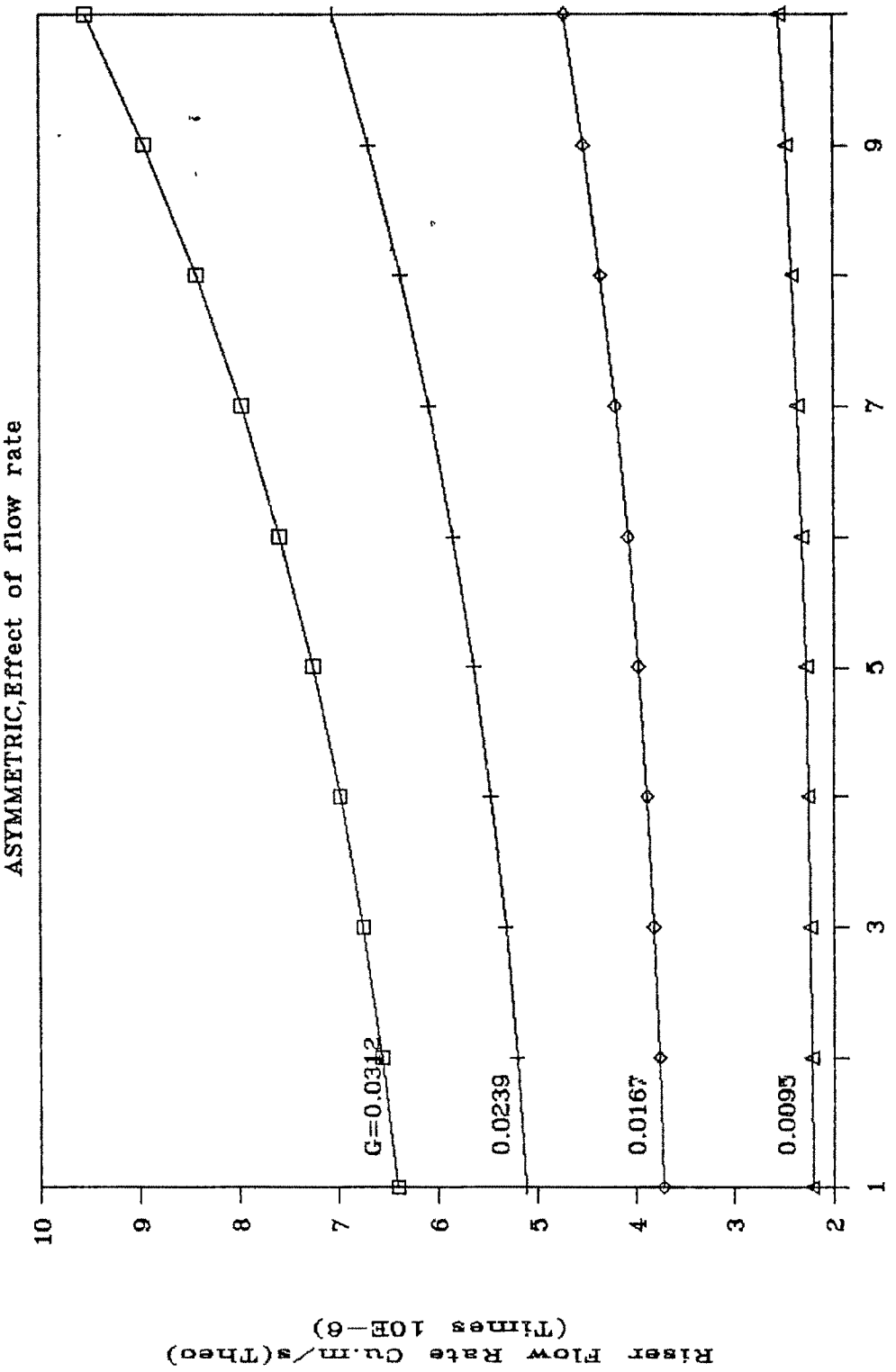

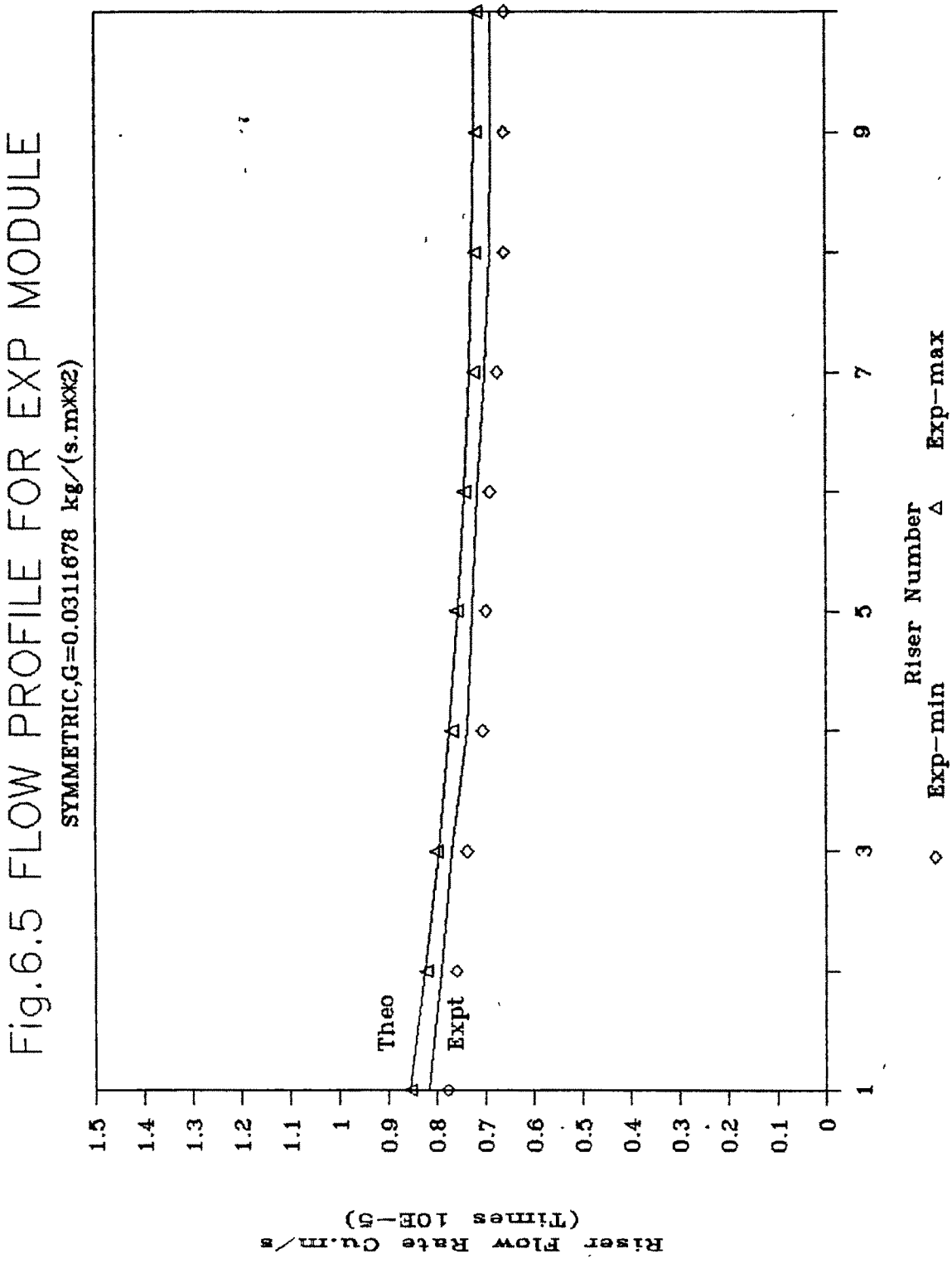
Fig.6.5 FLOW PROFILE FOR EXP MODULE
SYMMETRIC,G=0.0311678 kg/(s.mXX2)
Riser Flow Rate Cu.m/s
(Times 10E-5)
1.5
1.4
1.3
1.2
1.1
1
0.9
0.8
0.7
0.6
0.5
0.4
0.3
0.2
0.1
0
Theo
Expt
1
3
5
7
9
Riser Number
Exp-min
Exp-max

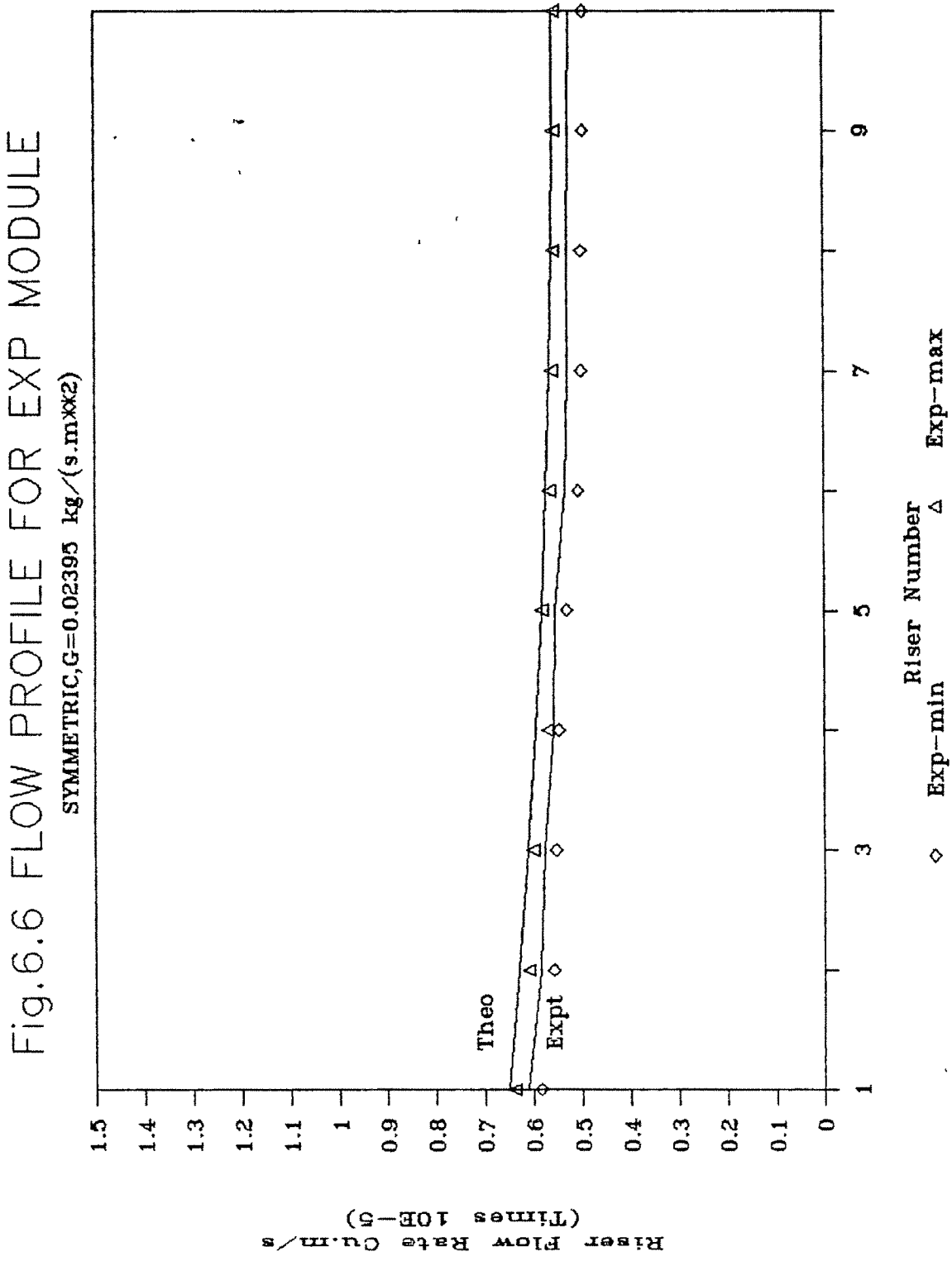
Fig.6.6 FLOW PROFILE FOR EXP MODULE
SYMMETRIC,G=0.02395 kg/(s.m**2)
Riser Flow Rate Cu.m/s
(Times 10E-5)
1.5
1.4
1.3
1.2
1.1
1
0.9
0.8
0.7
0.6
0.5
0.4
0.3
0.2
0.1
0
Theo
Expt
1
3
5
7
9
Riser Number
Exp-min
Exp-max

Fig.6.7 FLOW PROFILE FOR EXP MODULE

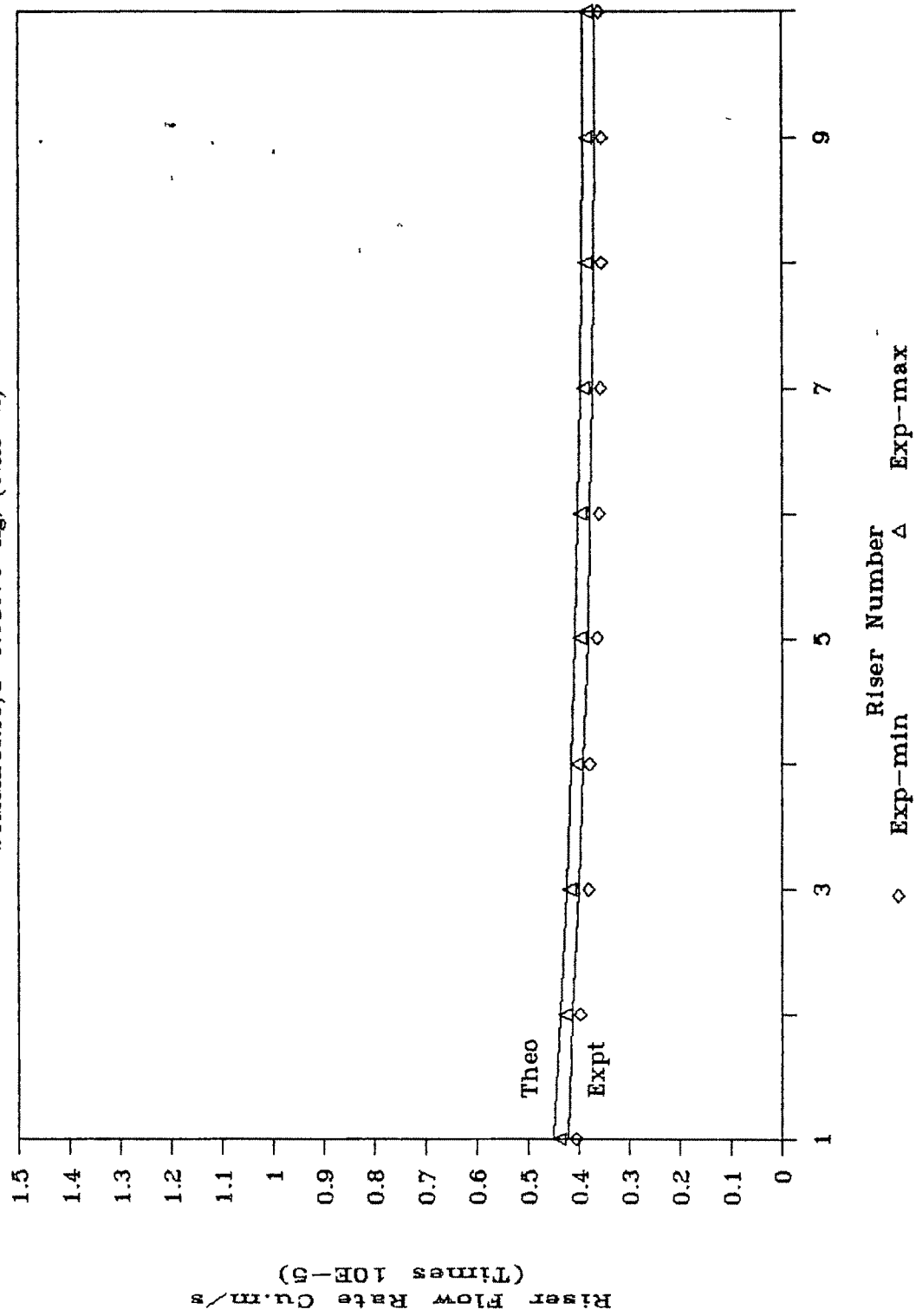

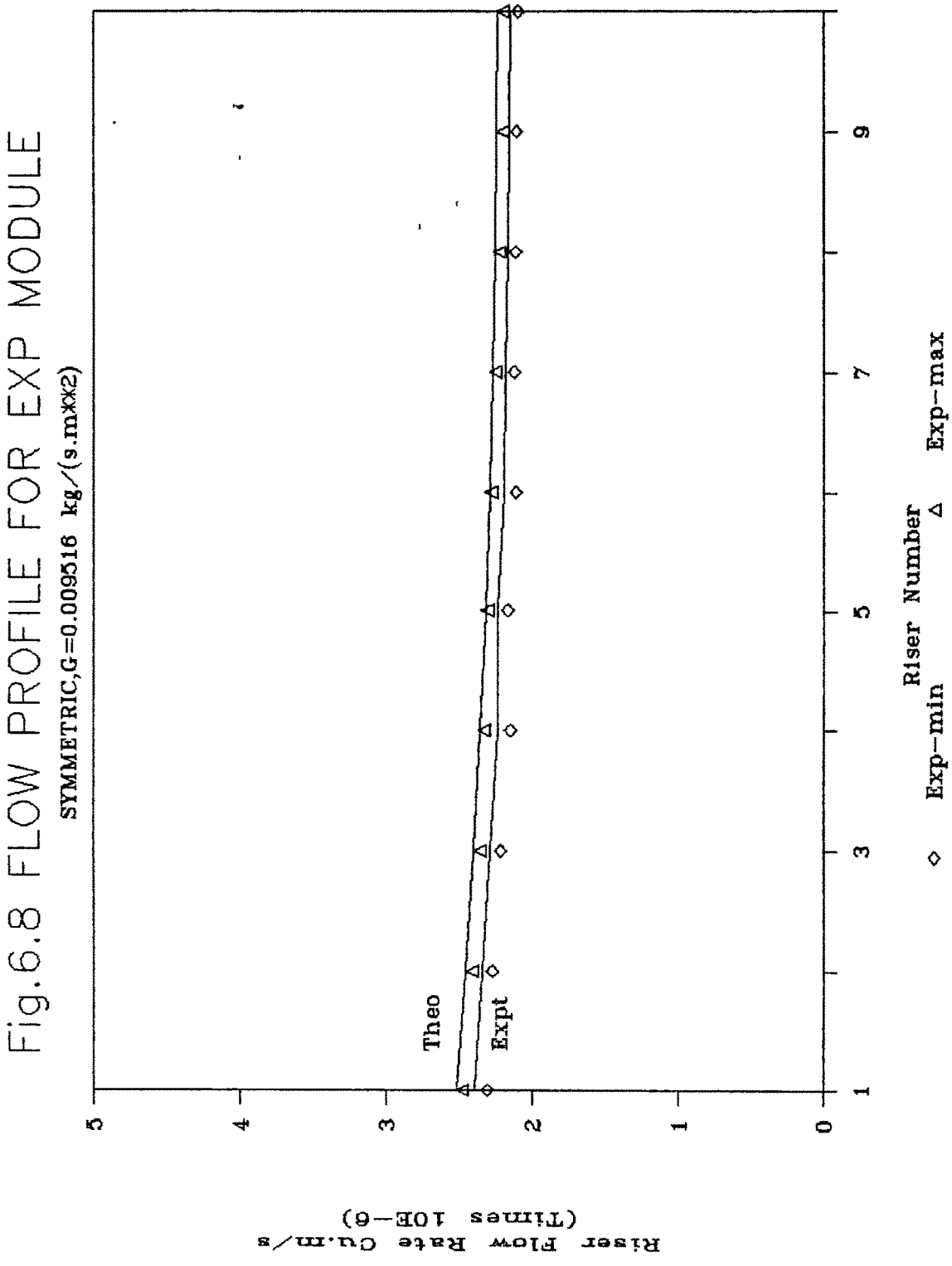
Fig.6.8 FLOW PROFILE FOR EXP MODULE
SYMMETRIC,G=0.009516 kg/(s.mxx2)
Riser Flow Rate Cu.m/s
(Times 10E-6)
0
1
2
3
4
5
Theo
Expt
1
3
5
7
9
Riser Number
◇ Exp-min
△ Exp-max

Fig.6.8a COMPARATIVE FLOW FOR EXP MODULE

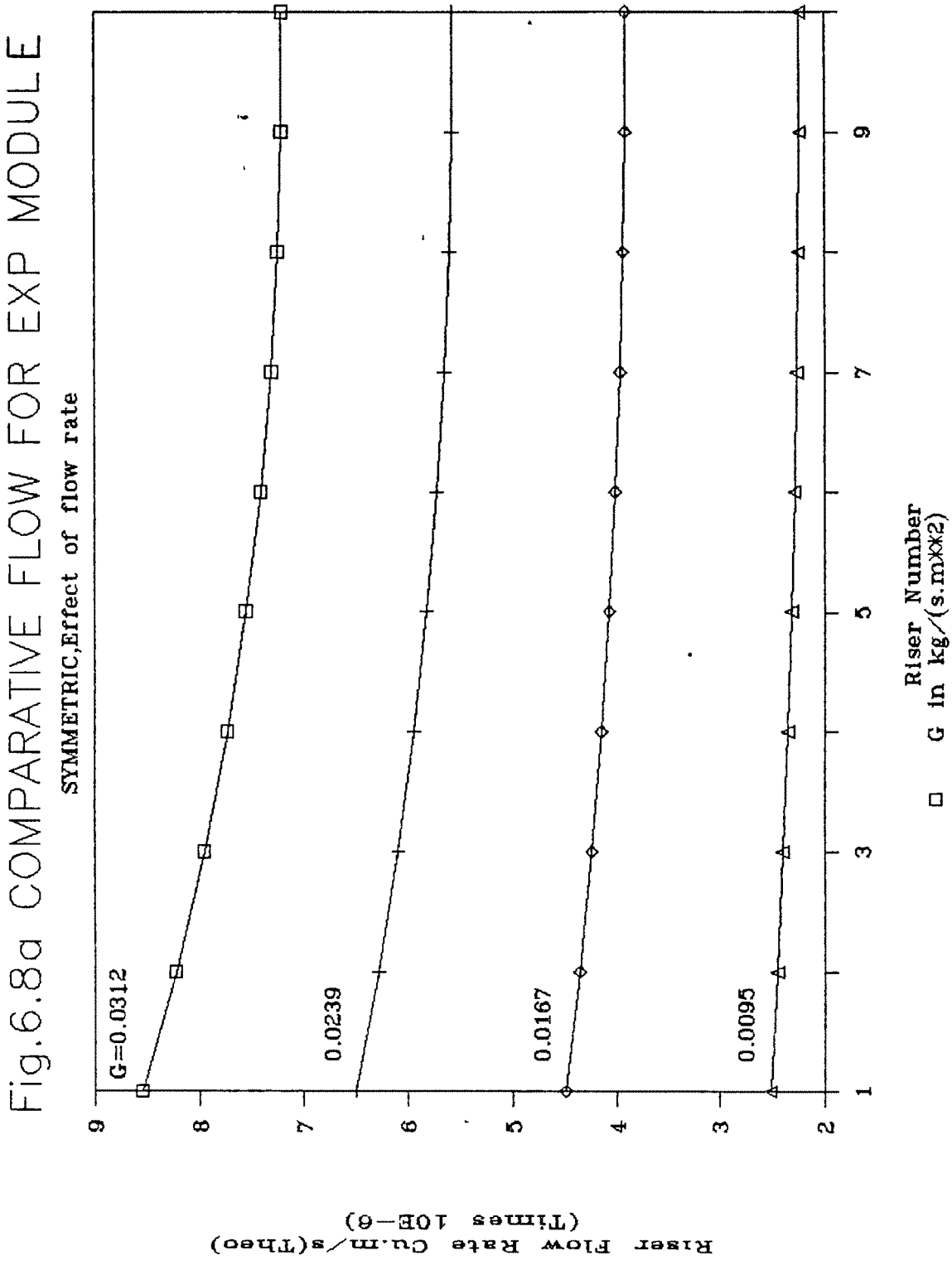

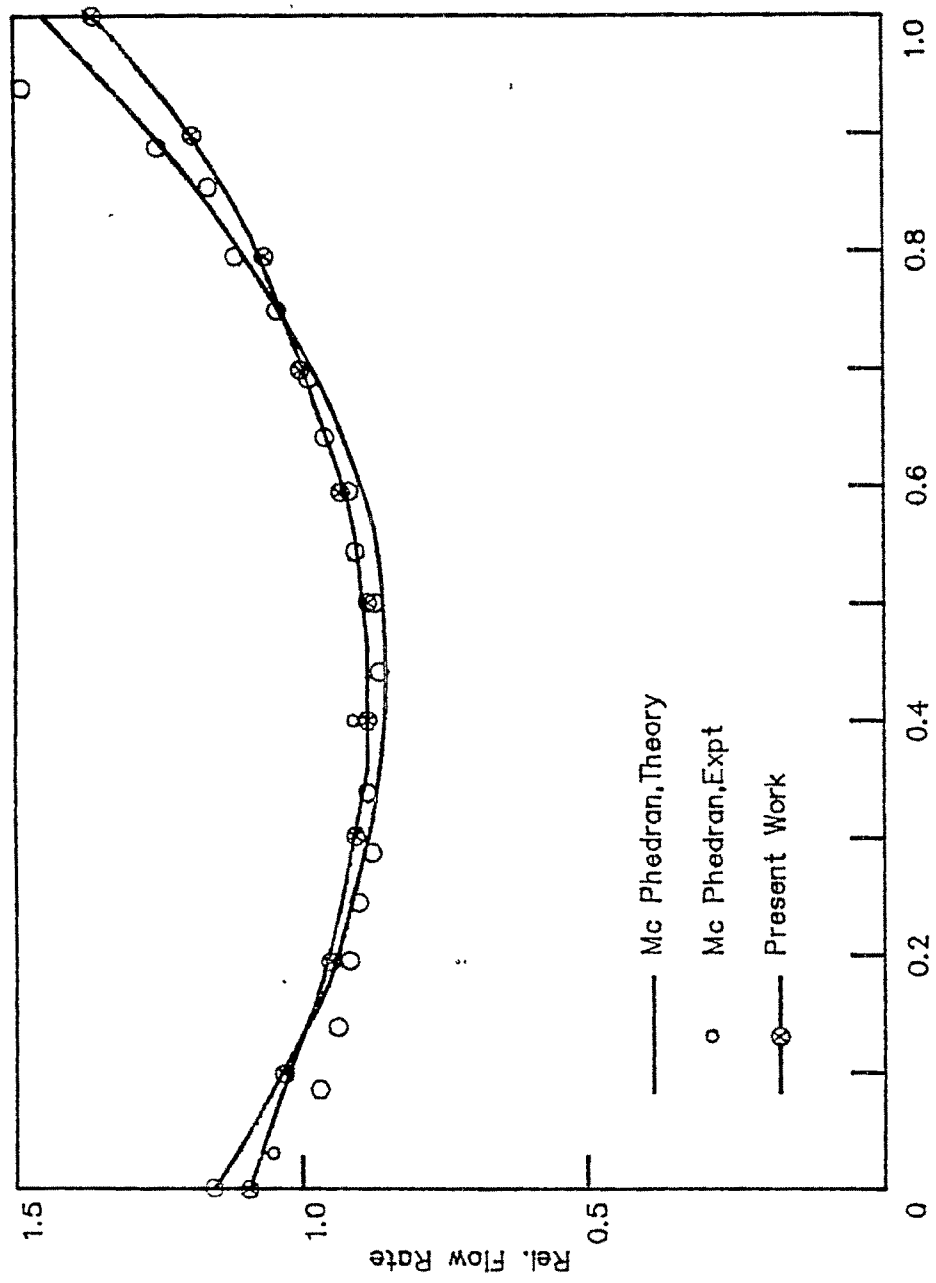

Fig.6.8b Comparison of Present Model with Mc Phedarn(1983) for Evacuated Solar Collector

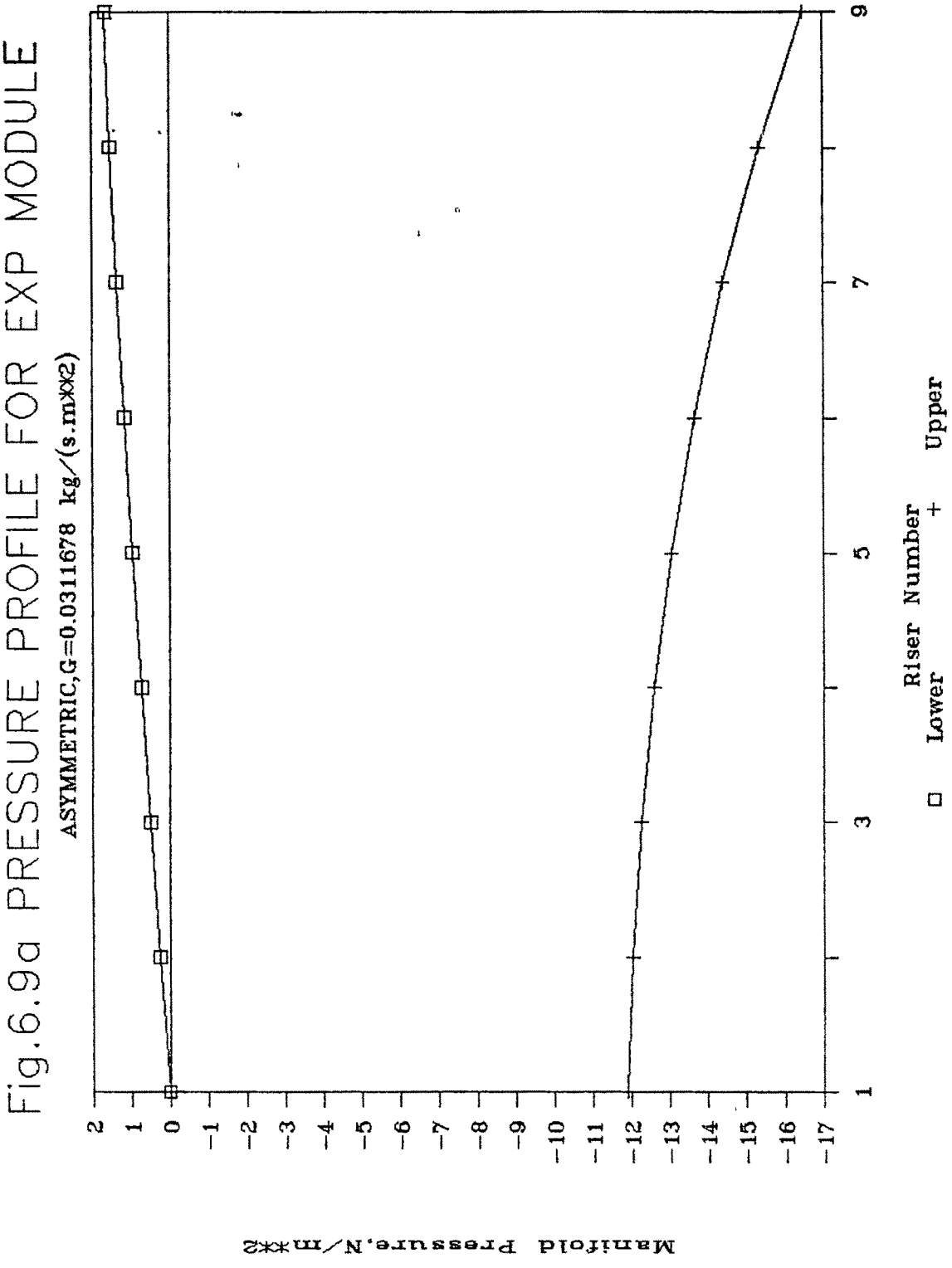
Fig.6.9a PRESSURE PROFILE FOR EXP MODULE
ASYMMETRIC,G=0.0311678 kg/(s.m**2)
Manifold Pressure,N/m**2
2
1
0
-1
-2
-3
-4
-5
-6
-7
-8
-9
-10
-11
-12
-13
-14
-15
-16
-17
1
3
5
7
9
Riser Number
□ Lower + Upper

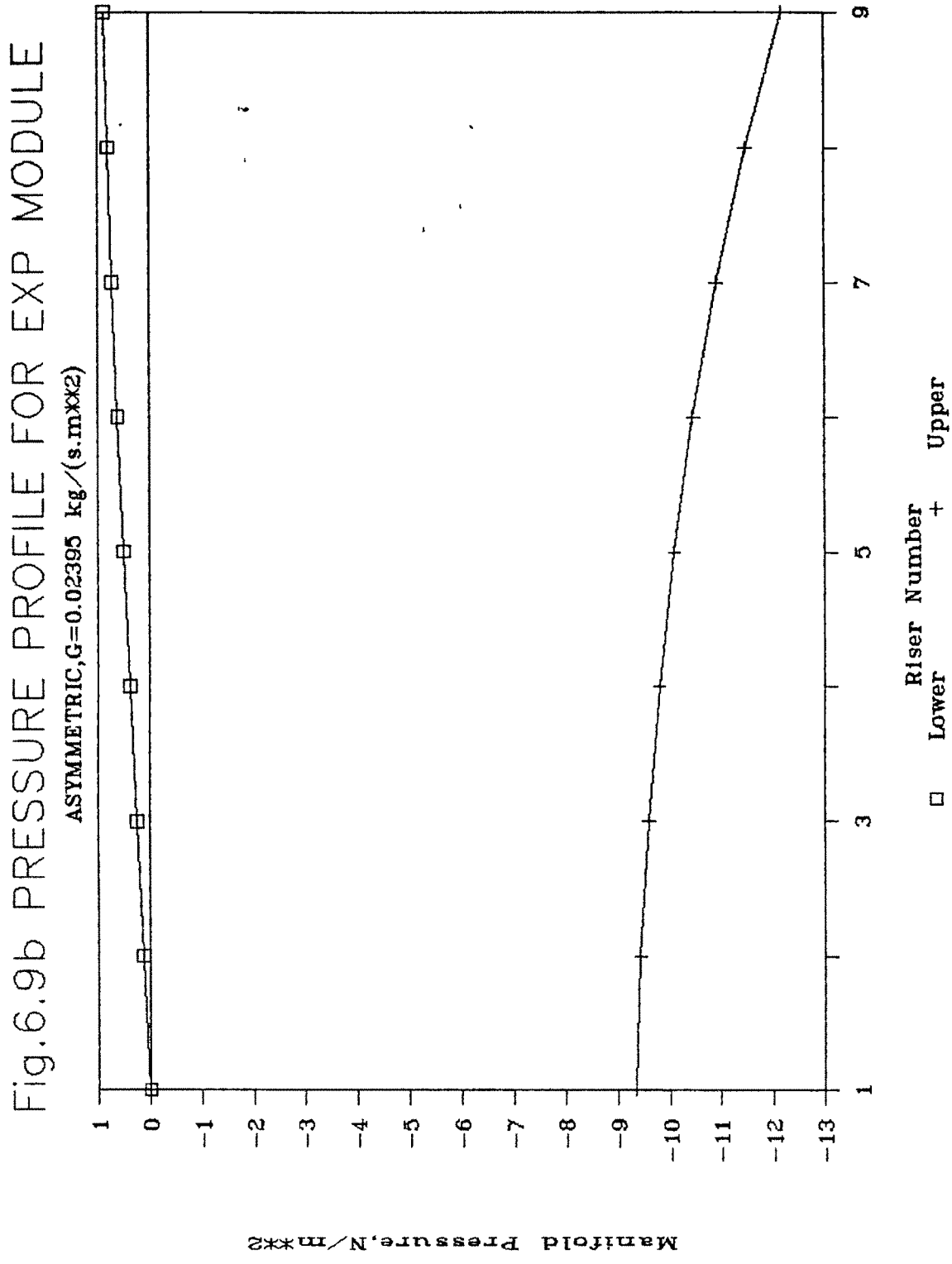
Fig.6.9b PRESSURE PROFILE FOR EXP MODULE
ASYMMETRIC,G=0.02395 kg/(s.m**2)
Manifold Pressure,N/m**2
1
0
-1
-2
-3
-4
-5
-6
-7
-8
-9
-10
-11
-12
-13
1
3
5
7
9
Riser Number
Lower
Upper

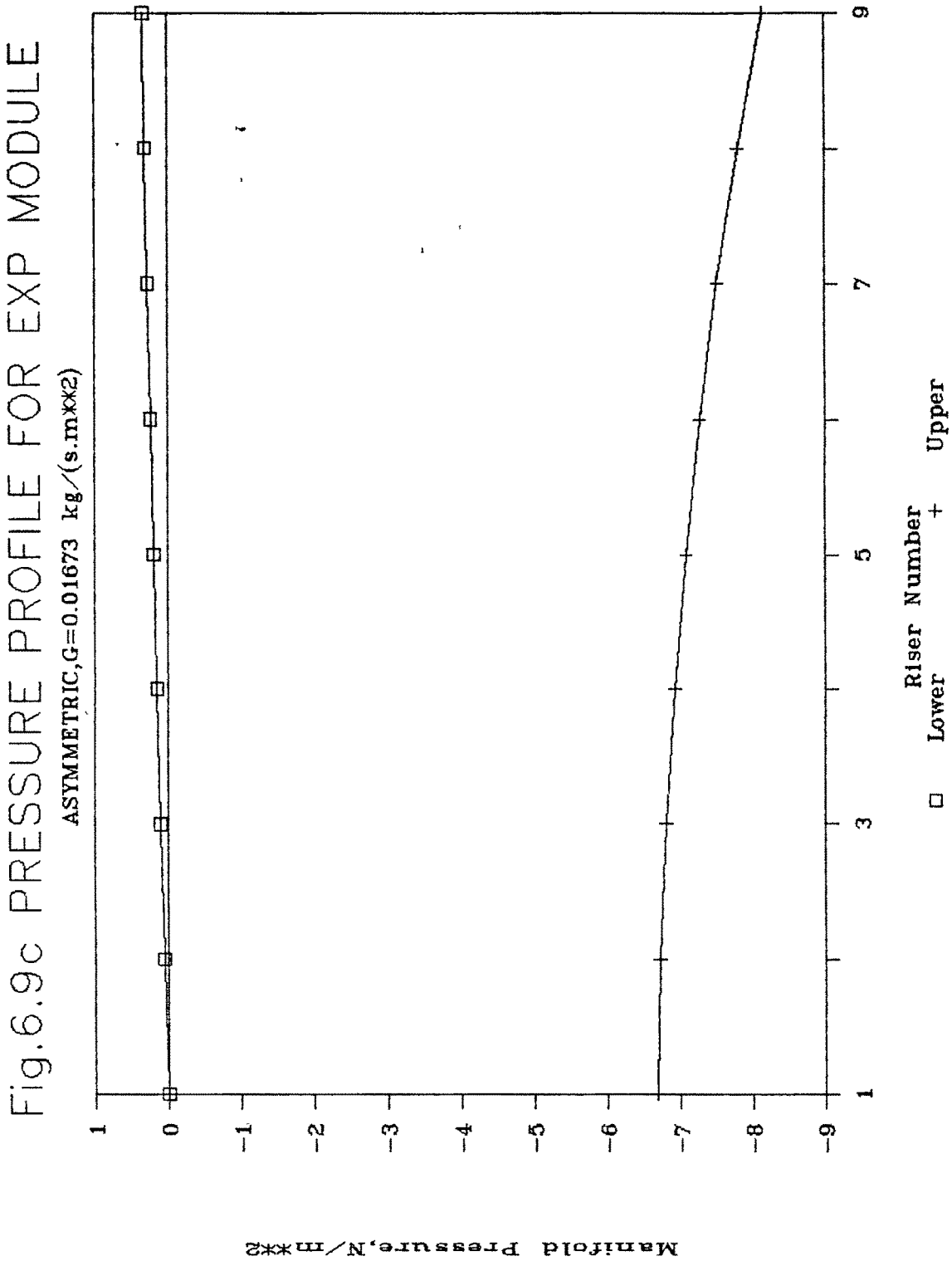
Fig.6.9c PRESSURE PROFILE FOR EXP MODULE
ASYMMETRIC,G=0.01673 kg/(s.m**2)
Manifold Pressure,N/m**2
1
0
-1
-2
-3
-4
-5
-6
-7
-8
-9
1
3
5
7
9
Riser Number
□ Lower
+ Upper

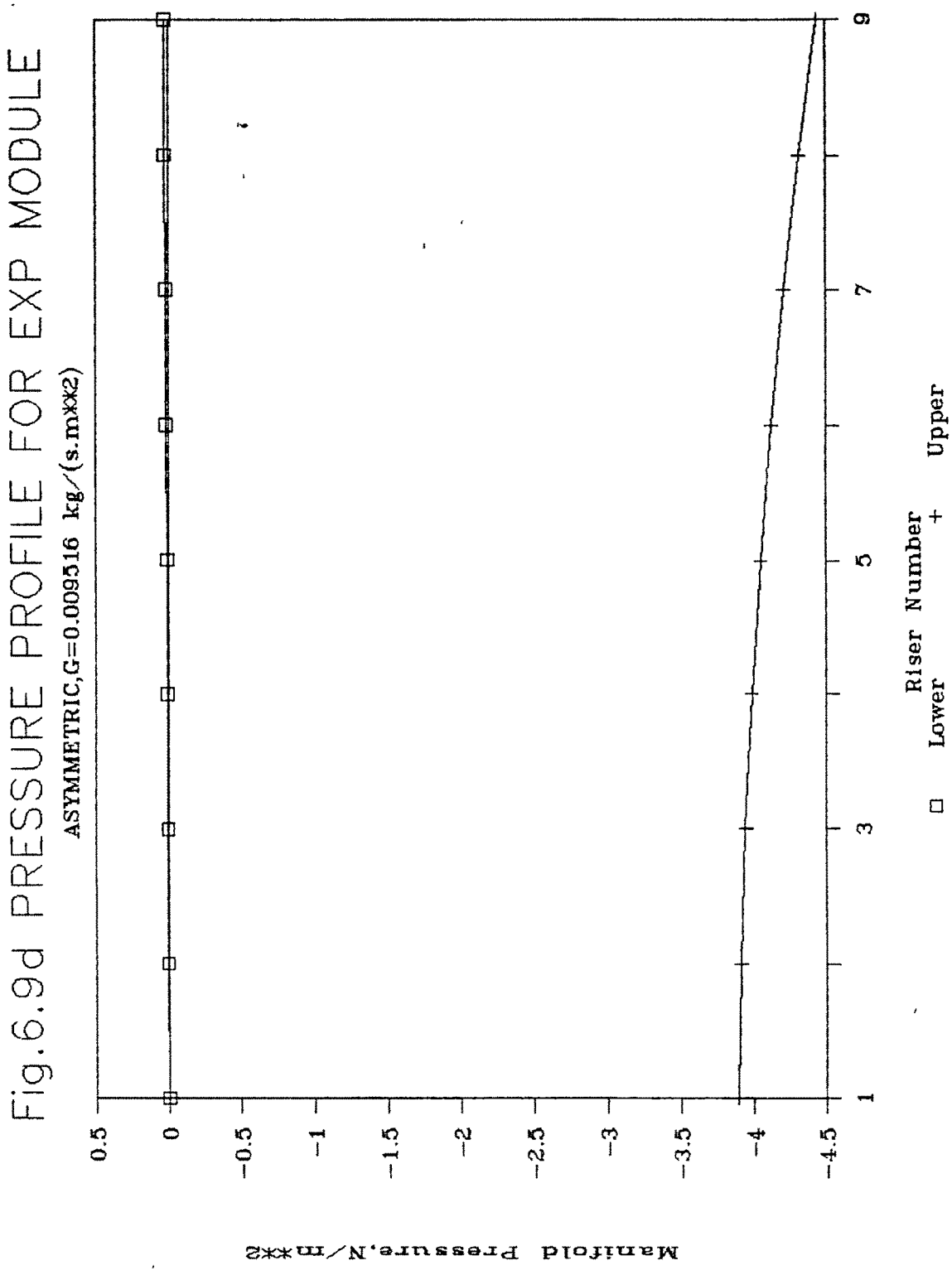
Fig.6.9d PRESSURE PROFILE FOR EXP MODULE
ASYMMETRIC,G=0.009516 kg/(s.m**2)
Manifold Pressure,N/m**2
0.5
0
-0.5
-1
-1.5
-2
-2.5
-3
-3.5
-4
-4.5
1
3
5
7
9
Riser Number
□ Lower
+ Upper

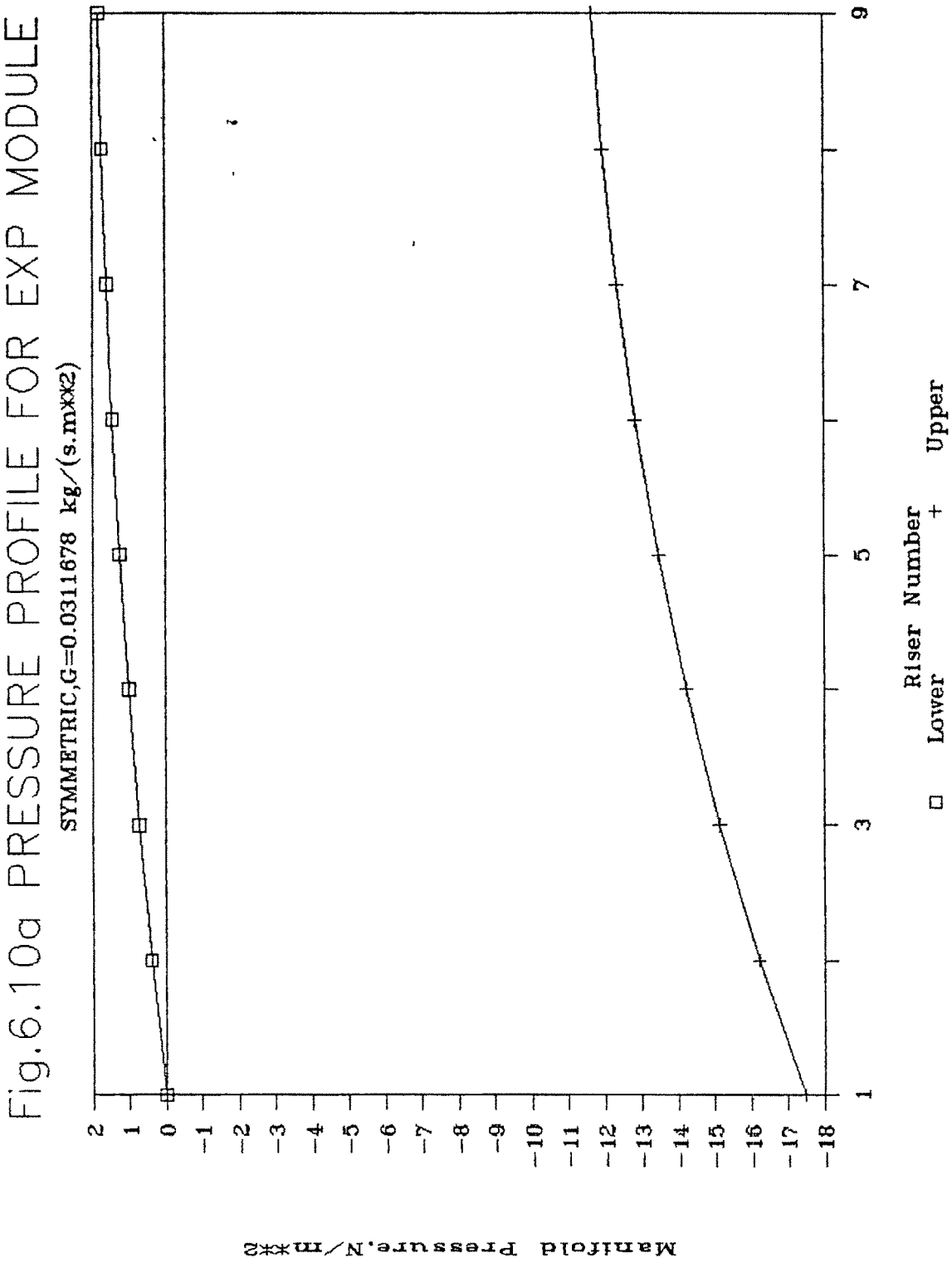
Fig.6.10a PRESSURE PROFILE FOR EXP MODULE
SYMMETRIC,G=0.0311678 kg/(s.mXX2)
Manifold Pressure,N/m**2
2
1
0
-1
-2
-3
-4
-5
-6
-7
-8
-9
-10
-11
-12
-13
-14
-15
-16
-17
-18
1
3
5
7
9
Riser Number
□ Lower
+ Upper

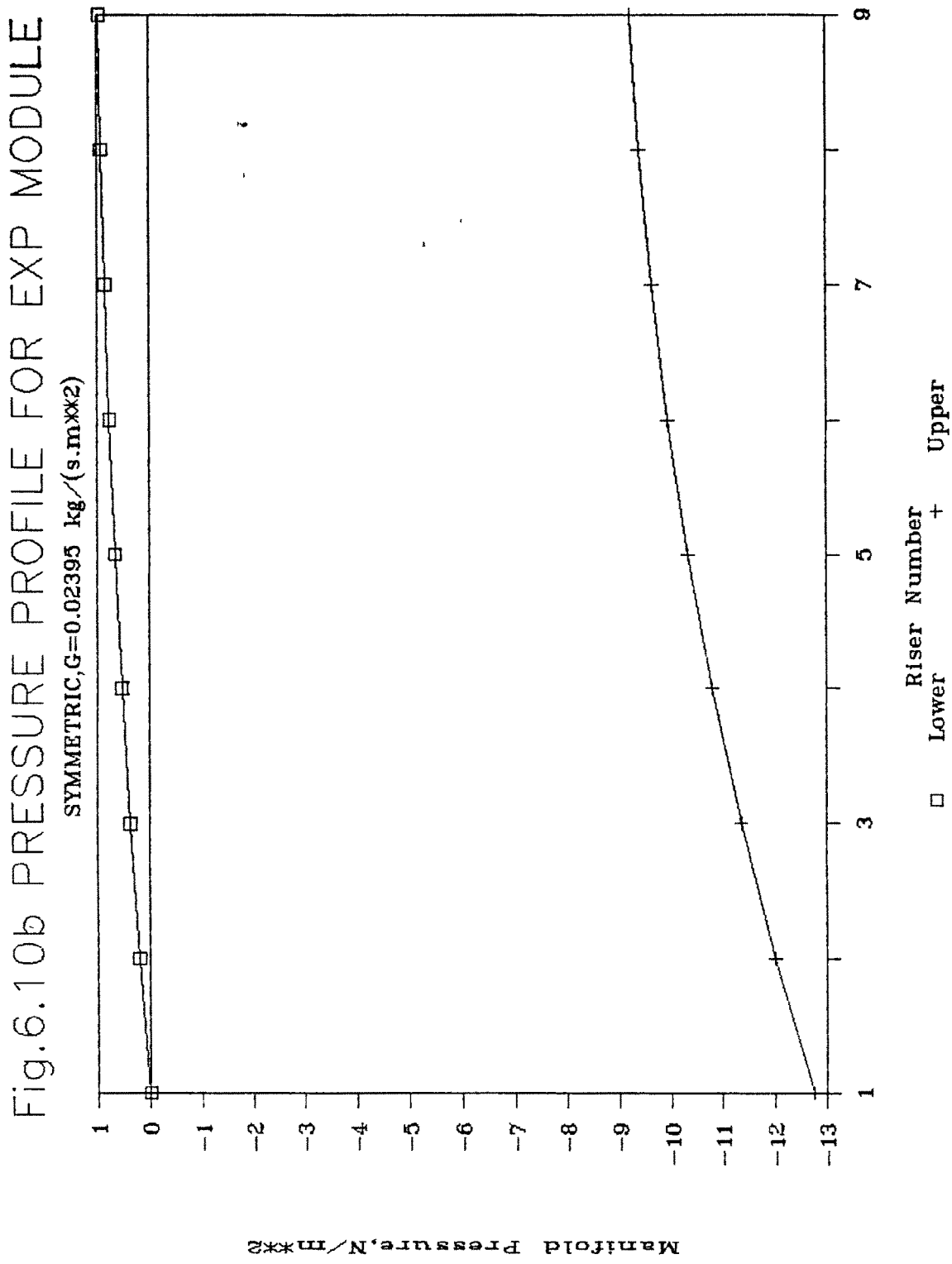
Fig.6.10b PRESSURE PROFILE FOR EXP MODULE
SYMMETRIC,G=0.02395 kg/(s.m**2)
Manifold Pressure,N/m**2
1
0
-1
-2
-3
-4
-5
-6
-7
-8
-9
-10
-11
-12
-13
1
3
5
7
9
Riser Number
□ Lower
+ Upper

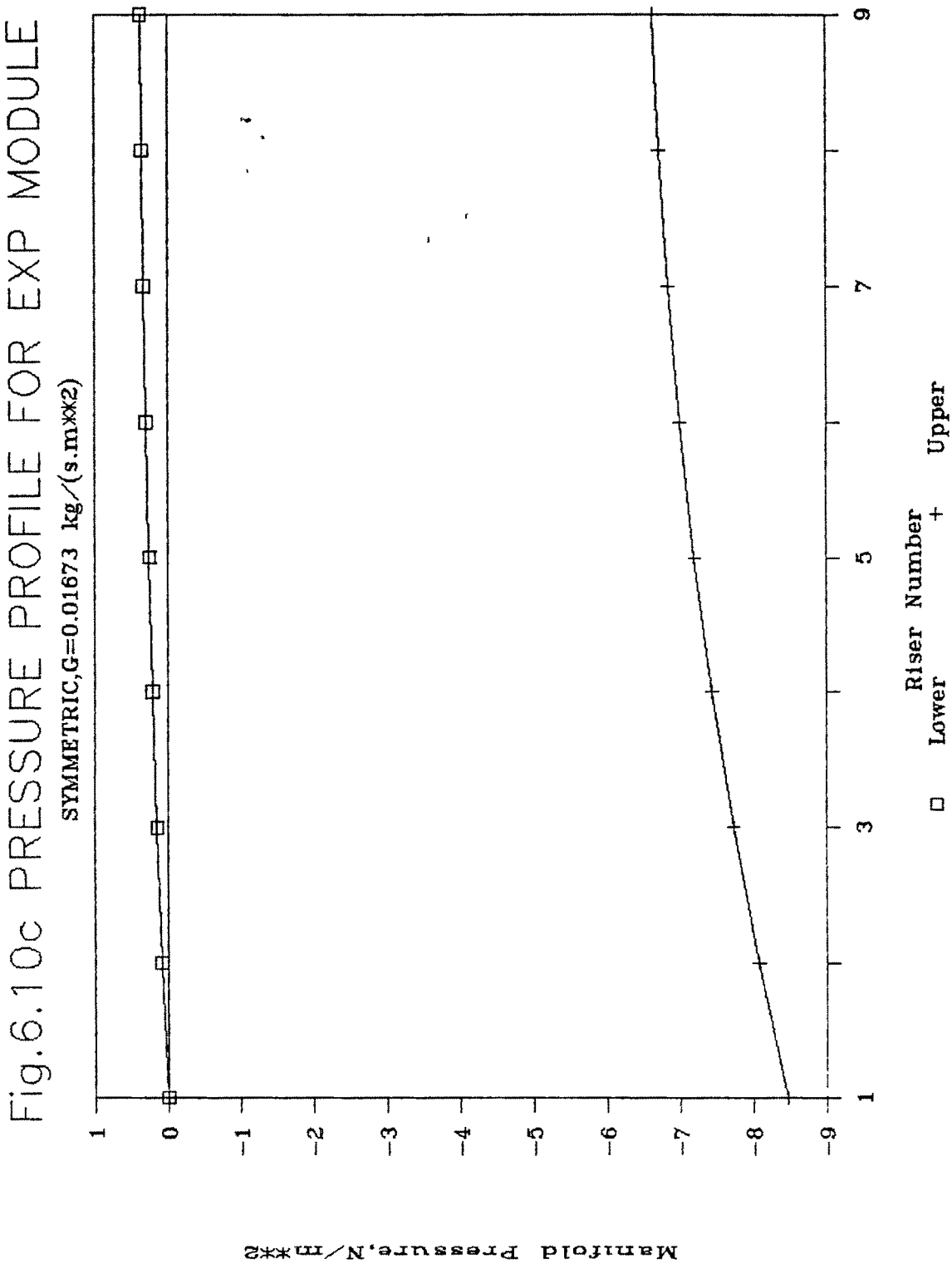
Fig.6.10c PRESSURE PROFILE FOR EXP MODULE
SYMMETRIC,G=0.01673 kg/(s.m**2)
Manifold Pressure,N/m**2
1
0
-1
-2
-3
-4
-5
-6
-7
-8
-9
1
3
5
7
9
Riser Number
□ Lower
+ Upper

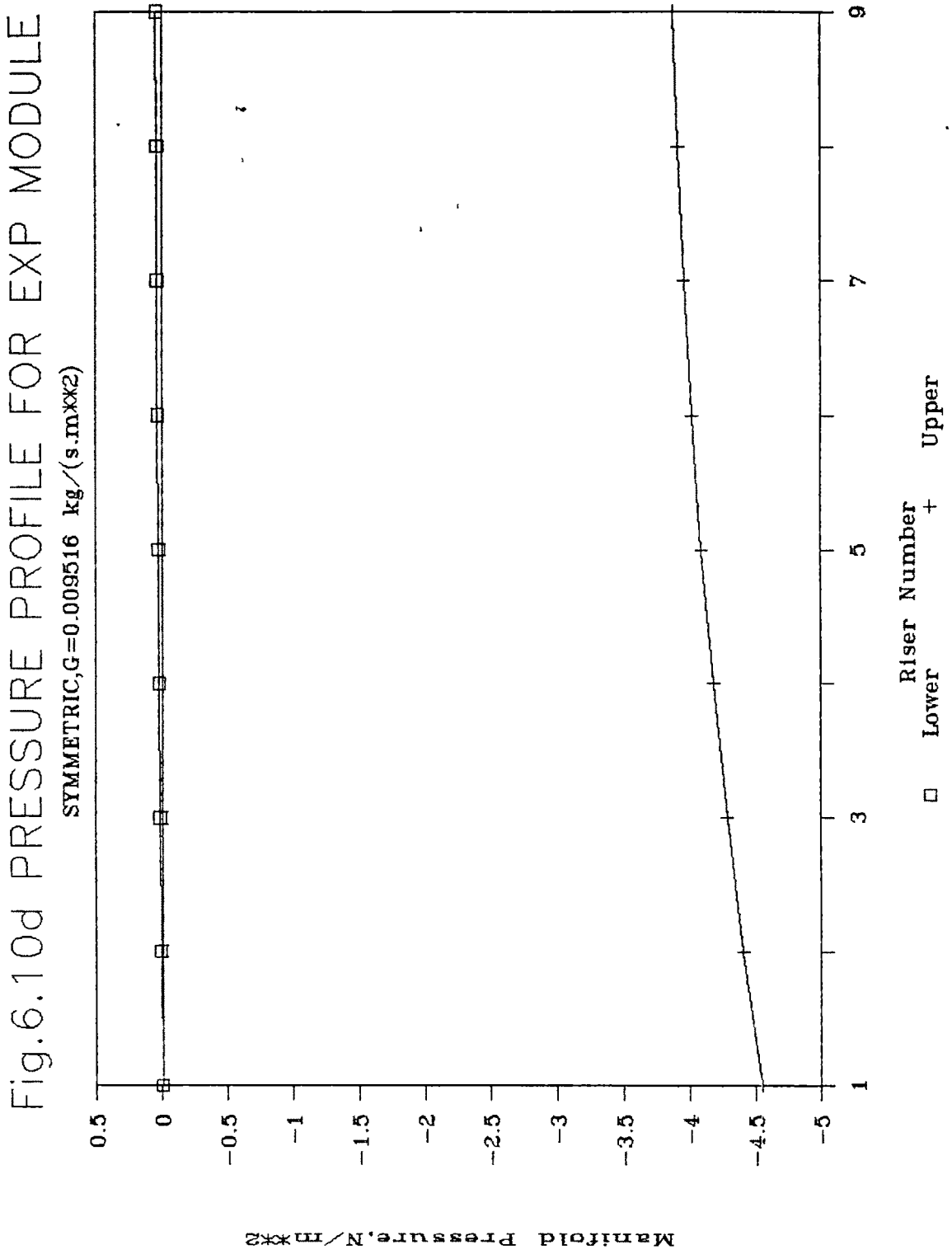
Fig.6.10d PRESSURE PROFILE FOR EXP MODULE
SYMMETRIC,G=0.009516 kg/(s.m**2)
Manifold Pressure,N/m**2
0.5
0
-0.5
-1
-1.5
-2
-2.5
-3
-3.5
-4
-4.5
-5
1
3
5
7
9
Riser Number
□ Lower
+ Upper

6.1.3 Comparison with McPhedran's model

The present-discrete model employs the flow coefficients of Gardel(1957) and Miller(1978) as discussed in Chapter 3, which are defined differently from the conventional momentum coefficients. McPhedran's continuous model (1983) for the evacuated solar collector on the other hand employs momentum coefficients, which were assumed to be inedependent of flow and area ratio. It will be worthwhile to compare both the models which have different basis of modelling. The evacuated solar collector geometry and the flow rate employed by McPhedran were used to predict the riser flow rates. The evacuated solar collector comprised of 4 modules, each with 15 risers of 4.4 mm each with a total flow rate of 4 l/min. Further deatails are given below. The riser tube has an 180 degree U-bend. The additional resistance is considered in the model.

Fig 6.8b gives the comparison of the relative riser flow rates obtained by the present model and that made by McPhedran for asymmetric flow. It is observed from Fig. 6.8b that there is an excellent agreement between the present model and that of McPhedran.

This implies that the isothermal model can be employed to predict the performance of an actual solar collector array, where the flow maldistribution is low. The assumptions made in Chap. 3 were thus valid.

McPhedrans Evacuated Solar Collector Details

-Riser :	.diameter	0.0044	m
	.spacing	0.0600	m
	.length	2.9000	m
	.projection in header	<0.0010	m
-Manifold diameter		0.0171	m
-Interconnecting pipe diameter		0.020	m
-Riser spacing between adjacent collectors		0.160	m

6.1.4 Observations on the experimental results

Asymmetric

For all the four flow rates studied it is observed that the riser flow rates continuously increases towards the exit. This increases with collector flow rate as shown in Fig. 6.4a . For the lowest flow rate of 0.0095 kg $s^{-1}m^{-2}$, the flow is practically uniform.

The riser flows behaviour can be explained by examining the manifold pressure distribution shown in Figs. 6.9a - 6.9d. The reference zero pressure is taken where the fluid just enters the first dividing tee junction in the lower manifold. It may also be noted that the pressure in the upper manifold refers to the point after the fluid leaves the combining tee junction. Thus the pressure differential at any riser shown comprises of the pressure changes at dividing tee, the riser and the combining tee. This is due to the equivalent resistance network chosen for the solution of the network equations as described in Chapter 3.

In general, the lower manifold pressure increases towards the exit as the static pressure rise at the tee junction outweighs the frictional loss in the manifold thereby the net effect is continuously increasing manifold pressure. On the other hand the upper manifold pressure continuously falls since the combining tee pressure loss reinforces the frictional loss in the manifold.

For higher flow rates both the manifold pressures exhibit faster changes along the manifold with the result the pressure differential continuously increases towards the exit. This results in higher riser flow rates correspondingly.As the collector flow rate decreases the pressure changes along the manifold are smaller. For the lowest flow rate the lower manifold pressure is nearly constant throughout and the upper one is practically constant. This explains the almost uniform riser flow rates for G = 0.0095 $kgs^{-1}m^{-2}$.

This suggests that for a given collector geometry and flow rate it is possible to obtain uniform flow distribution.

Symmetric

In regards to the flow distribution similar observations can be made here that the flow is more uniform for lower flow rates as shown in Fig. 6.8a.

Similar arguments also apply here for the manifold pressure distribution. However, the upper manifold pressure distribution is different as the pressure continuously rises away from the exit as shown in Figs. 6.10a - 6.10d since the total pressure has to decrease towards the exit. The overall effect is a pressure differential which results in more uniform flow distribution. This can be appreciated by comparing Figs.6.4a and 6.8a. For the higher

flow rates the flow is more uniform in symmetric mode rather than in asymmetric. This can be observed from Table 6.9 which gives the value of non-uniformity factors.

Table 6.9 Non-uniformity factors for the experimental collector module.

Collector Flow Rate $kgs^{-1}m^{-2}$	Asymmetric	Symmetric
0.0312	0.0173	0.0033
0.0239	0.0113	0.0028
0.0167	0.0061	0.0022
0.0095	0.0022	0.0016

The flow rate in the first riser is always the highest since this is the shortest path for the fluid. For the rest of the fluid as it is diverted into the risers traverses longer path. The fluid entering the last riser has the longest path. Since the pressure drop through any path has to be the same the first riser being of lowest resistance has the highest flow while that in the last riser the lowest.

6.2 Flow distribution studies in large solar collector array.

In the previous sections the model proposed here has been validated by the experiments as well as momentum model of McPhedran(1983). The model thus can be used for studying flow distributions in large solar collector array. In actual practise 5-15 collectors can be placed in parallel depending upon site constraints. In the following sections flow distributions will be studied in 5-module collector array, both in asymmetric and symmetric flow configurations.

In the previous sections it was observed that collector flow rate affect the flow distribution. In the earlier study [Soin(1983)] it was also observed that the area ratio play a significant role in the flow distribution. These two parameters will be studied here. The effect of longer or shorter riser tubes is not studied separately here as the effect of length variation possible within the practical size of collector would be small compared to that due to area ratio. In general, however, longer tubes will provide more uniform flow distribution, keeping other parameters the same.

The effects of riser and collector spacing on the flow distribution are also examined.

The area ratio referred here is the cross-setional ratio of a single riser to that of the manifold. It should be differentiated

with the area ratio defined by other workers, e.g. Bajura and Jones(1976) where it represents the cross sectional area ratio of total number of risers to that of the manifold. The later is also called the porosity of a manifold.

It is found that the optimum collector flow rate range is 0.0050 - 0.0075 kg $s^{-1}m^{-2}$ which maximises the energy collection in a solar water heating systems [Soin(1982,1985), Shil and Soin(1987)]. The collector flow rate, G, selected for the study is 0.0075 $kgs^{-1}m^{-2}$, which is the baseline value. The collector geometry details are given in Table 6.10.

The four manifold diameters shown above correspond to area ratio of 0.05, 0.10, 0.20 and 0.40. The riser diameter has been kept constant. The collector geometry given in Table 6.10 corresponds to the typical present day solar collector. This is considered as the baseline collector.

The results are presented as the actual riser flow rates and relative riser flow rates. The relative riser flow rate provides a quick appreciation of the extent of flow maldistribution with respect to uniform value. Also within limits it can be utilised to have a quick estimate for similar collector geometry, flow rate and area ratio. The collector array efficiency is calculated as described in Sec. 3.9 to provide an estimate of collector efficiency degradation due to flow maldistribution. The manifold pressure are also presented for each flow rate-area ratio.

Table 6.10 Details of collector geometry

.Manifold diameter	a. 0.04025	m
	b. 0.02846	m
	c. 0.02012	m
	d. 0.01423	m
.Riser diameter	0.009	m
length	2.2	m
.No. of risers per module	8	
.Riser spacing	0.110	m
.Inter-connecting pipe length	0.110	m
.Fin thickness	0.0003	m
.Absorber optical properties		
-absorptivity	0.95	
-emissivity	0.10	
.No. of glass cover	1	
.Insulation thickness	0.050	m

6.2.1 Simulations of 5-module solar collector array

6.2.1.1 Asymmetric-Effect of area ratio

Keeping the collector flow rate constant at 0.0075 $kgs^{-1}m^{-2}$, the manifold diameters were varied to obtain the desired area ratios. Figs. 6.11 to 6.14 gives the riser flow profiles (absolute and relative) for area ratios of 0.05 to 0.40. It is seen that as the area ratio increases the flow maldistribution increases. The riser flow rates in the middle tend to decrease much below that of uniform value as the area ratio increases.

Fig. 6.15 gives very clearly the effect of area ratio. For area ratio of 0.05, the riser flow profile is practically uniform. At a value of 0.10 the maldistribution is still quite low. For area ratios of 0.20 and 0.40 the maldistribution has increased relatively.

It may be emphasised here that as the number of collectors in parallel is increased the total flow rate (kgs^{-1} or m^3s^{-1}) entering the collector array increases in proportion to the collector area, the collector flow rate being expressed as kgs^{-1} per unit collector area. This is a basic design requirement in a solar collector. In other words, irrespective of series or parallel connection or combination, the collector flow rate expressed in kg $s^{-1}m^{-2}$ remains the same so as to keep the temperature rise across the collector in

series the same. For a collector array purely in parallel this implies temperature rise across the collector riser. Thus, for a collector array having uniform flow distribution the collector array efficiency will be identical to that of a single collector at the same flow rate, G, kg $s^{-1}m^{-2}$.

The manifold pressure distributions are given in Figs. 6.17a to 6.17c. Unlike for single collector module (experimental), the lower manifold pressure changes much more rapidly for higher area ratios. This in combination with that of upper manifold results in low pressure differential across the manifold which reduces the riser flow rates in the middle of the array while that of the end risers increases. The rapid change in the manifold pressure in the lower manifold is due to increase in the frictional losses which outweighs the static pressure gain at the tee junctions.

As the area ratio increases the pressure drop across the manifold changes more rapidly. It is more predominant in the upper manifold, because of the reinforcement of pressure loss due to friction and combining flow tee junction. This suggests that a better flow distribution can be obtained by keeping the upper manifold diameter greater than the lower one.

To understand better the behaviour, a 3-module array with an area ratio of 0.20 was also studied at the same flow rate. Fig. 6.13c and 6.13d show the riser flow profiles, while Fig. 6.17d indicate the pressure profile.

Based on the results of 1-,3- and 5-module array of an area ratio of 0.20, the followings can be observed :

a. The riser flow rates monotonically increases for a single collector module (Fig.6.4a). However, when several collectors are connected in parallel, the riser flow rates show a minimum (Figs. 6.13c-d and 6.13a-b). It may be seen from these figures that the minimum riser flow rate has shifted towards the middle of the array.

b. This can be explained by the manifold pressure profiles. The pressure drop across the manifold increases significantly due to increase in the total flow rate as the number of collectors in parallel increases. The presure changes rapidly in the lower manifold at the inlet where the flow rate is highest. The pressure changes slowly away from the inlet by the time most of the fluid is diverted into the risers. On the other hand in the upper manifold the pressure changes rapidly at the outlet (see Figs. 6.17c and 6.17d). The zones of rapid pressure change in the manifold being at the inlet and exit, the pressure distributions thus result in higher flow rates in the extreme risers with a corresponding decrease in the risers between these two zones resulting in flow maldistribution. Higher the frictional pressure drop offered by the manifold with an increase in the flow rate higher the flow maldistribution.

c. As the manifold length increases due to more number of collectors in parallel, other factors remaining the same, the pressure change across the manifold becomes predominant compared to that across the riser. For a single collector, the riser pressure drop is controlling (Fig. 6.9d approximates the situation). On the other hand, by the time the number of collector modules are 5, the pressure drop across the lower manifold is comparable and that in the upper manifold is 3-4 times that of the riser (Fig.6.17c). The riser pressure drop for uniform flow is about 30 Nm^{-2} (Fig.6.17a).

It can be observed that **'riser to manifold length ratio'** is an important parameter affecting the flow distribution. In the present study, or in general where the riser length is fixed, this necessarily implies increase in flow maldistribution with increase in number of collector modules in parallel, other parameters remaining the same.

The above suggests that as the number of collectors in parallel increase, the area ratio should be decreased to obtain uniform flow distribution. This implies a choice of higher manifold diameter so as to keep pressure drop across the manifold much lower in comparison to that in the riser. This can be observed for area ratios of 0.05 and 0.10 for 5-module array. Fig. 6.17a indicate that the riser pressure drop is controlling for area ratio of 0.05. For area ratio of 0.10, the pressure drop in the upper manifold

becomes comparable to that in the riser, but that in the lower manifold is much smaller. For an area ratio of 0.20 as explained above the manifold pressure drop is controlling.

Thus, for a fixed riser diameter and length, the **'length to diameter ratio of the manifold'** emerges as an important parameter.

The author had earlier studied the flow distribution in a large solar collector array [Soin(1983)]. However, the manifold diameter was kept constant while the riser diameter was varied to obtain different area ratios. Similar observations were made. It would be interesting to compare the behaviour with the present collector where the riser diameter is fixed and the manifold diameter varied. The flow distribution are obtained for the collector geometry given in Table 6.10, except that the manifold diameter is kept constant at 0.025 m. Riser diameters of 0.056, 0.008 and 0.0112 m are chosen to obtain area ratios of 0.05, 0.10 and 0.20 respectively.

The riser flow profiles are given in Figs. 6.15a to 6.15f. It is observed that the riser flow rates are practically equal to that of fixed riser diameter for the same area ratio. The pressure profile is also nearly identical for the same area ratio. However, the magnitude of the pressure drop is quite different. The array pressure drops for fixed riser diameter are given in Table 6.11, while that for fixed manifold diameter are given in Table 6.13. In Table 6.13 the results of previous studies [Soin(1983)] of different collector geometry are given alongwith those obtained for the

present collector geometry. In the previous studies the riser spacing was 0.070 m instead of 0.110 in the present collector.

It may be noted that the collector array pressure drop decreases with area ratio (as riser diameter increases for a fixed manifold diameter) in Table 6.13, while the reverse is true for fixed riser diameter as the manifold diameter increases as shown in Tables 6.11 and 6.12.

In case the diameter is fixed, as in the present case, the average pressure drop across the risers remain very near to the one for uniform value. The pressure variation in the manifold affects the flow distribution. On the other hand, when the manifold diameter is kept constant the pressure drop across the manifold remains nearly the same as the area ratio changes, but the riser pressure drop increases with decrease in the area ratio. In this case the riser pressure drop affects the flow distribution.

It is seen that in either case uniform flow distribution is obtained by keeping a low area ratio. In the present study the uniform flow is obtained by increasing the manifold diameter (riser diameter fixed) thereby keeping the manifold pressure differential nearly constant due to small frictional loss in the manifold. On the other hand when the manifold diameter is fixed it is obtained by reducing the riser diameter thereby increasing the riser pressure drop. In both the cases it is important to note that the riser pressure drop is significantly higher than that across the manifold

(e.g. see Figs. 6.17a and 6.17e) to obtain uniform flow distribution.

The area ratio is, therefore, the most important parameter of a solar collector to ensure uniform flow distribution.

6.2.1.2 Asymmetric-Effect of flow rate

Keeping the area ratio constant the collector flow rates of 0.0050 and 0.0150 $kgs^{-1}m^{-2}$ were studied. The results are given in Figs.6.16a to 6.16f. The area ratio of 0.20 was chosen to illustrate clearly the effect of flow rate on the flow distribution. The comparison of the three flow rates is given in Fig. 6.16g. It is observed that flow maldistribution increases with flow rate. This is due to increase in the frictional pressure drop in the manifold as the flow rate is doubled. This is evident from the pressure profile shown in Fig. 6.16f. On the other hand, the flow distribution improves for lower flow rate of 0.0050 $kgs^{-1}m^{-2}$ as can be seen in Fig. 6.16a-b. The corresponding pressure profile is given by Fig. 6.16c.

It may be inferred that for a collector geometry designed at a particular flow rate, lower flow rates can be used and the flow maldistribution will be lower as shown in Fig. 6.16g. This is an important observation in that a designer can opt for a single design applicable for a range of flow rates below the design value.

6.2.2.1 Symmetric-Effect of area ratio

Keeping the collector flow rate constant at 0.0075 $kgs^{-1}m^{-2}$, the area ratio was varied from 0.05 to 0.40. The results are given in Figs. 6.18 to 6.21. The riser flow rates continuously decreases away from the exit. It is observed that the flow maldistribution increases with area ratio. The comparative riser flow rates for all the four area ratios are given in Fig. 6.22. The riser flow rates are practically uniform for area ratio of 0.05. The flow maldistribution is very low for area ratio of 0.10. For area ratios of 0.20 and greater it increases, with the risers near the exit having the higher flow rates.

The manifold pressure distributions are given in Figs. 6.24a to 6.24c. It is observed that the pressure change along the lower manifold is very slow compared to that in the upper manifold for all area ratios. This suggests that if the upper manifold is of greater diameter than the lower one flow distribution will improve.

The pressure profile for the 5-module array for higher area ratios is no longer conducive for uniform flow distribution as was the case in the single collector module. This is due to manifold pressure change controlling instead the riser one. To ensure uniform flow distribution lower area ratio is to be selected.

6.2.2.2 Symmetric-Effect of flow rate

Keeping the area ratio constant at 0.20 the collector flow rates of 0.0050 and 0.01560 kg $s^{-1}m^{-2}$ were studied. The results are given in Figs. 6.23 a to 6.23f. The comparison is given in Fig. 6.23g. It is observed that the flow maldistribution increases with flow rate.

The flow maldistribution decreases for lower flow rates when the collector geometry has been designed for a particular flow rate.

Fig.6.11a FLOW PROFILE FOR 5 MODULE

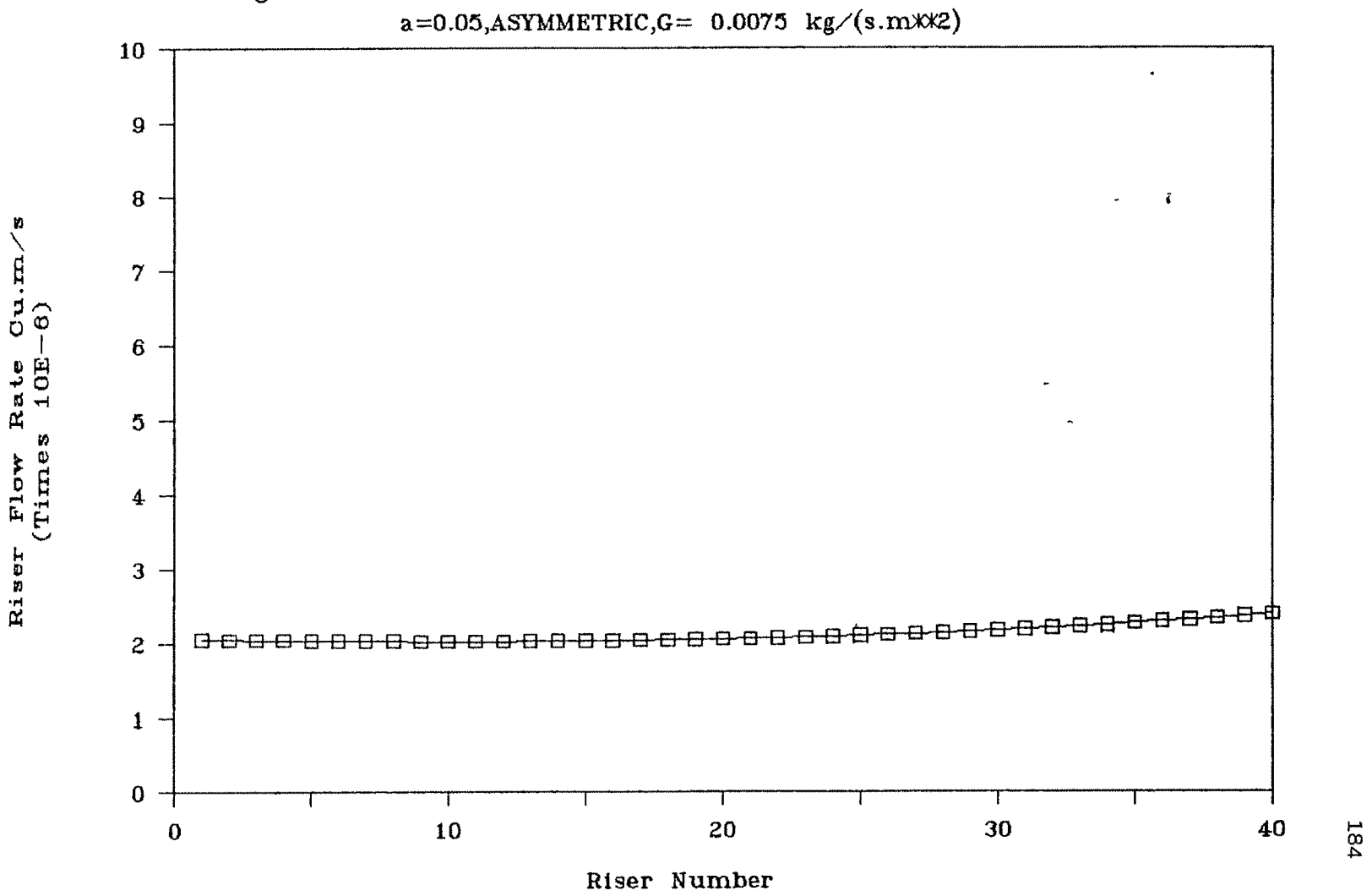

Fig.6.11b FLOW PROFILE FOR 5 MODULE

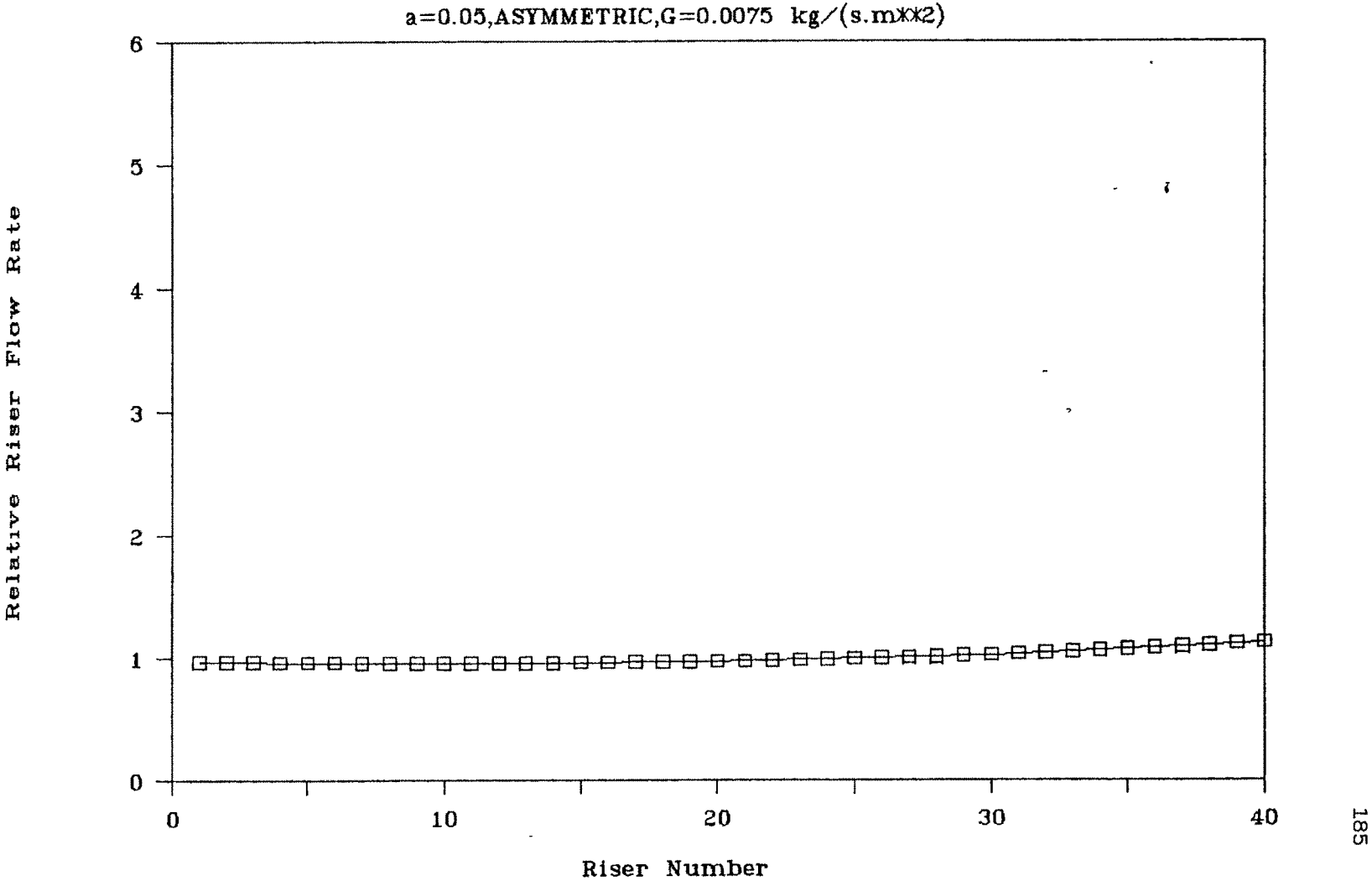

Fig.6.12a FLOW PROFILE FOR 5 MODULE

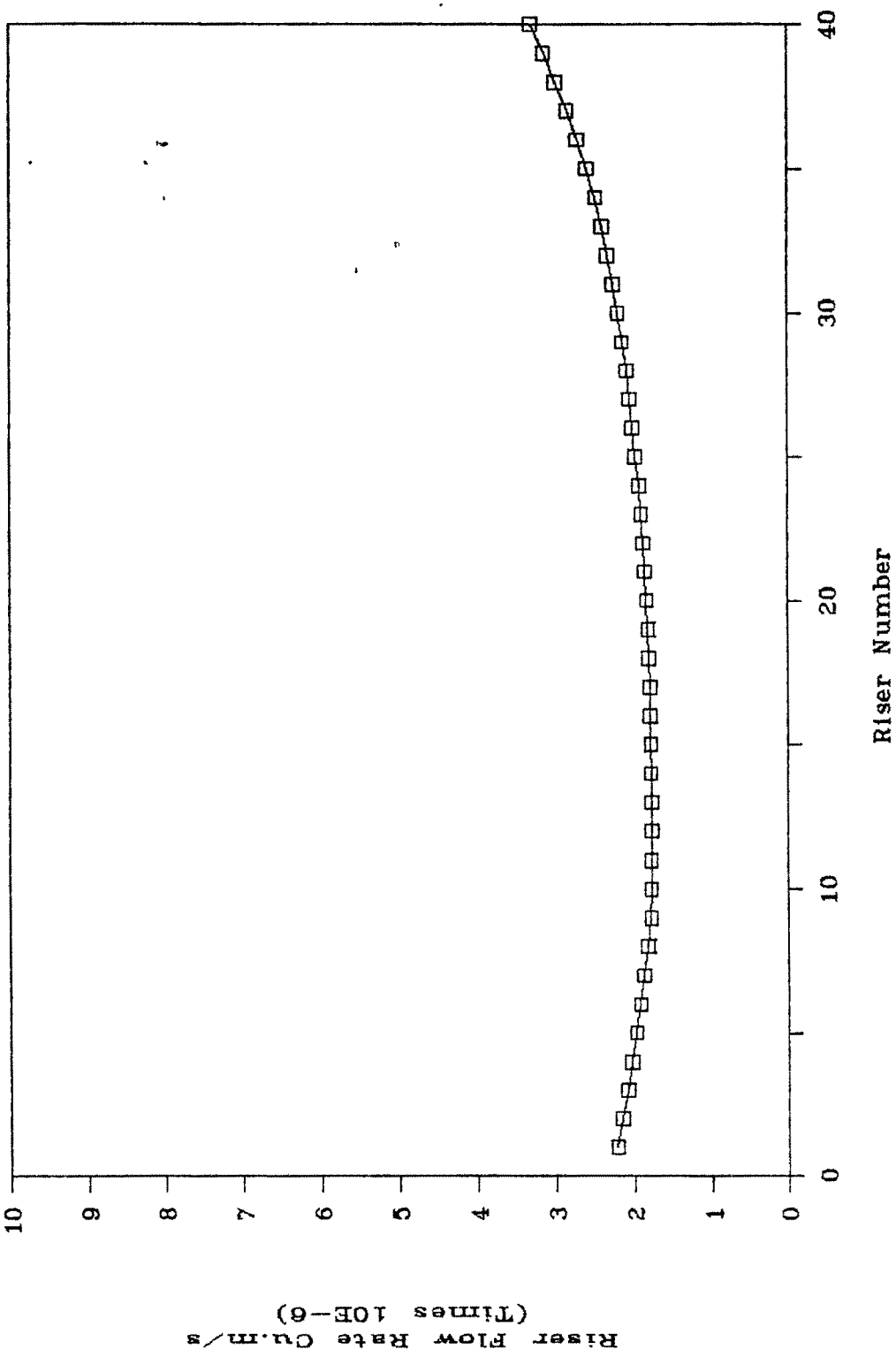

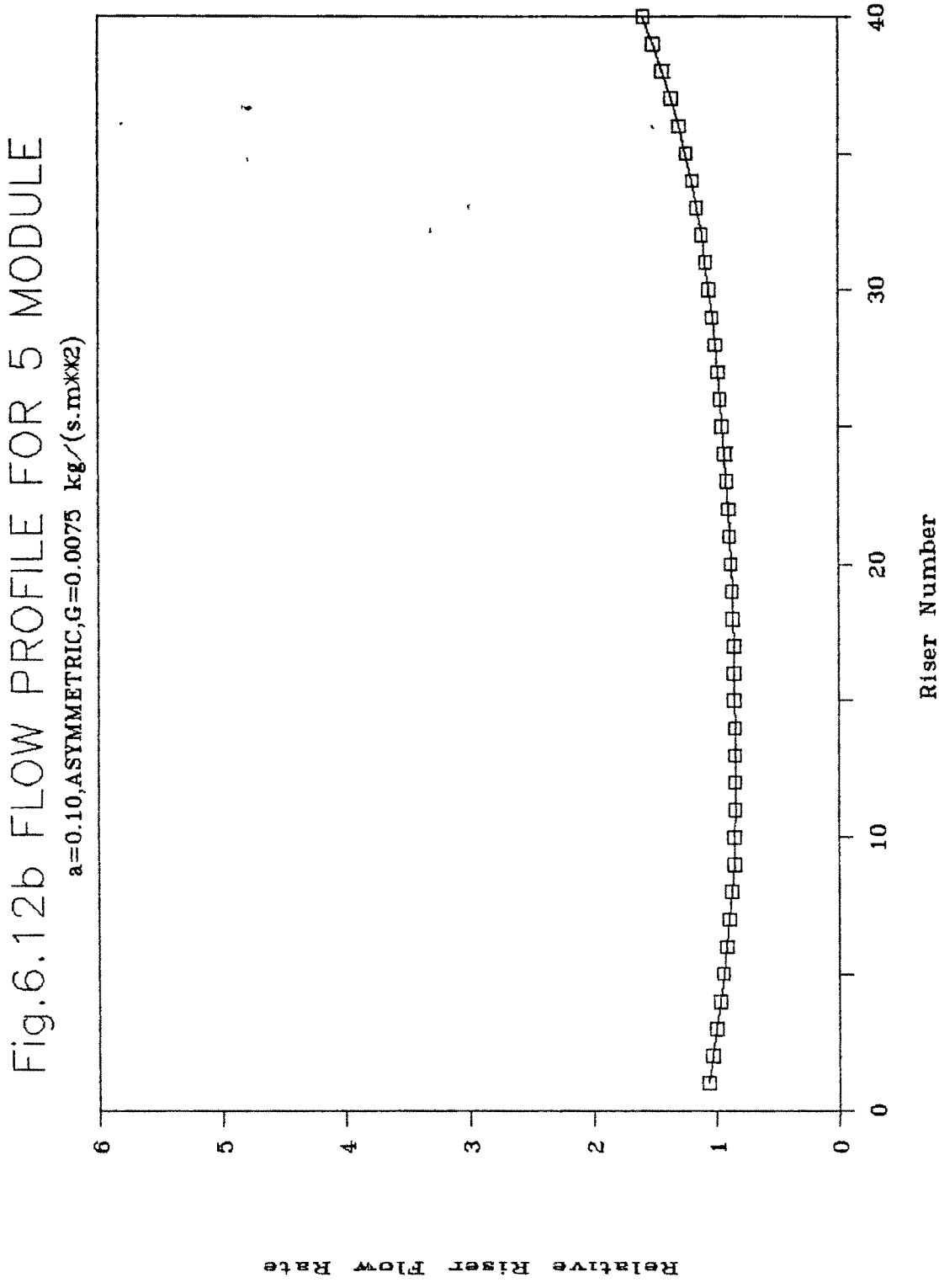
Fig.6.12b FLOW PROFILE FOR 5 MODULE
a=0.10,ASYMMETRIC,G=0.0075 kg/(s.m**2)
Relative Riser Flow Rate
Riser Number
0
1
2
3
4
5
6
0
10
20
30
40

Fig.6.13a FLOW PROFILE FOR 5 MODULE

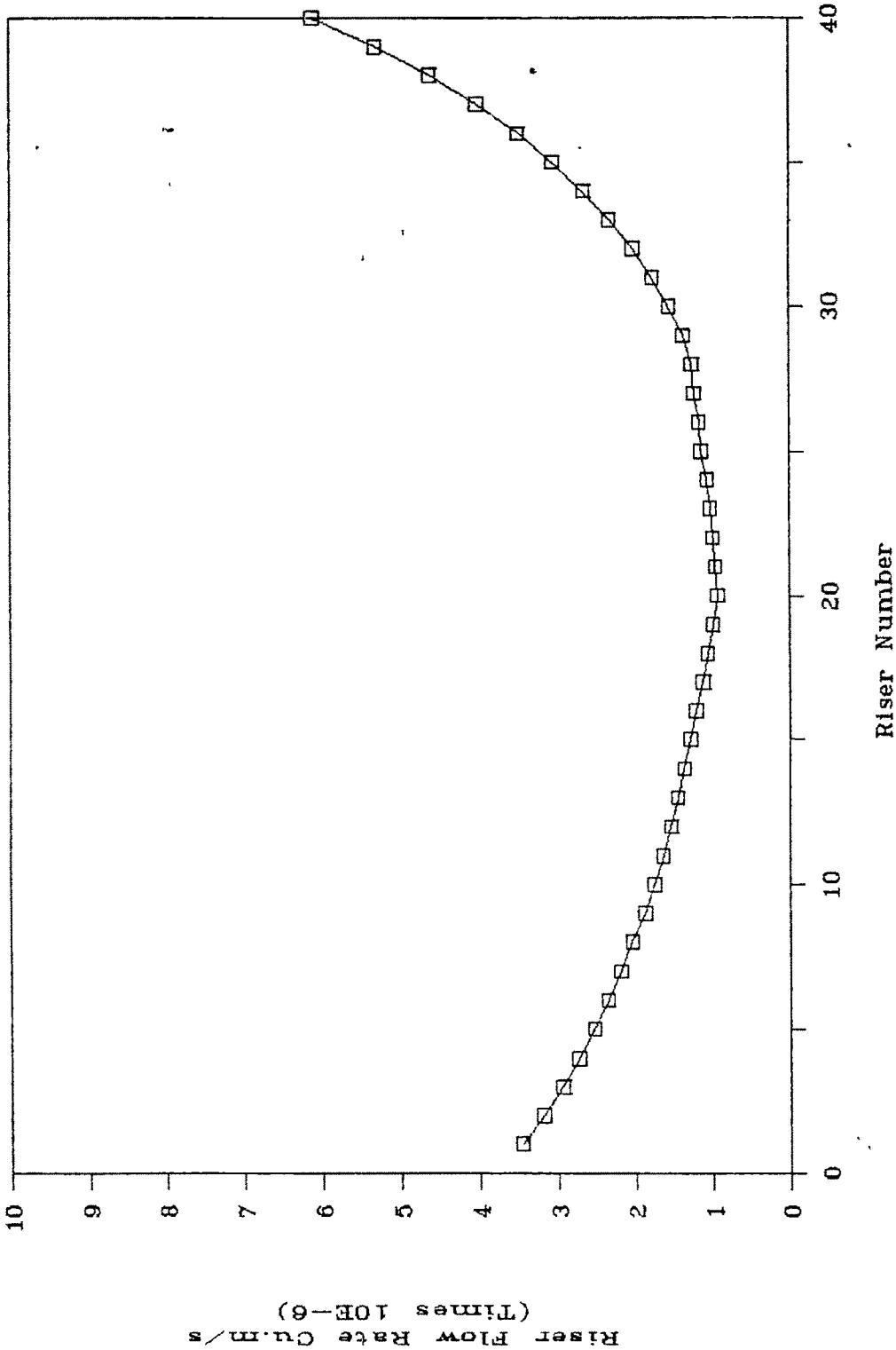

Fig.6.13b FLOW PROFILE FOR 5 MODULE

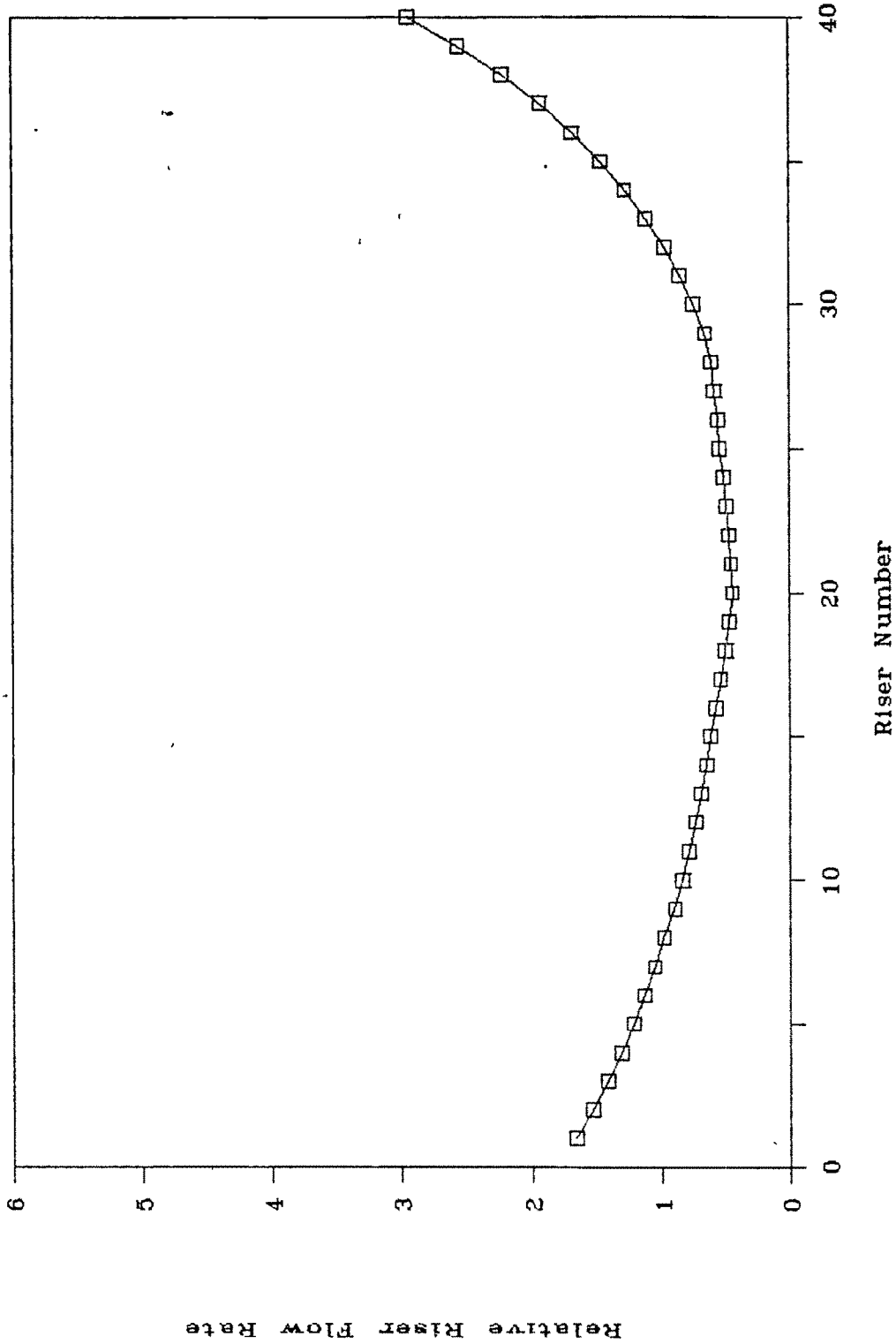

Fig.6.13c FLOW PROFILE FOR 3 MODULE

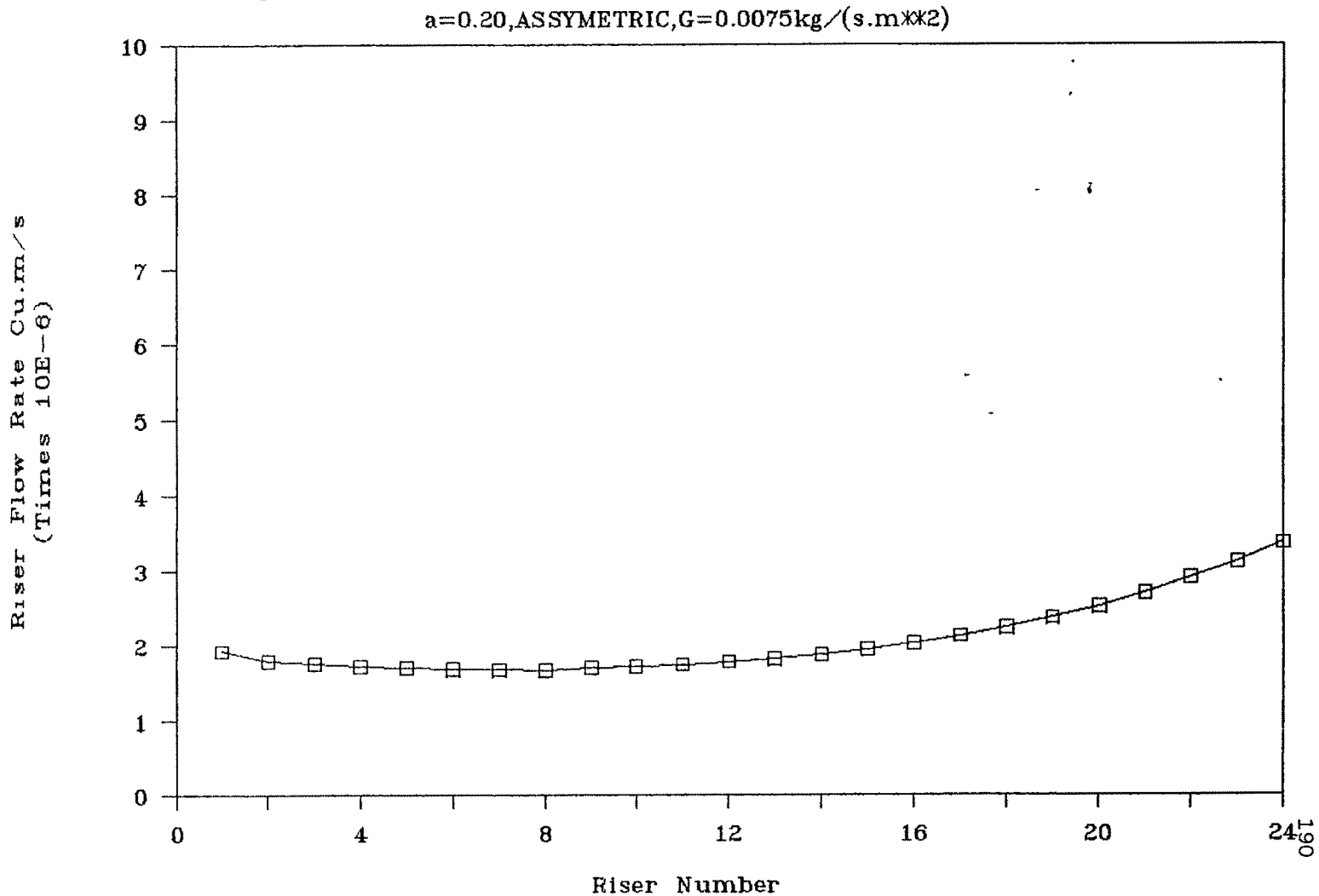

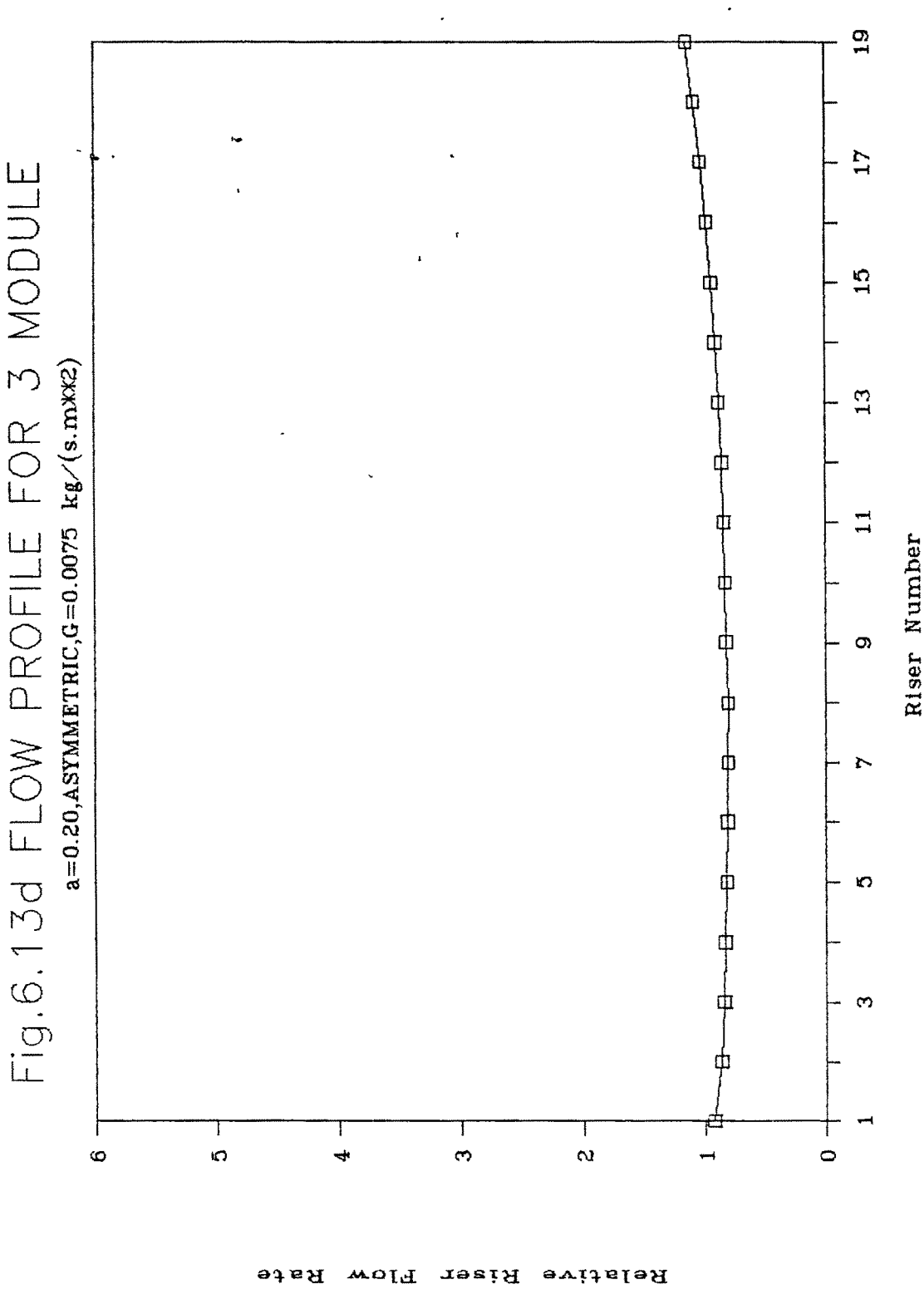
Fig.6.13d FLOW PROFILE FOR 3 MODULE
a=0.20,ASYMMETRIC,G=0.0075 kg/(s.m**2)
Relative Riser Flow Rate
0
1
2
3
4
5
6
1
3
5
7
9
11
13
15
17
19
Riser Number

Fig.6.14a FLOW PROFILE FOR 5 MODULE

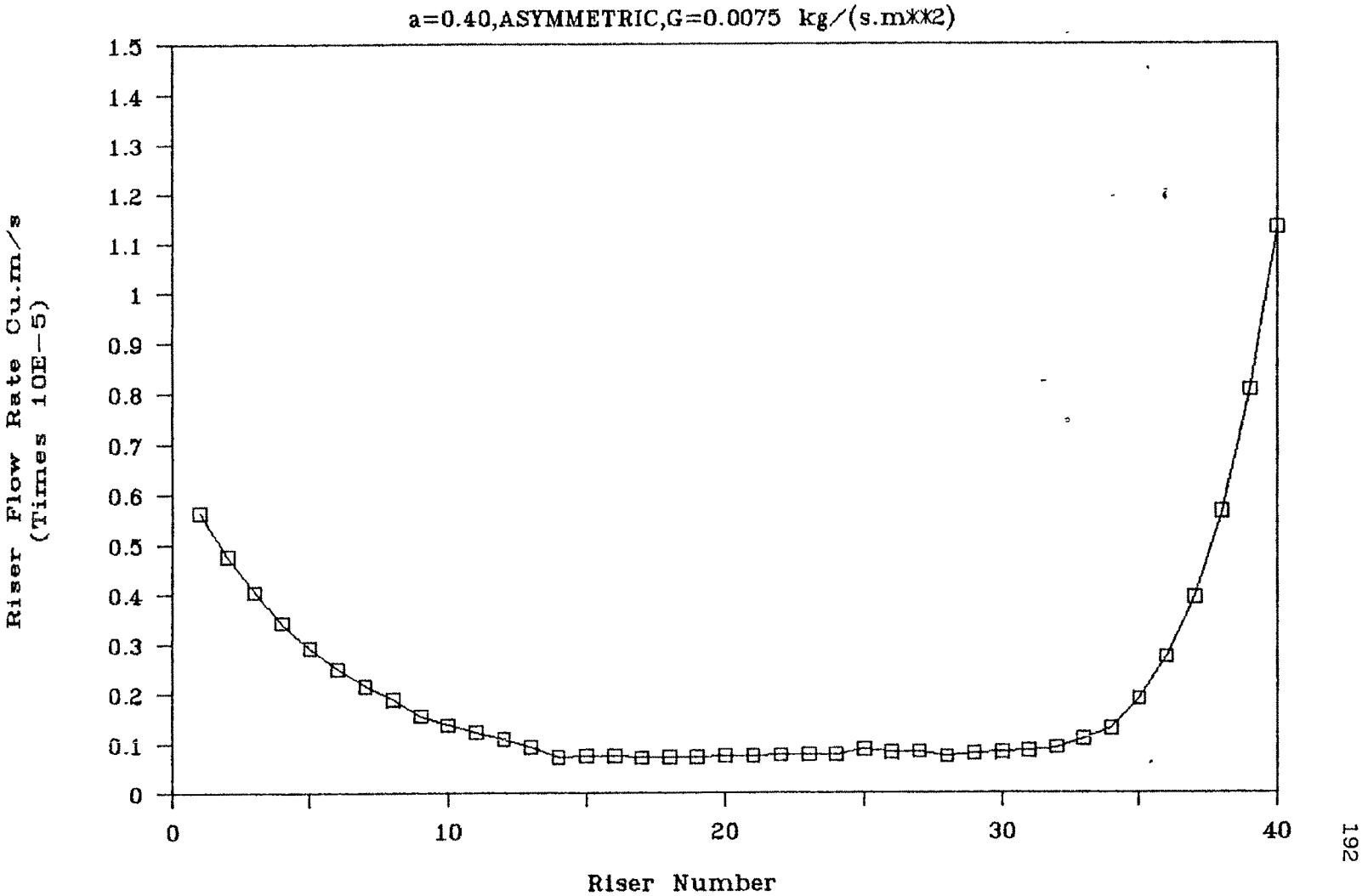

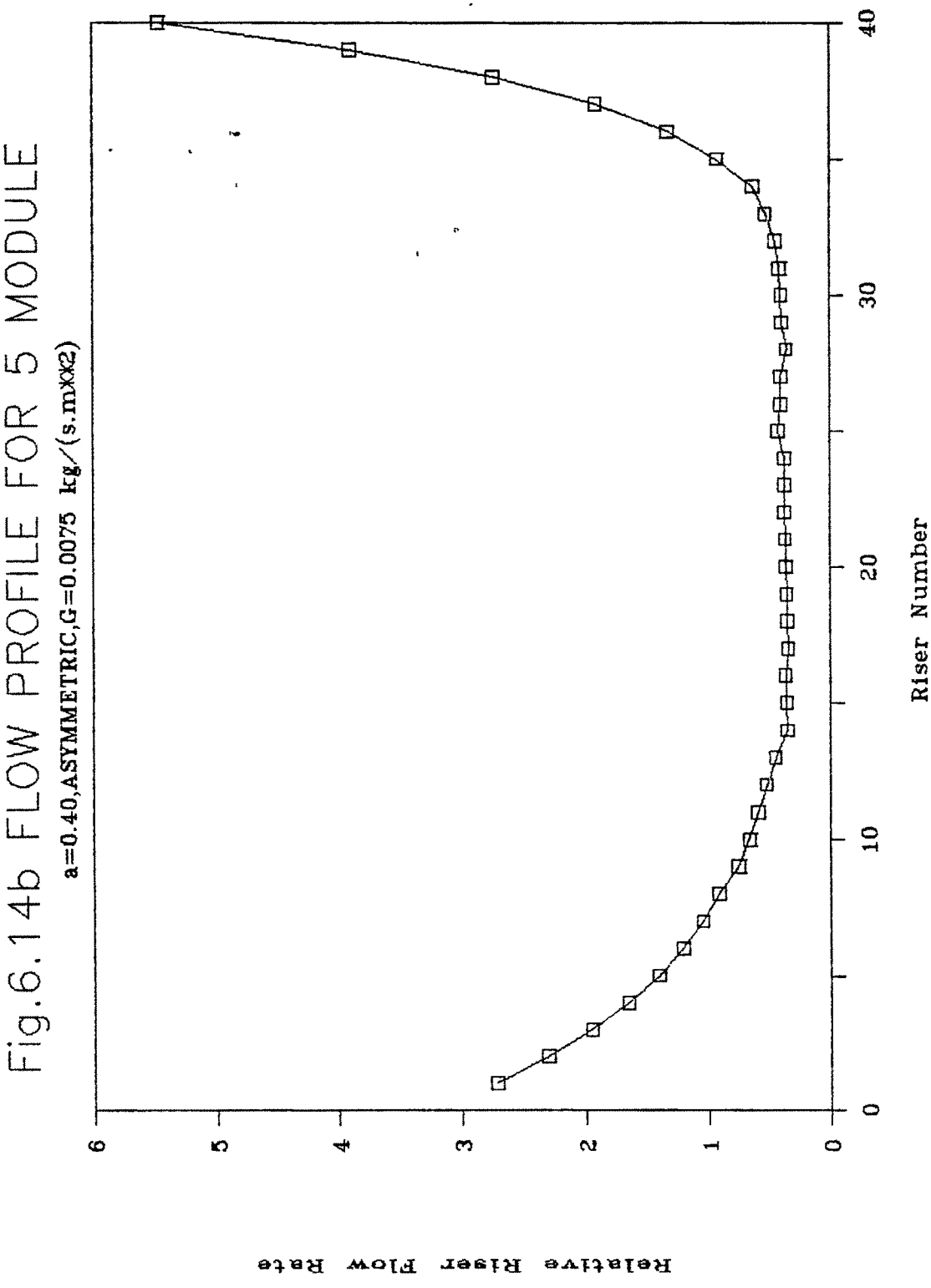
Fig.6.14b FLOW PROFILE FOR 5 MODULE
a=0.40,ASYMMETRIC,G=0.0075 kg/(s.mxx2)
Relative Riser Flow Rate
Riser Number
0
1
2
3
4
5
6
0
10
20
30
40

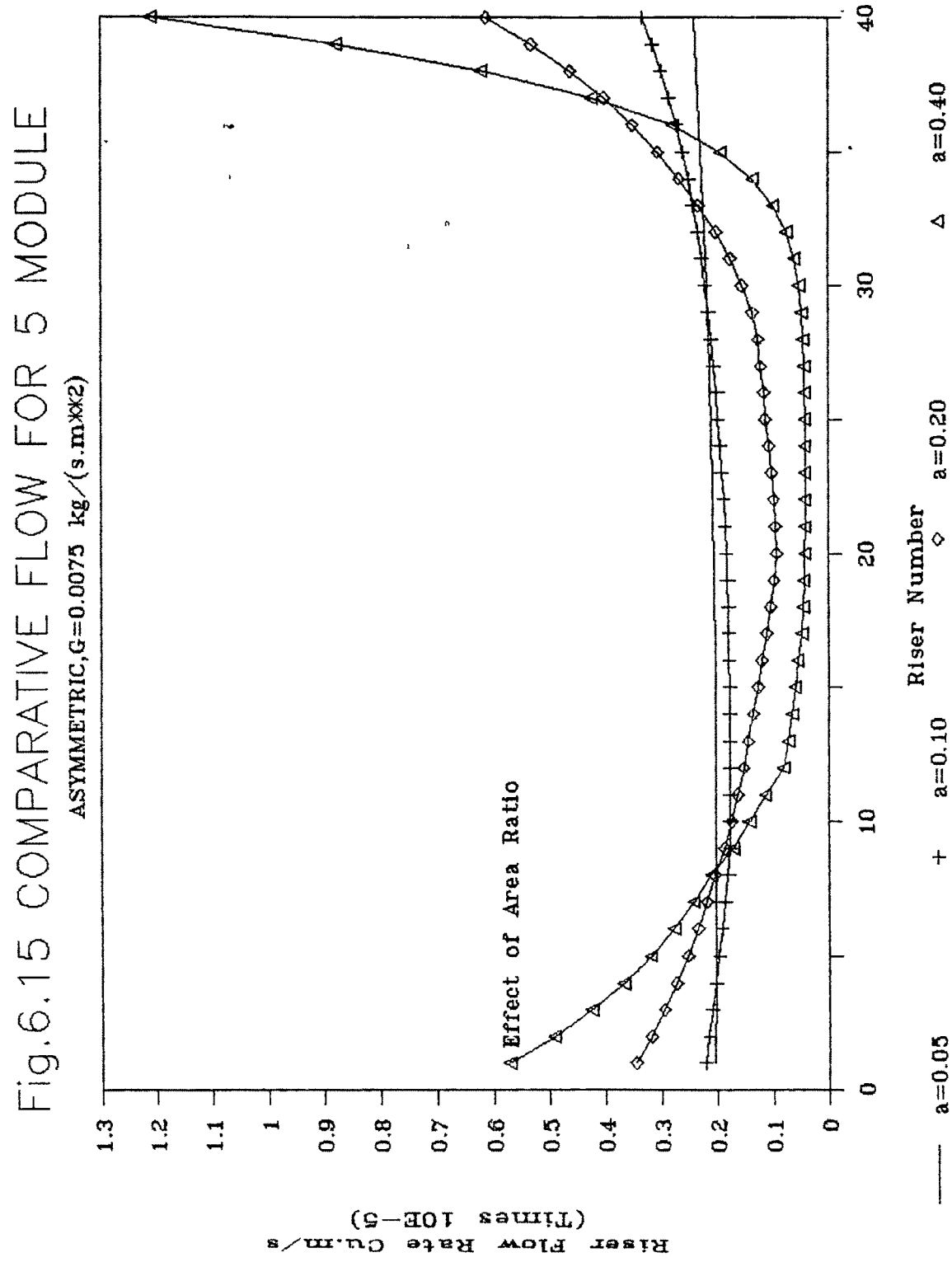
Fig.6.15 COMPARATIVE FLOW FOR 5 MODULE
ASYMMETRIC,G=0.0075 kg/(s.m**2)
Riser Flow Rate Cu.m/s
(Times 10E-5)
1.3
1.2
1.1
1
0.9
0.8
0.7
0.6
0.5
0.4
0.3
0.2
0.1
0
Effect of Area Ratio
0
10
20
30
40
Riser Number
a=0.05
a=0.10
a=0.20
a=0.40

Fig.6.15a FLOW PROFILE FOR 5 MODULES

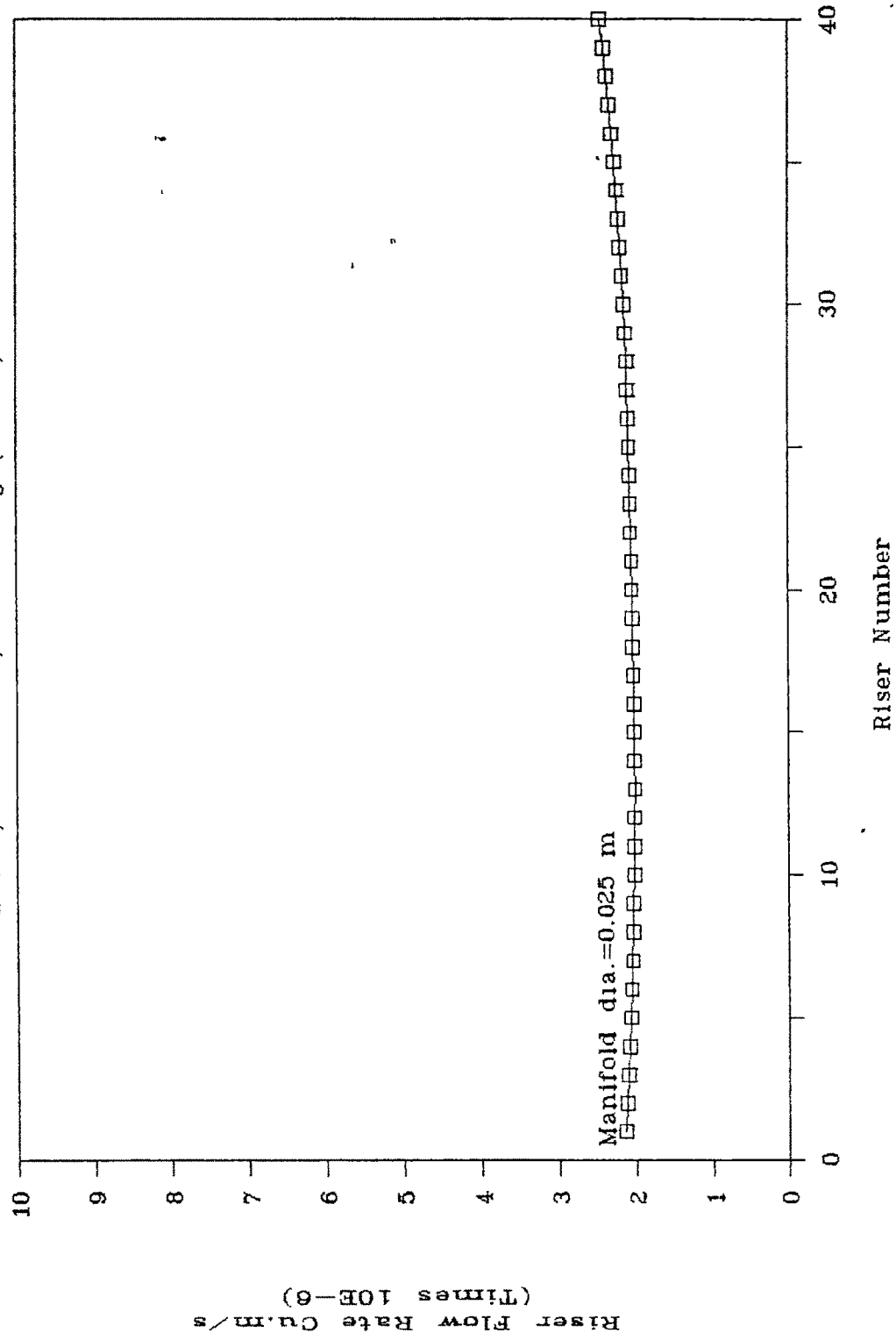

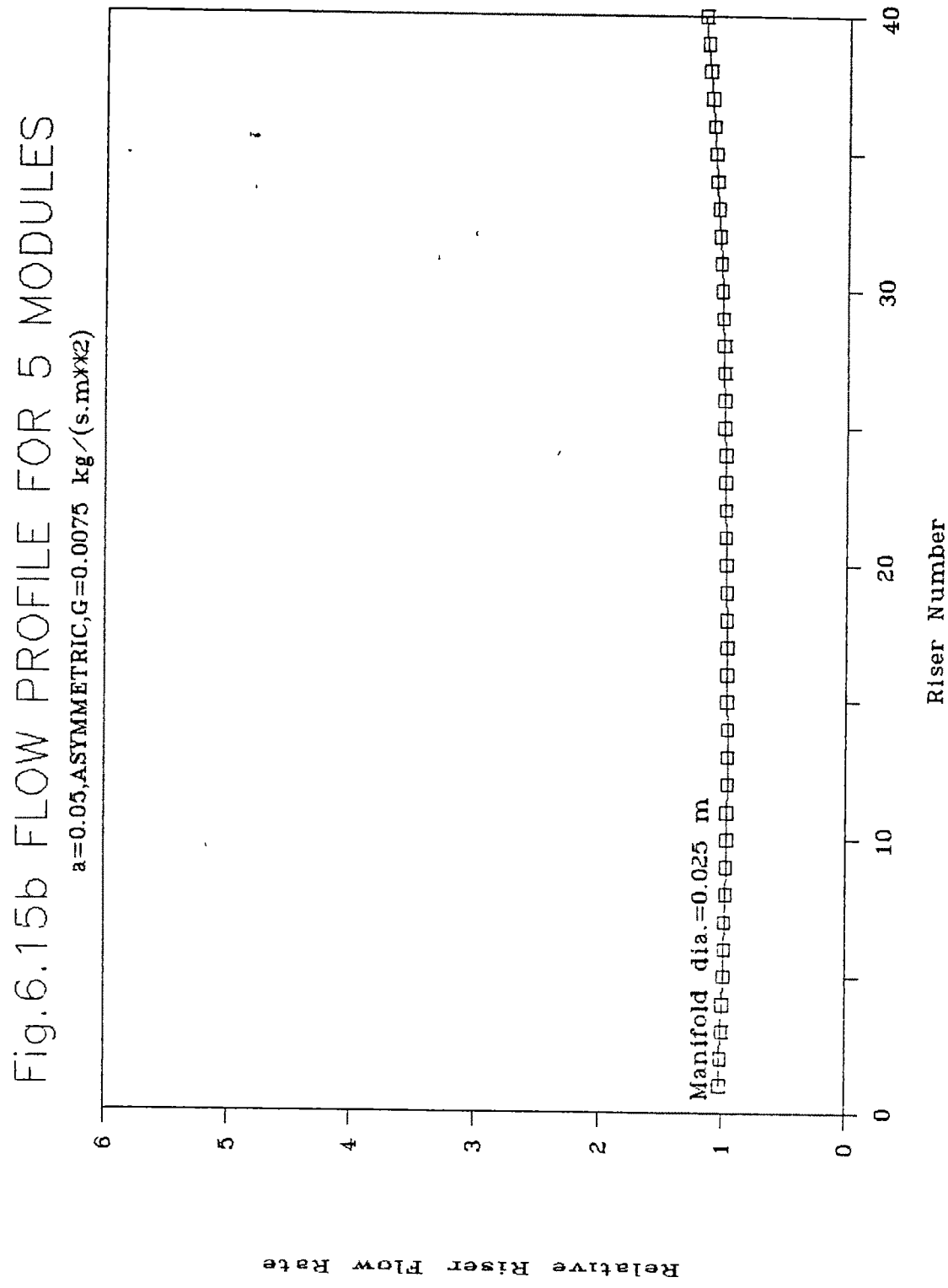
Fig.6.15b FLOW PROFILE FOR 5 MODULES
a=0.05,ASYMMETRIC,G=0.0075 kg/(s.m**2)
Manifold dia.=0.025 m
Relative Riser Flow Rate
Riser Number
0
1
2
3
4
5
6
0
10
20
30
40

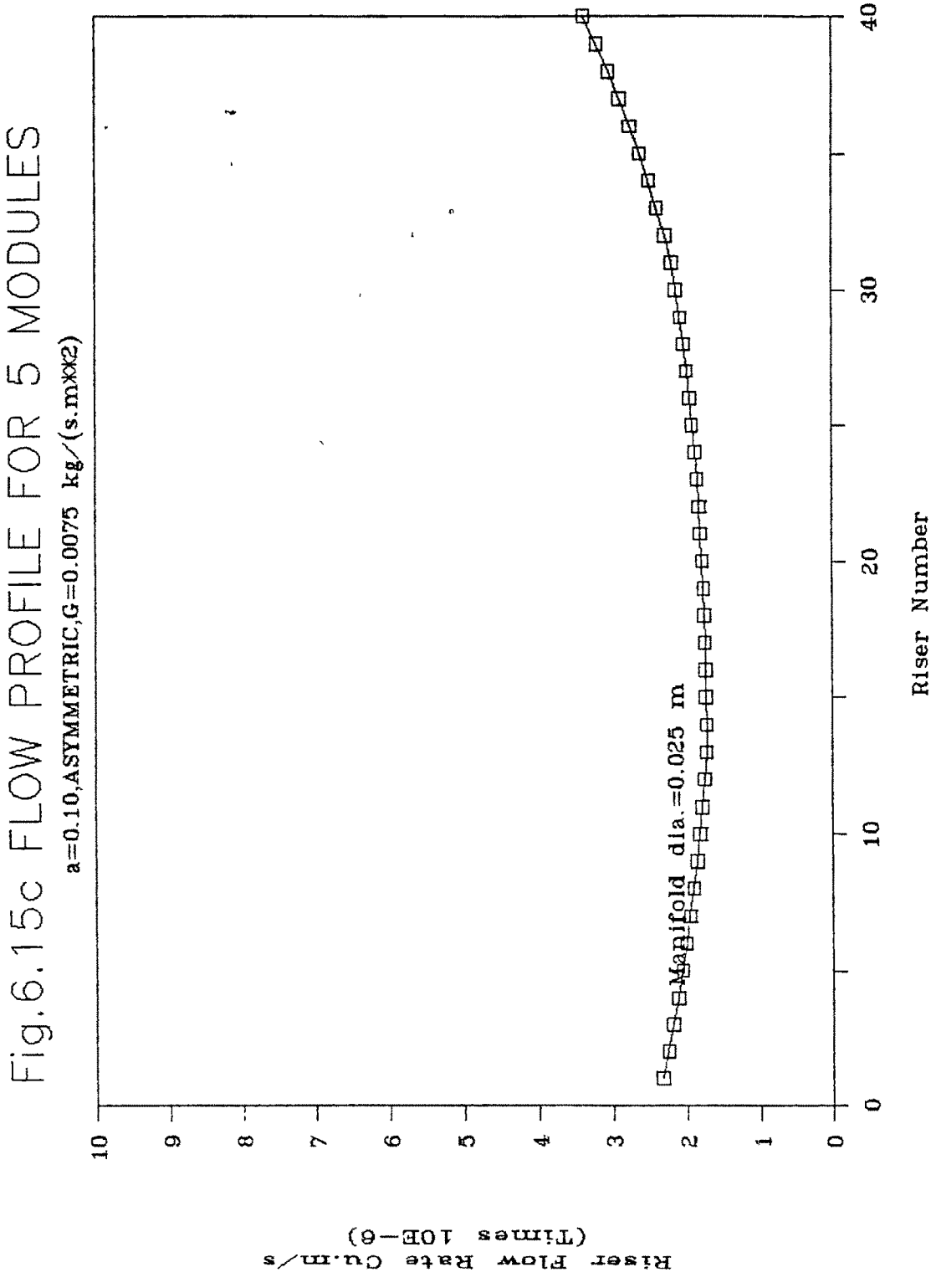
Fig.6.15c FLOW PROFILE FOR 5 MODULES
a=0.10,ASYMMETRIC,G=0.0075 kg/(s.m**2)
Riser Flow Rate Cu.m/s
(Times 10E-6)
Riser Number
Manifold dia.=0.025 m
0
1
2
3
4
5
6
7
8
9
10
0
10
20
30
40

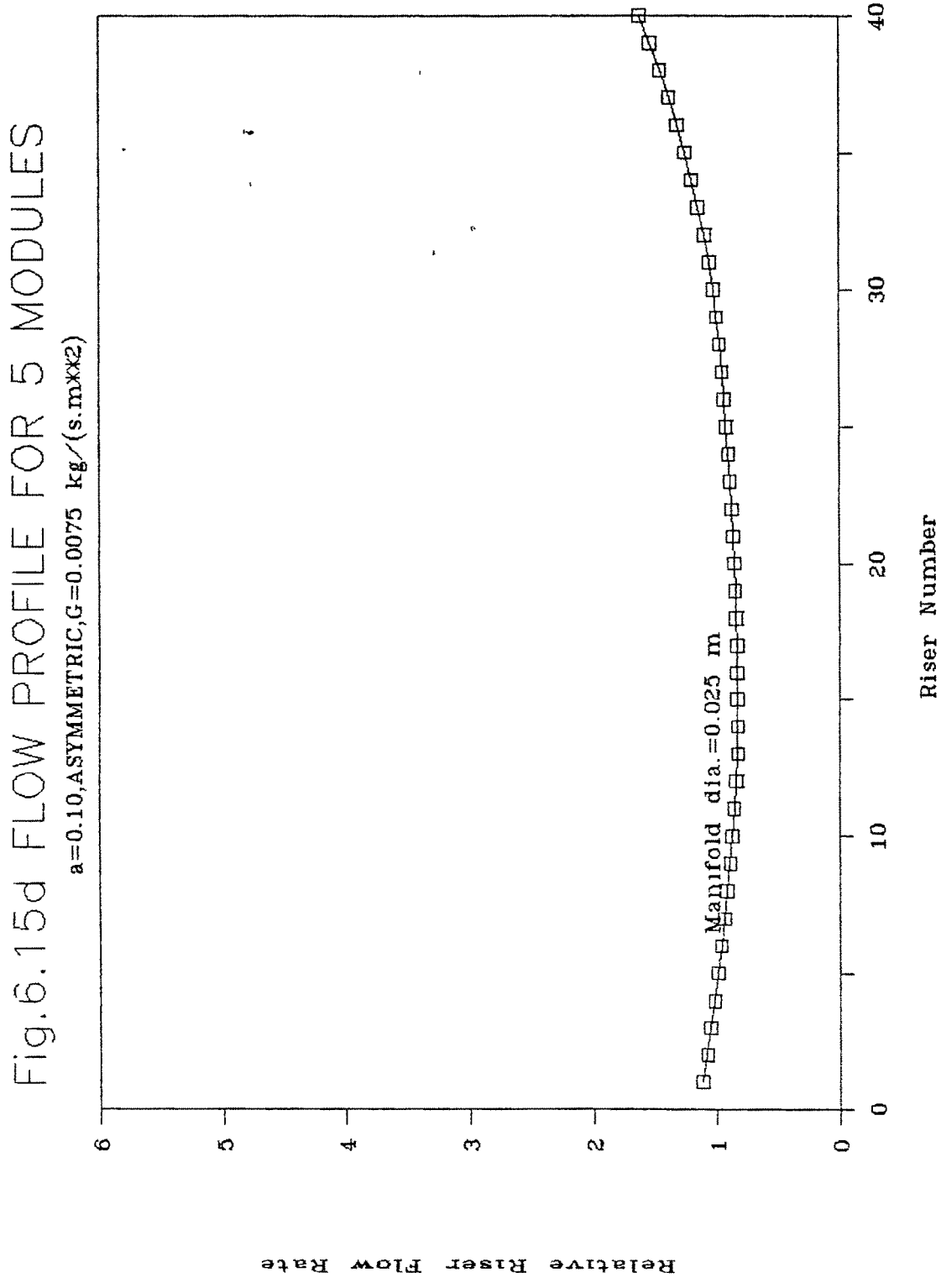
Fig.6.15d FLOW PROFILE FOR 5 MODULES
a=0.10,ASYMMETRIC,G=0.0075 kg/(s.mxx2)
Relative Riser Flow Rate
Riser Number
Manifold dia.=0.025 m
0
1
2
3
4
5
6
0
10
20
30
40

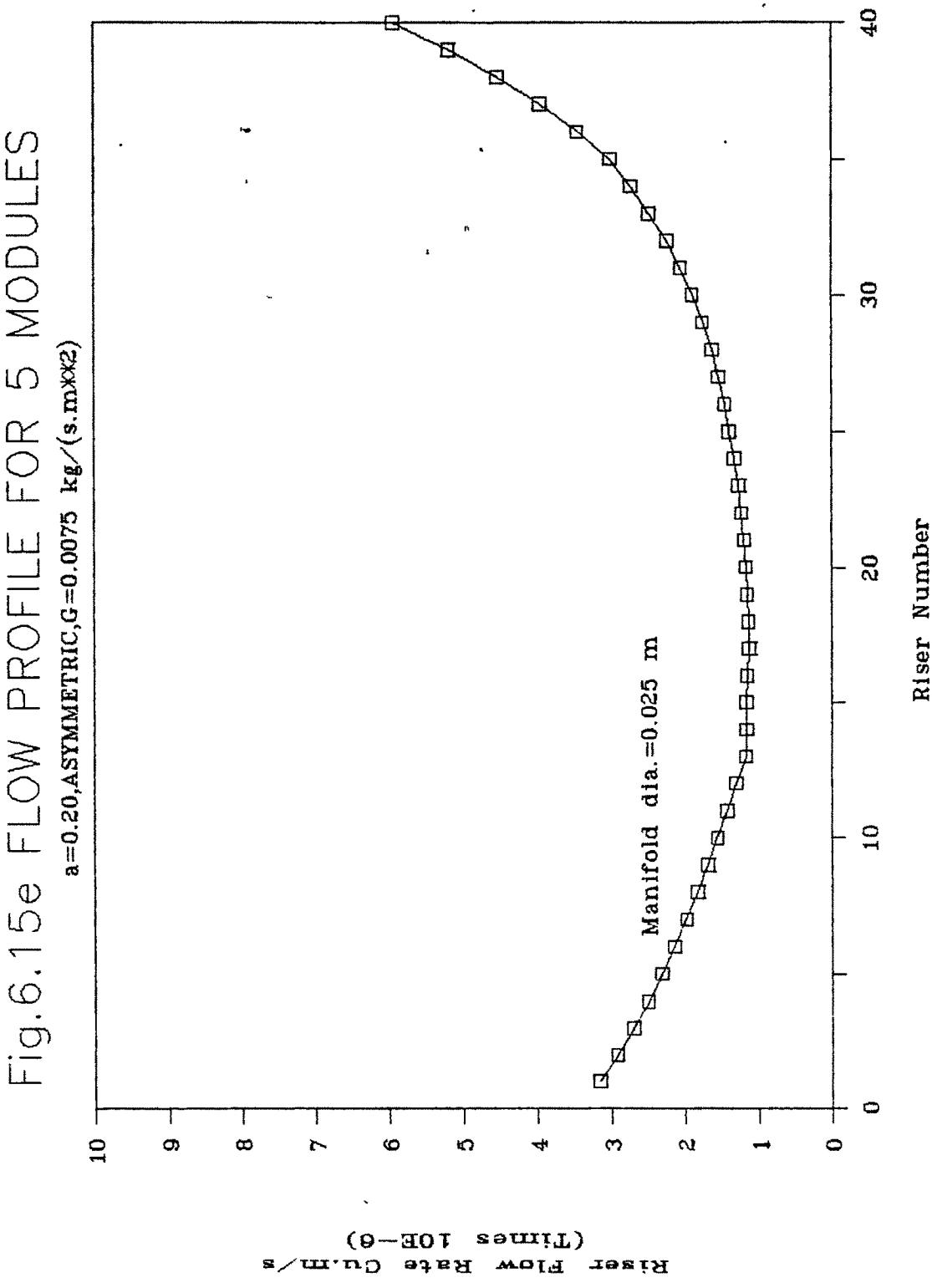
Fig.6.15e FLOW PROFILE FOR 5 MODULES
a=0.20,ASYMMETRIC,G=0.0075 kg/(s.m**2)
Manifold dia.=0.025 m
Riser Flow Rate Cu.m/s
(Times 10E-6)
Riser Number
0
1
2
3
4
5
6
7
8
9
10
0
10
20
30
40

Fig.6.15f FLOW PROFILE FOR 5 MODULES

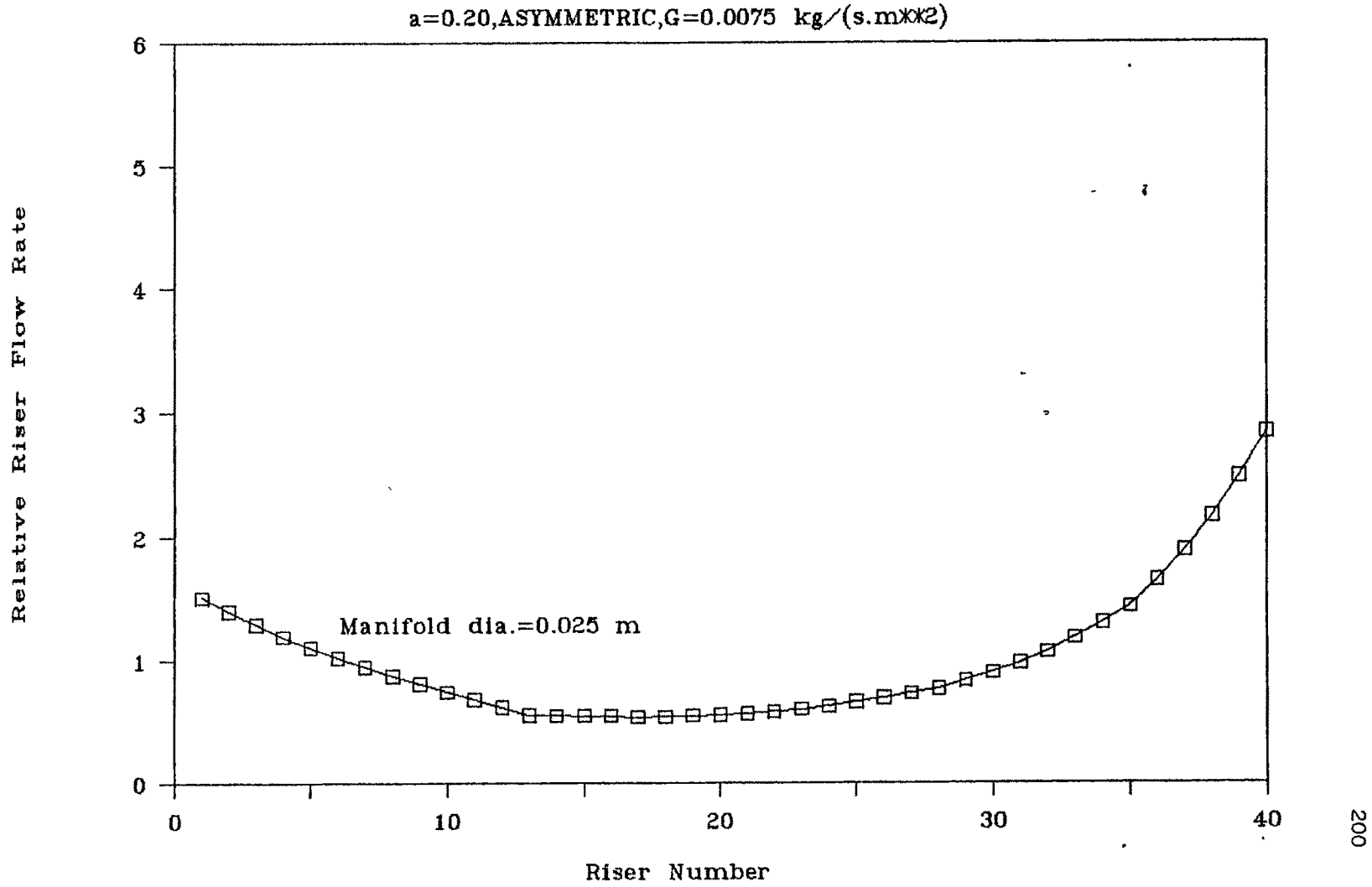

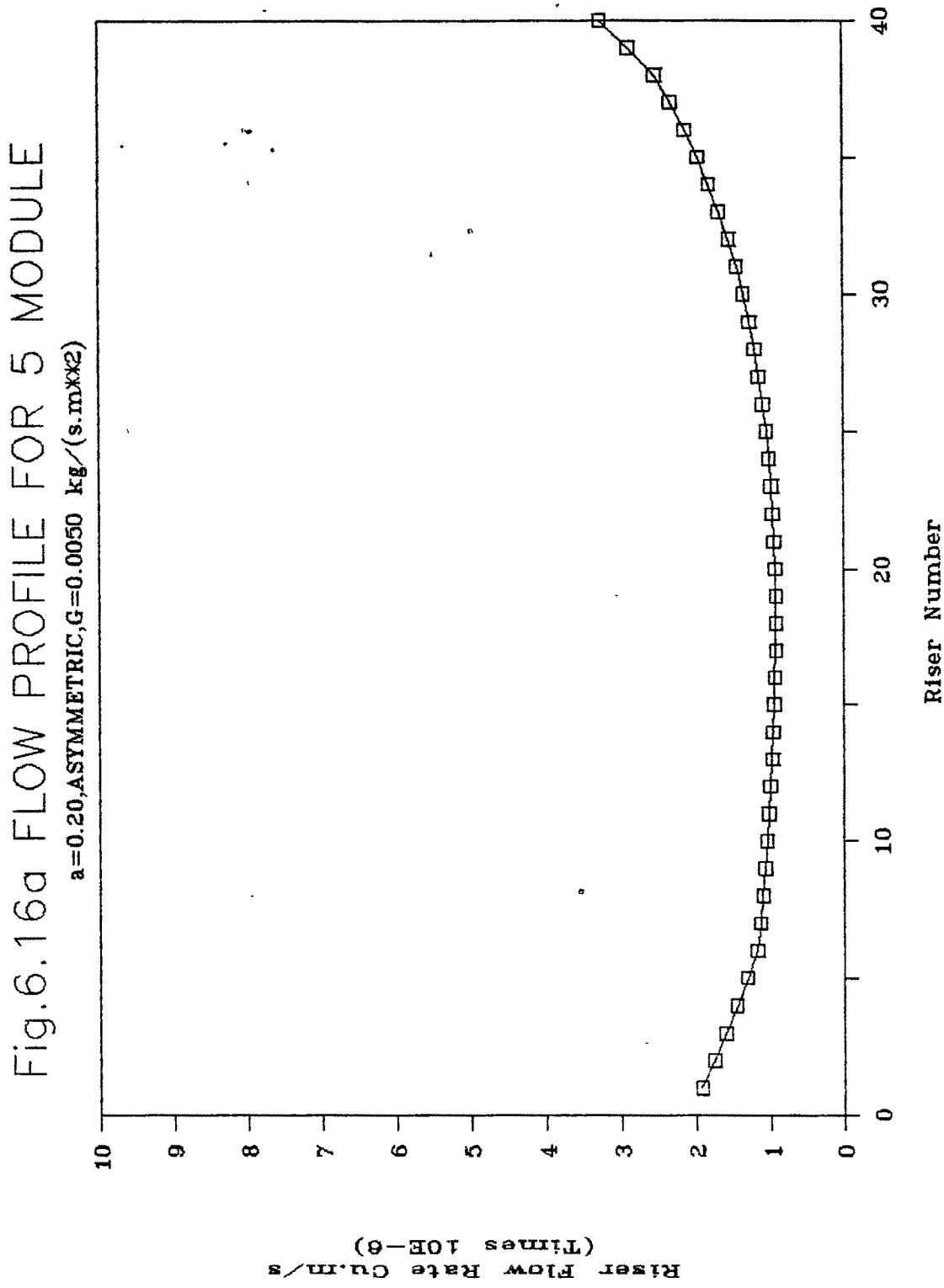
Fig.6.16a FLOW PROFILE FOR 5 MODULE
a=0.20,ASYMMETRIC,G=0.0050 kg/(s.m**2)
Riser Flow Rate Cu.m/s
(Times 10E-6)
0
1
2
3
4
5
6
7
8
9
10
0
10
20
30
40
Riser Number

Fig.6.16b FLOW PROFILE FOR 5 MODULE

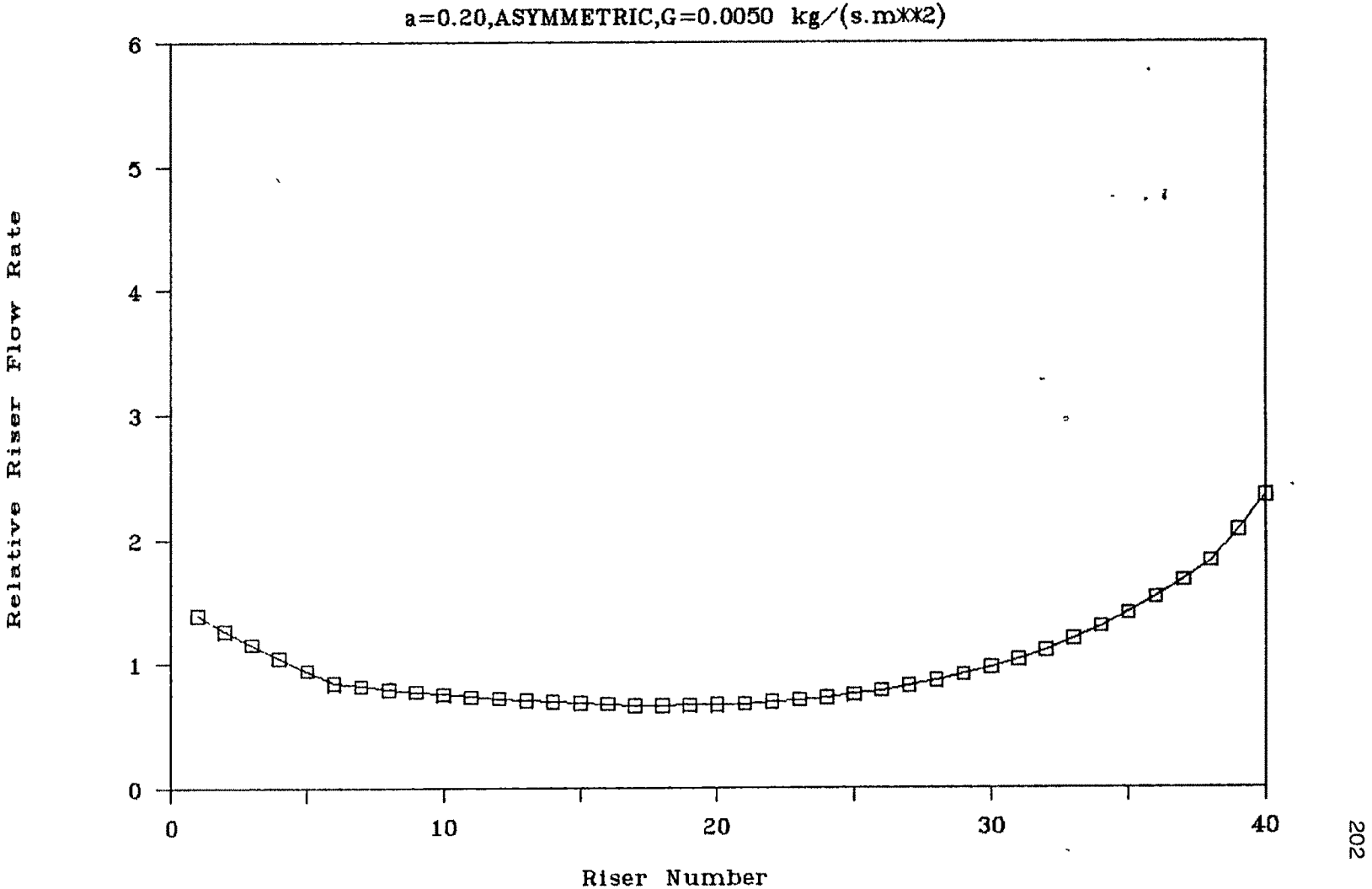

Fig.6.16c PRESSURE PROFILE FOR 5 MODULE

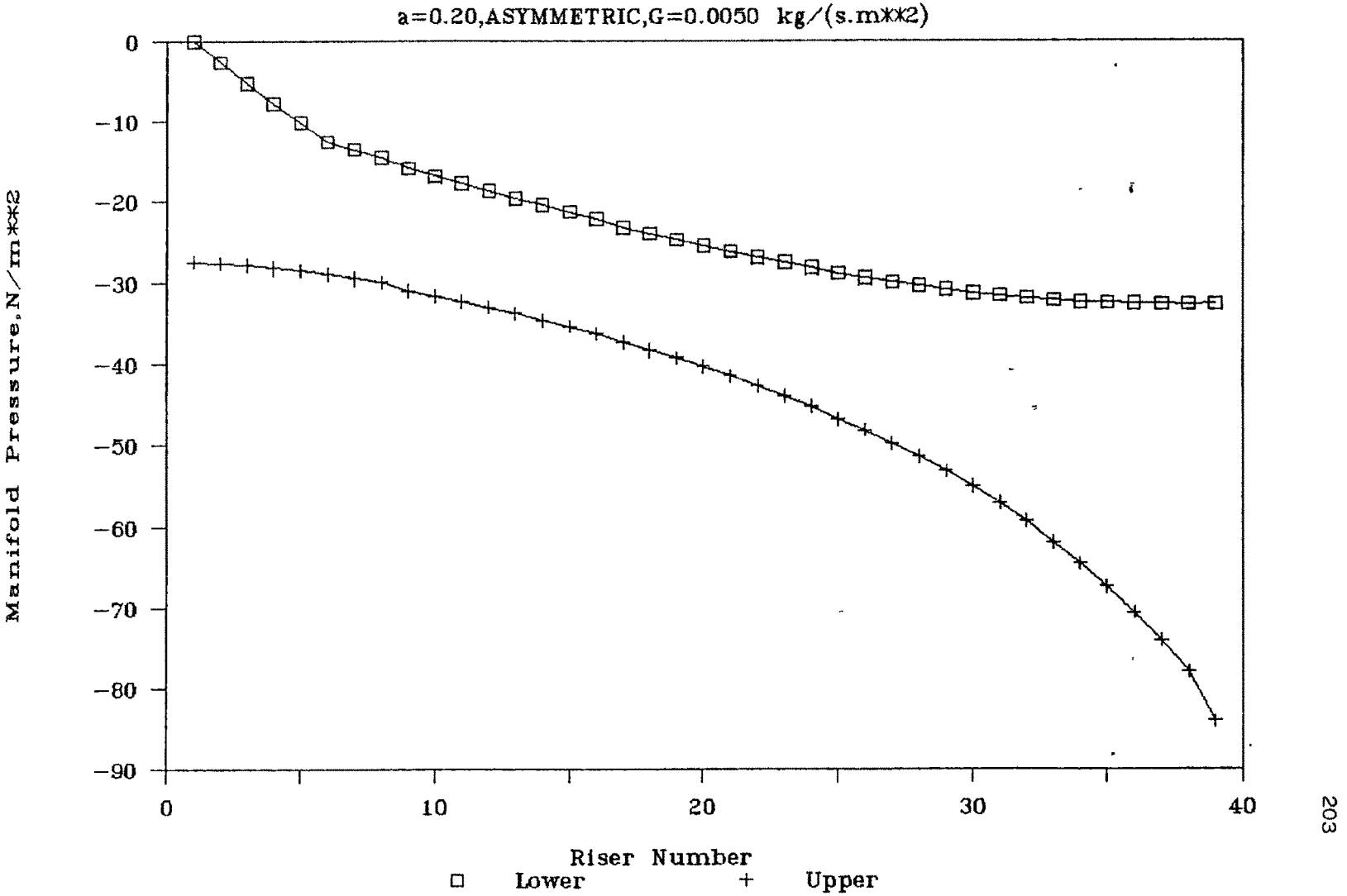

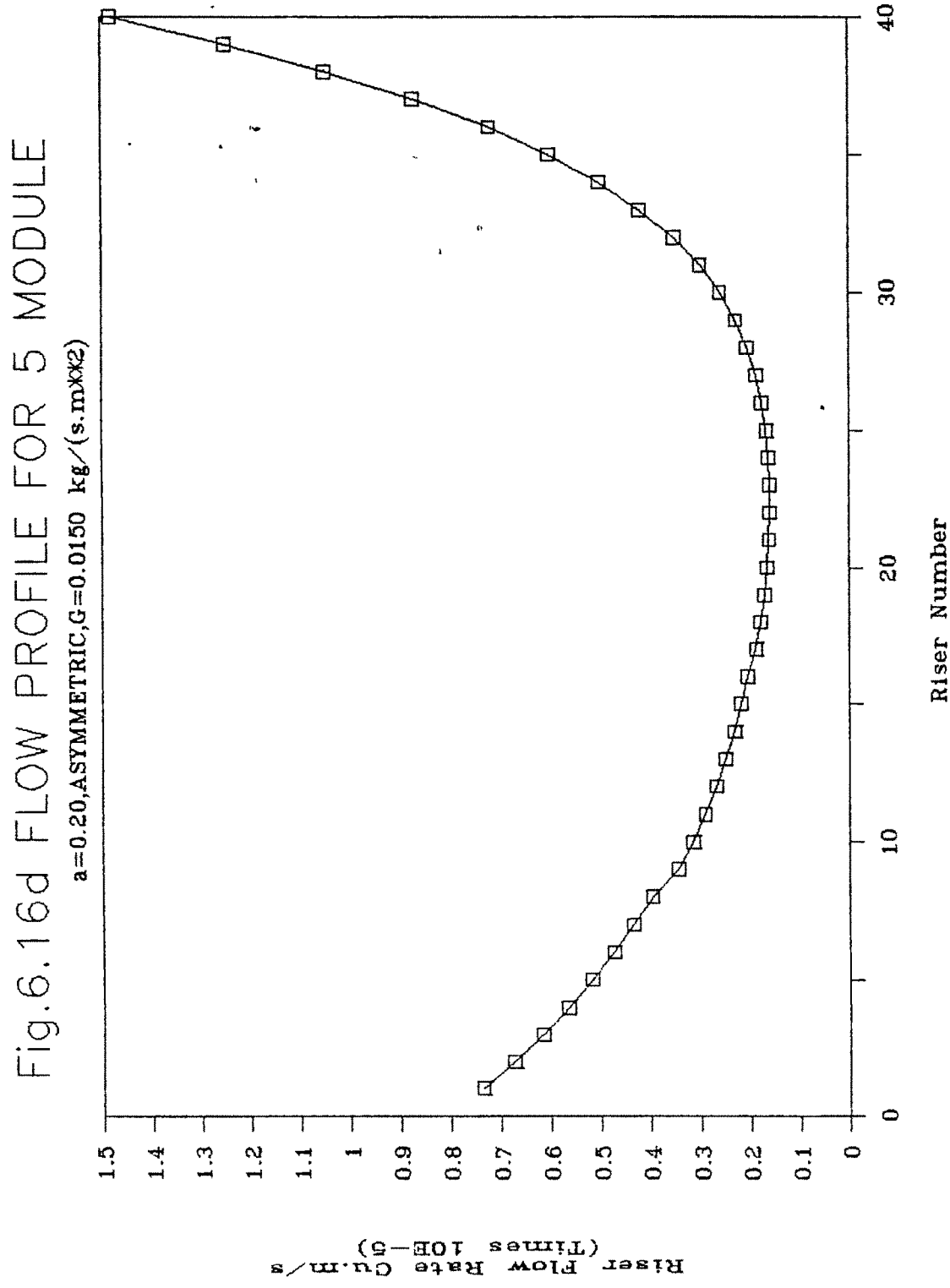
Fig.6.16d FLOW PROFILE FOR 5 MODULE
a=0.20,ASYMMETRIC,G=0.0150 kg/(s.mxx2)
Riser Flow Rate Cu.m/s
(Times 10E-5)
1.5
1.4
1.3
1.2
1.1
1
0.9
0.8
0.7
0.6
0.5
0.4
0.3
0.2
0.1
0
0
10
20
30
40
Riser Number

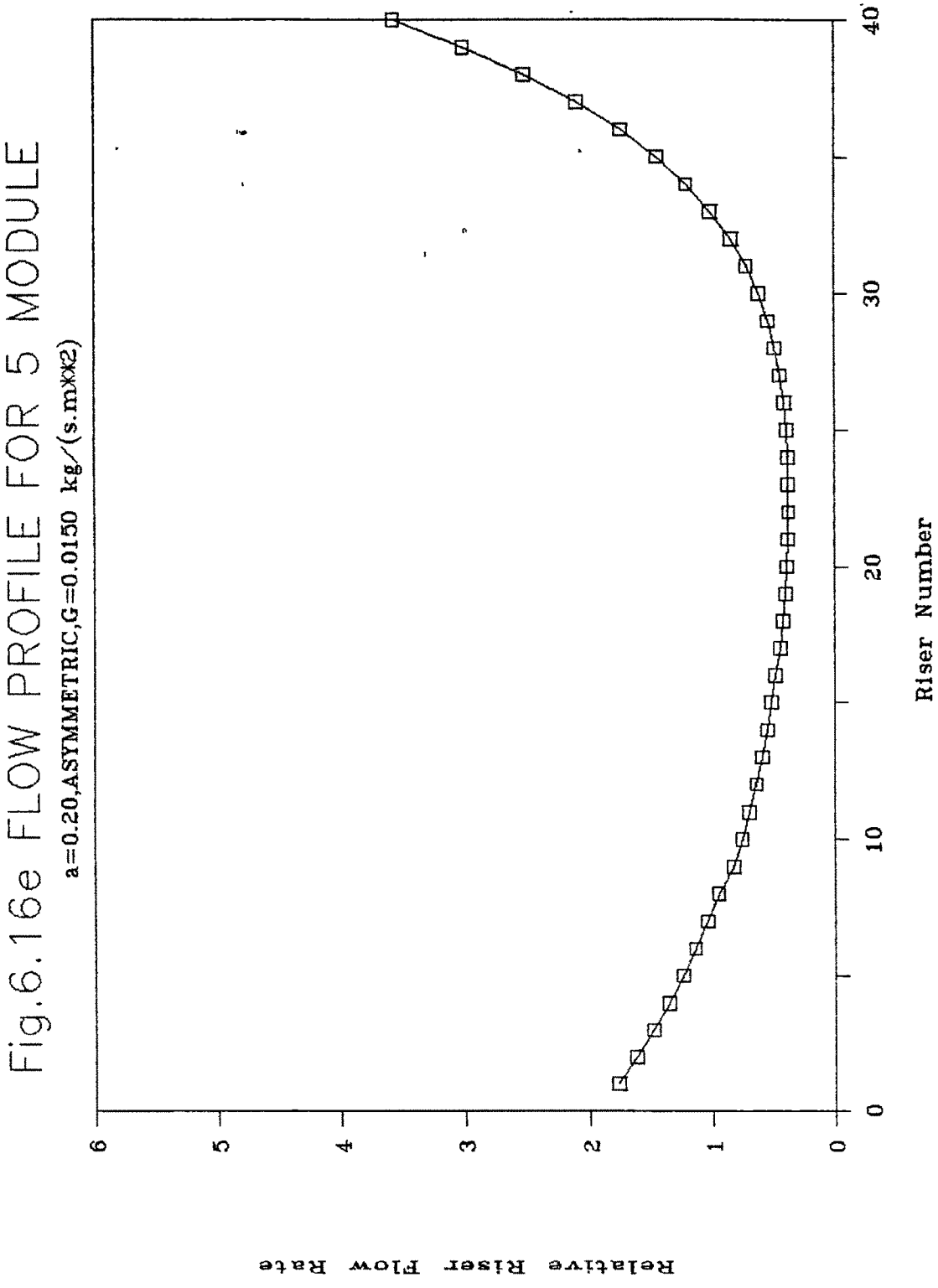
Fig.6.16e FLOW PROFILE FOR 5 MODULE
a=0.20,ASYMMETRIC,G=0.0150 kg/(s.m**2)
Relative Riser Flow Rate
Riser Number
0
1
2
3
4
5
6
0
10
20
30
40

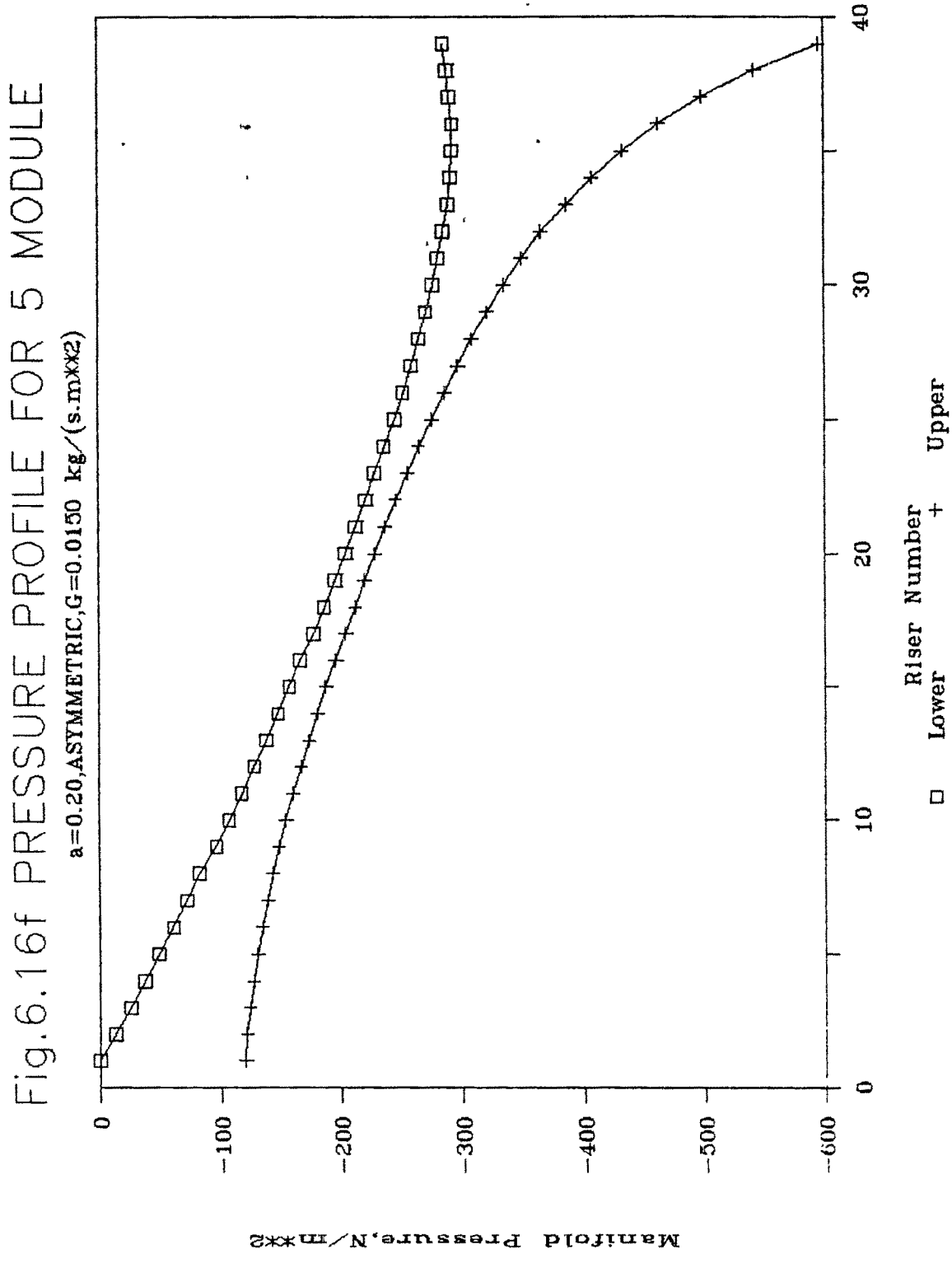
Fig.6.16f PRESSURE PROFILE FOR 5 MODULE
a=0.20,ASYMMETRIC,G=0.0150 kg/(s.m**2)
Manifold Pressure,N/m**2
0
-100
-200
-300
-400
-500
-600
0
10
20
30
40
Riser Number
□ Lower + Upper

Fig.6.16g COMPARATIVE FLOW FOR 5 MODULE

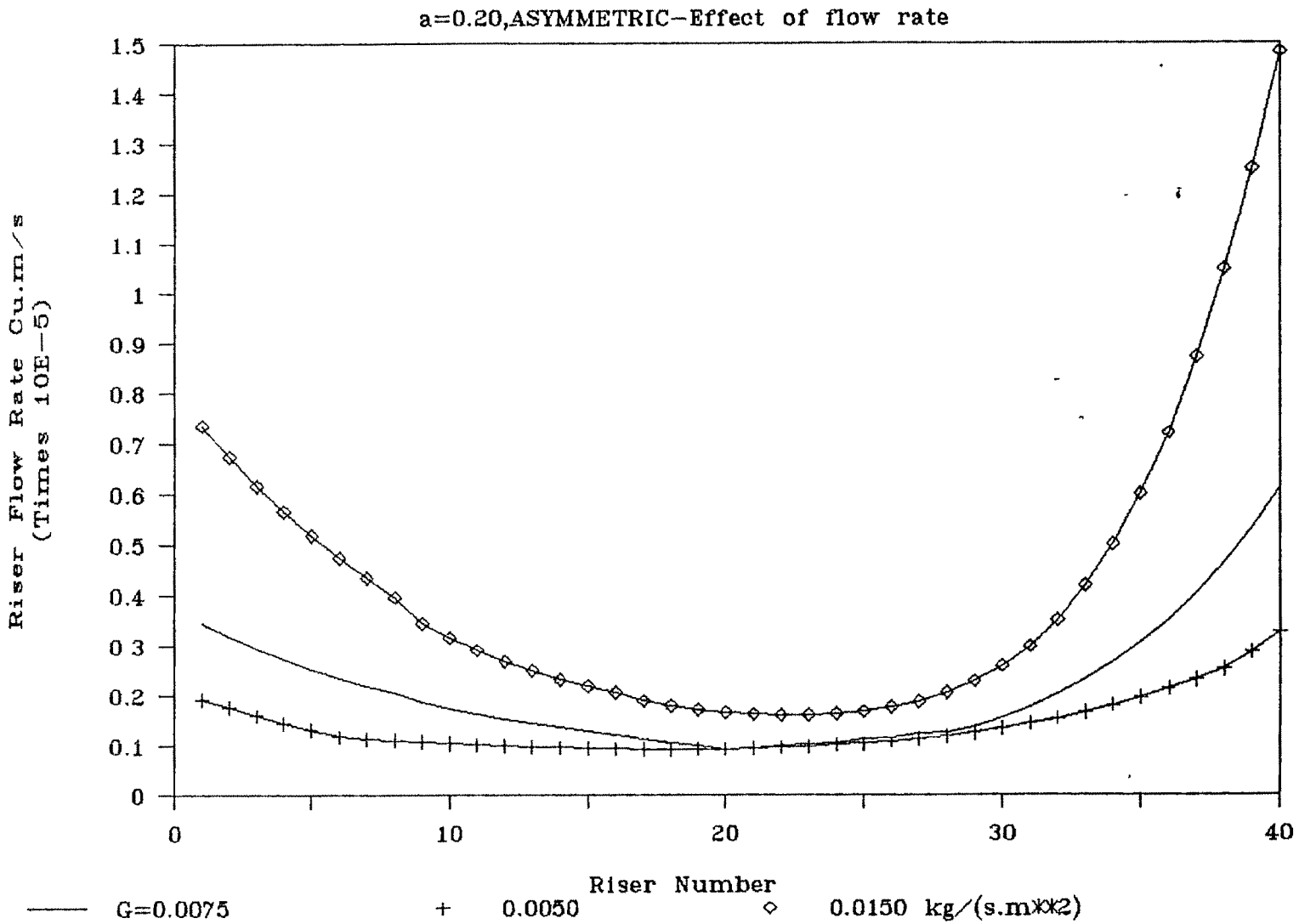

Fig.6.17a PRESSURE PROFILE FOR 5 MODULE

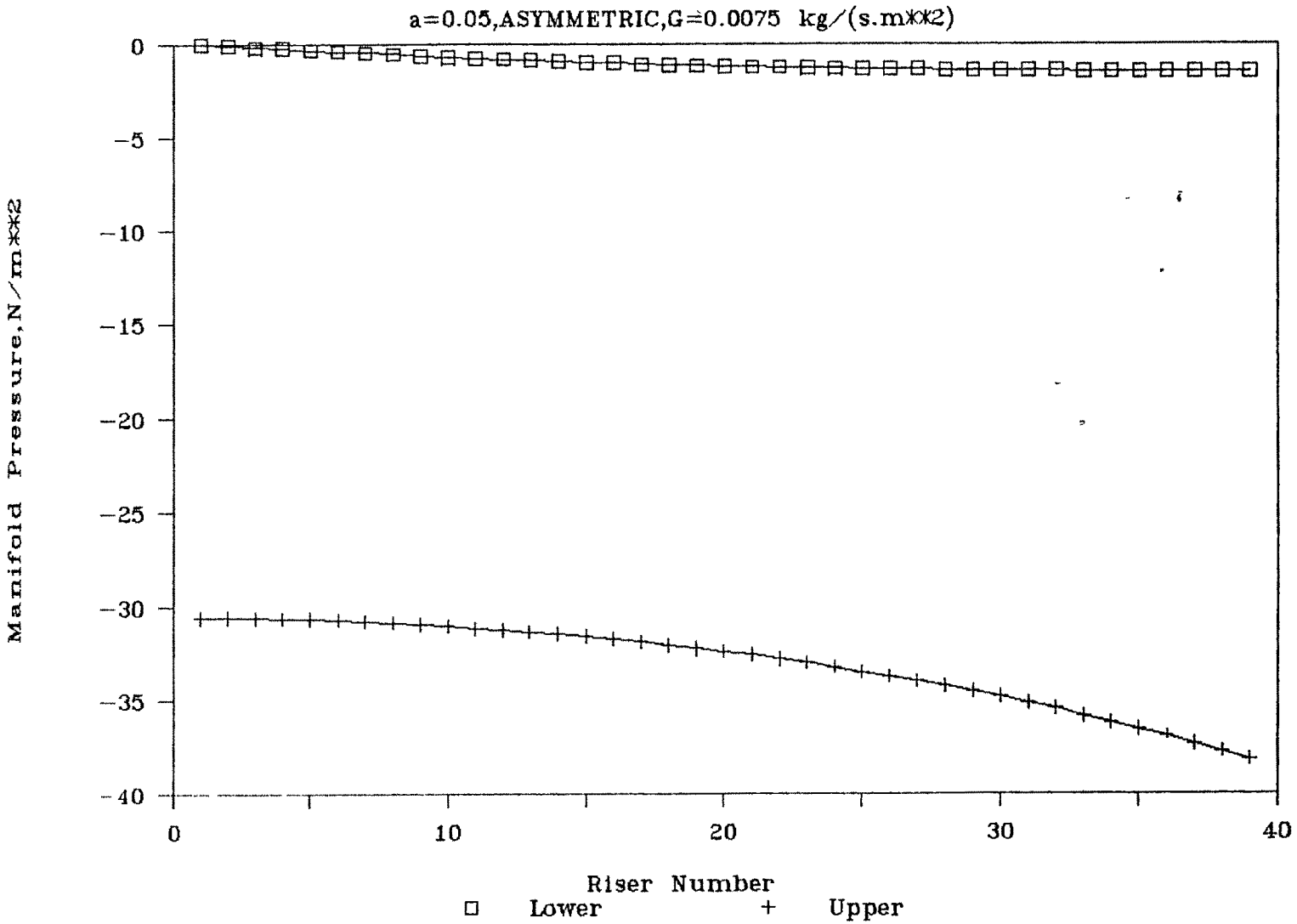

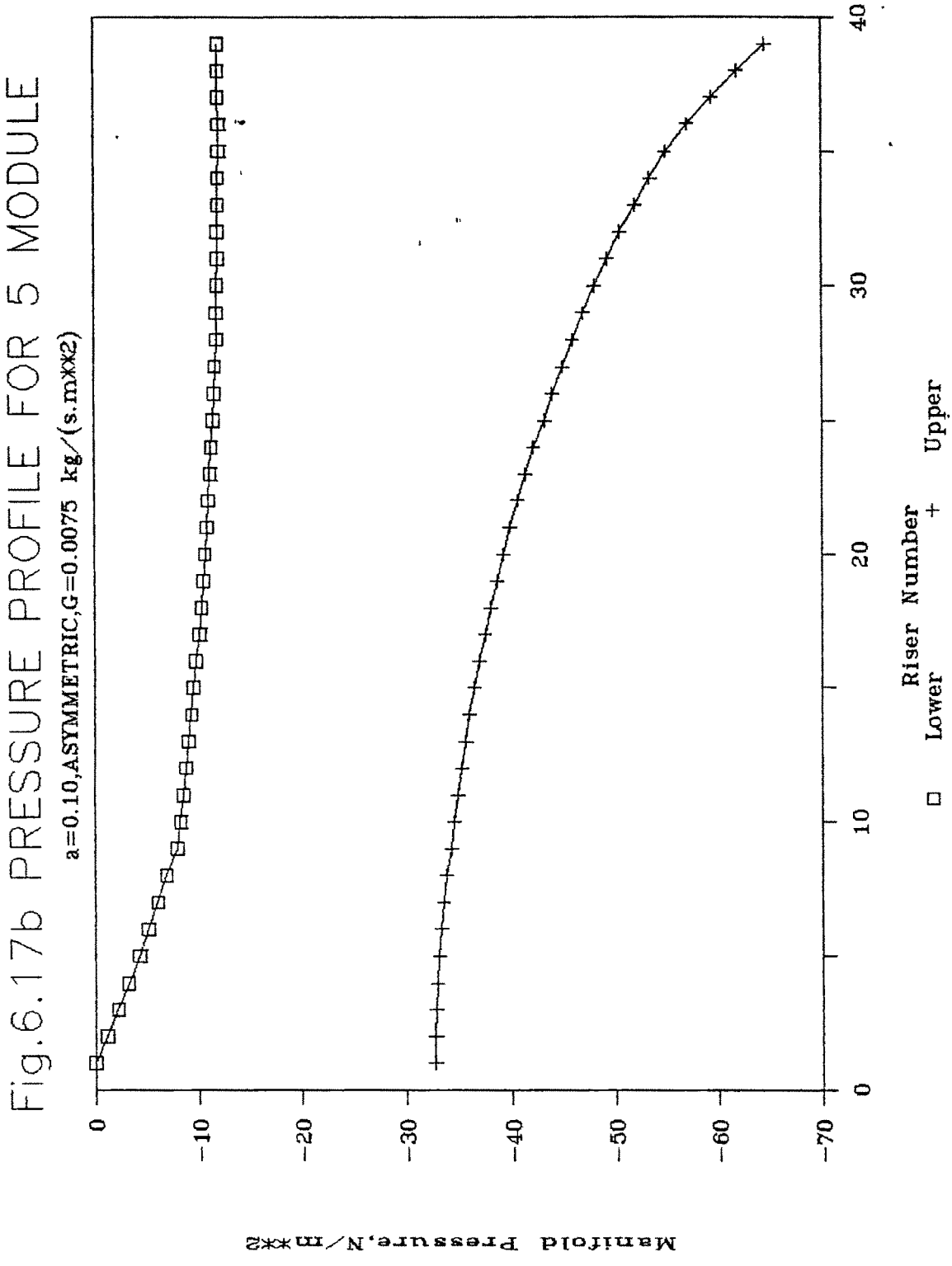
Fig.6.17b PRESSURE PROFILE FOR 5 MODULE
a=0.10,ASYMMETRIC,G=0.0075 kg/(s.m**2)
Manifold Pressure,N/m**2
0
-10
-20
-30
-40
-50
-60
-70
0
10
20
30
40
Riser Number
□ Lower
+ Upper

Fig.6.17c PRESSURE PROFILE FOR 5 MODULE

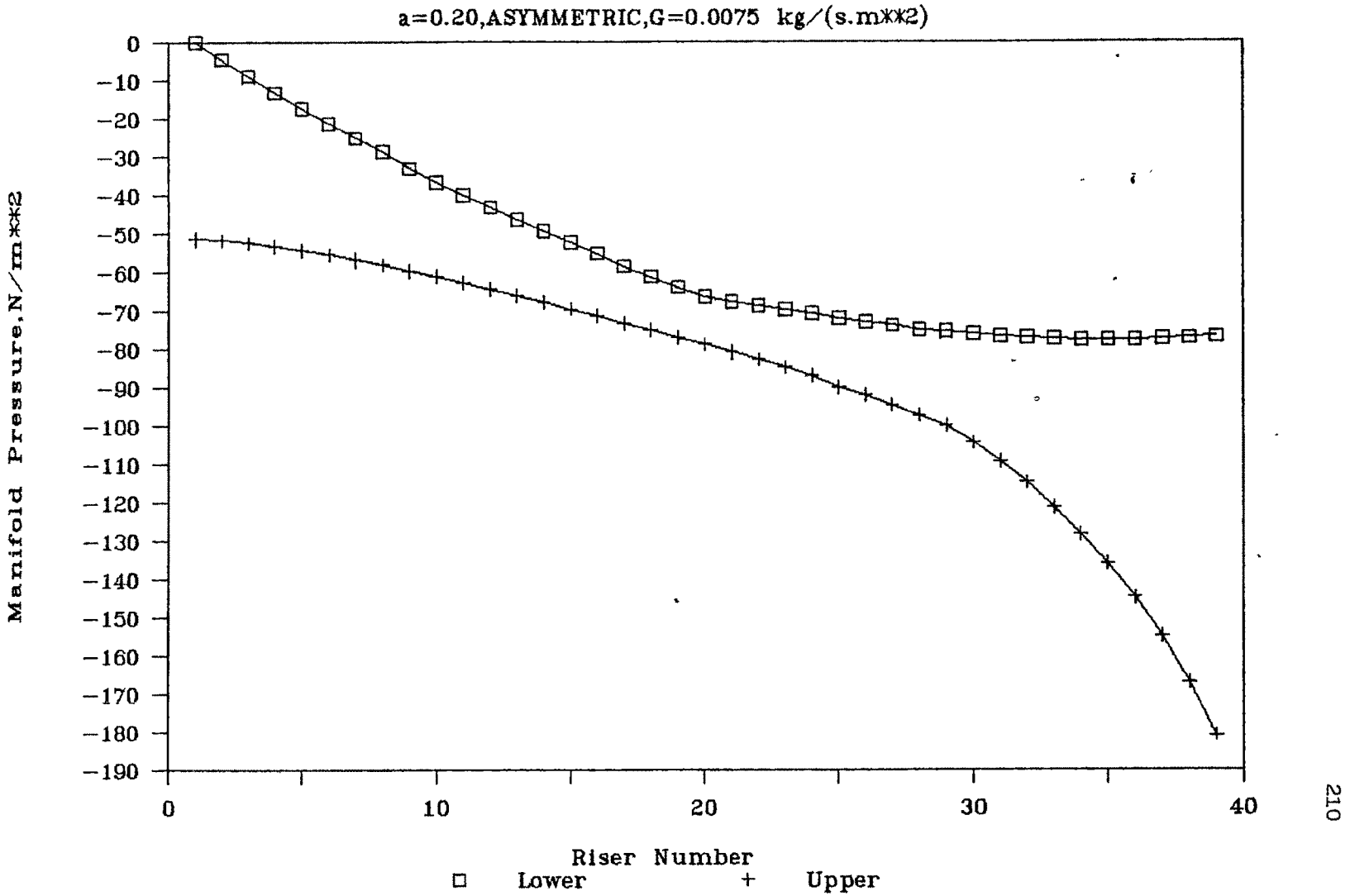

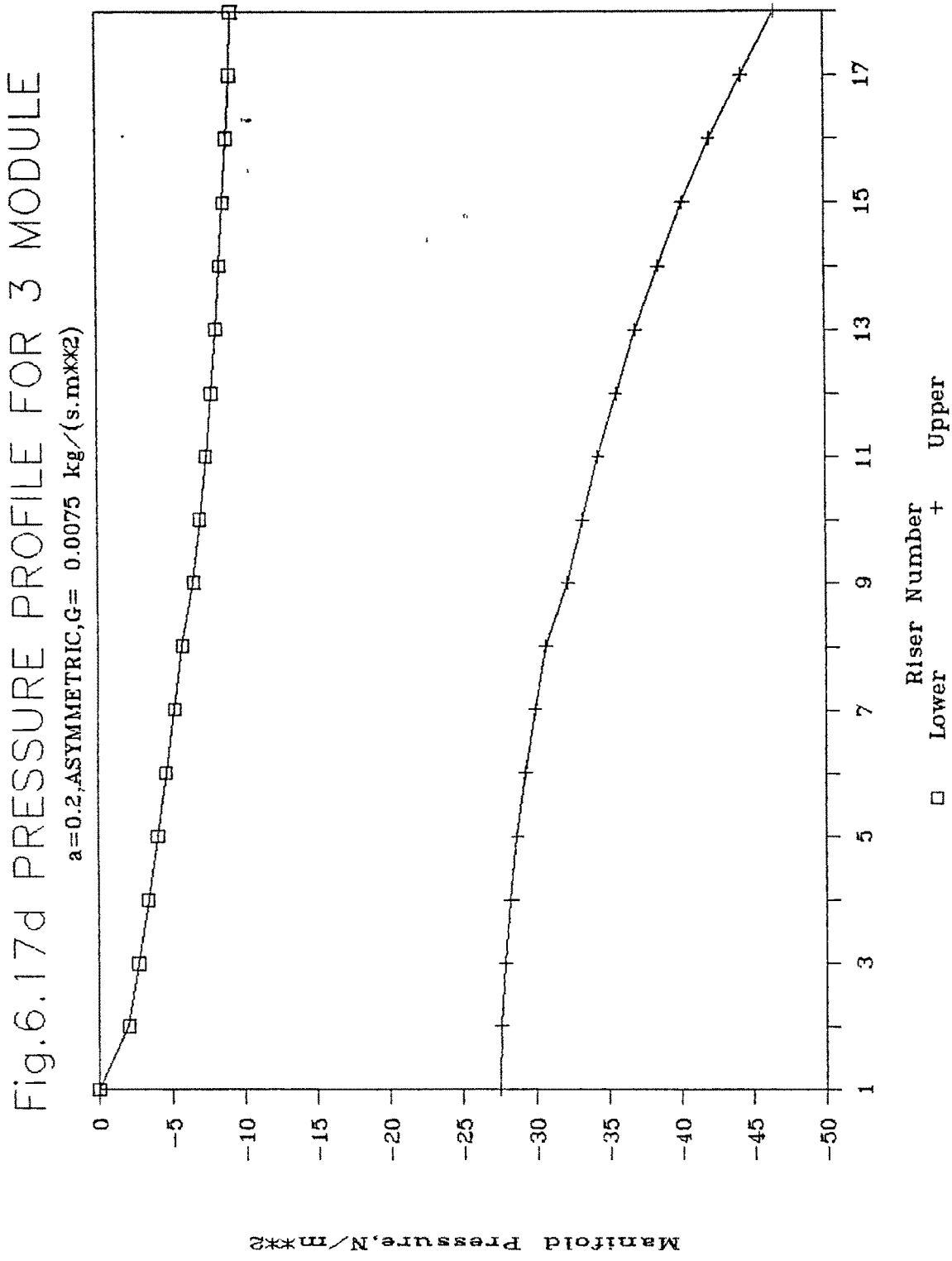
Fig.6.17d PRESSURE PROFILE FOR 3 MODULE
a=0.2,ASYMMETRIC,G= 0.0075 kg/(s.m**2)
Manifold Pressure,N/m**2
0
-5
-10
-15
-20
-25
-30
-35
-40
-45
-50
1
3
5
7
9
11
13
15
17
Riser Number
□ Lower
+ Upper

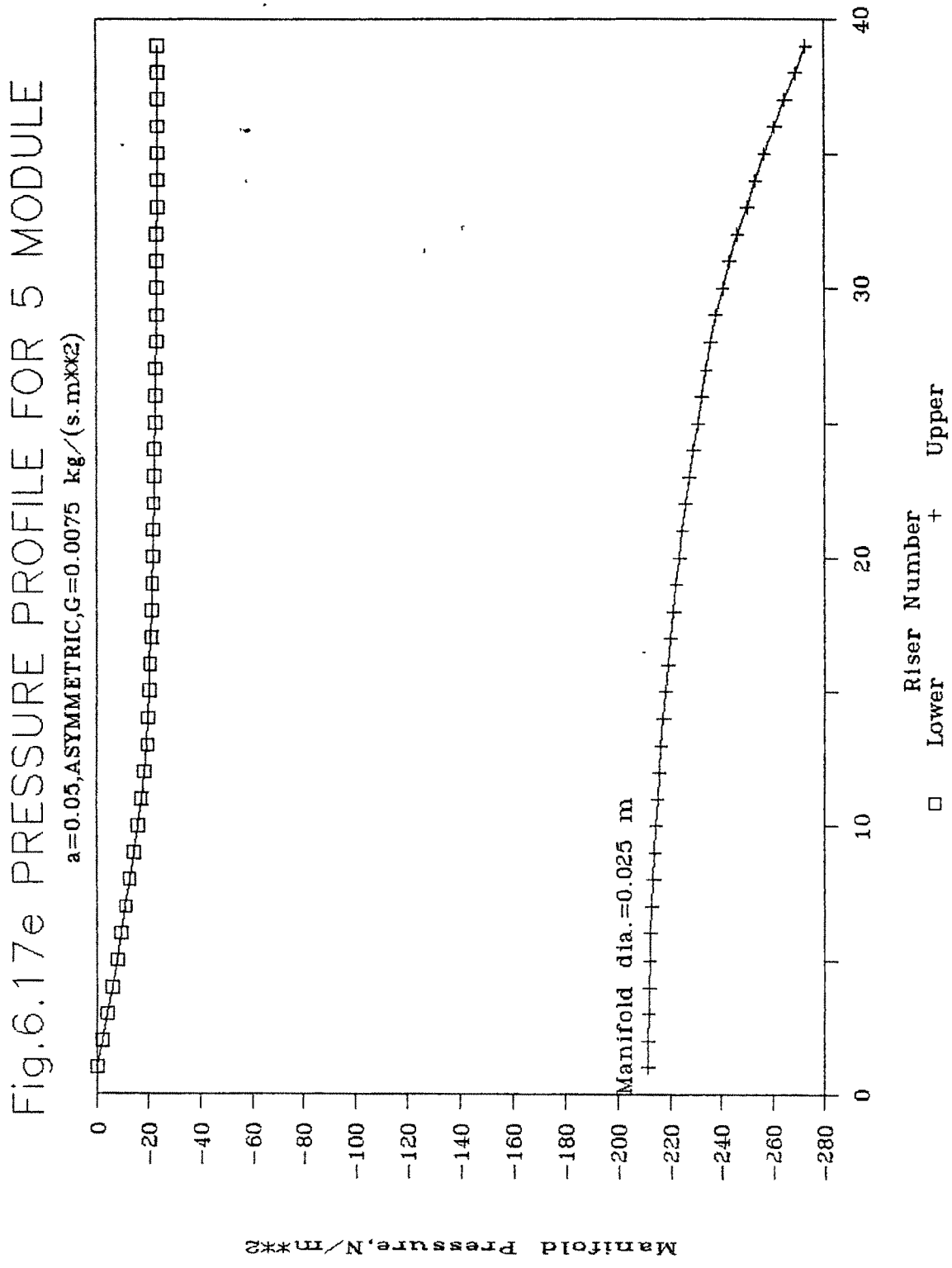
Fig.6.17e PRESSURE PROFILE FOR 5 MODULE
a=0.05,ASYMMETRIC,G=0.0075 kg/(s.m**2)
Manifold dia.=0.025 m
Manifold Pressure,N/m**2
0
-20
-40
-60
-80
-100
-120
-140
-160
-180
-200
-220
-240
-260
-280
0
10
20
30
40
Riser Number
Lower
Upper

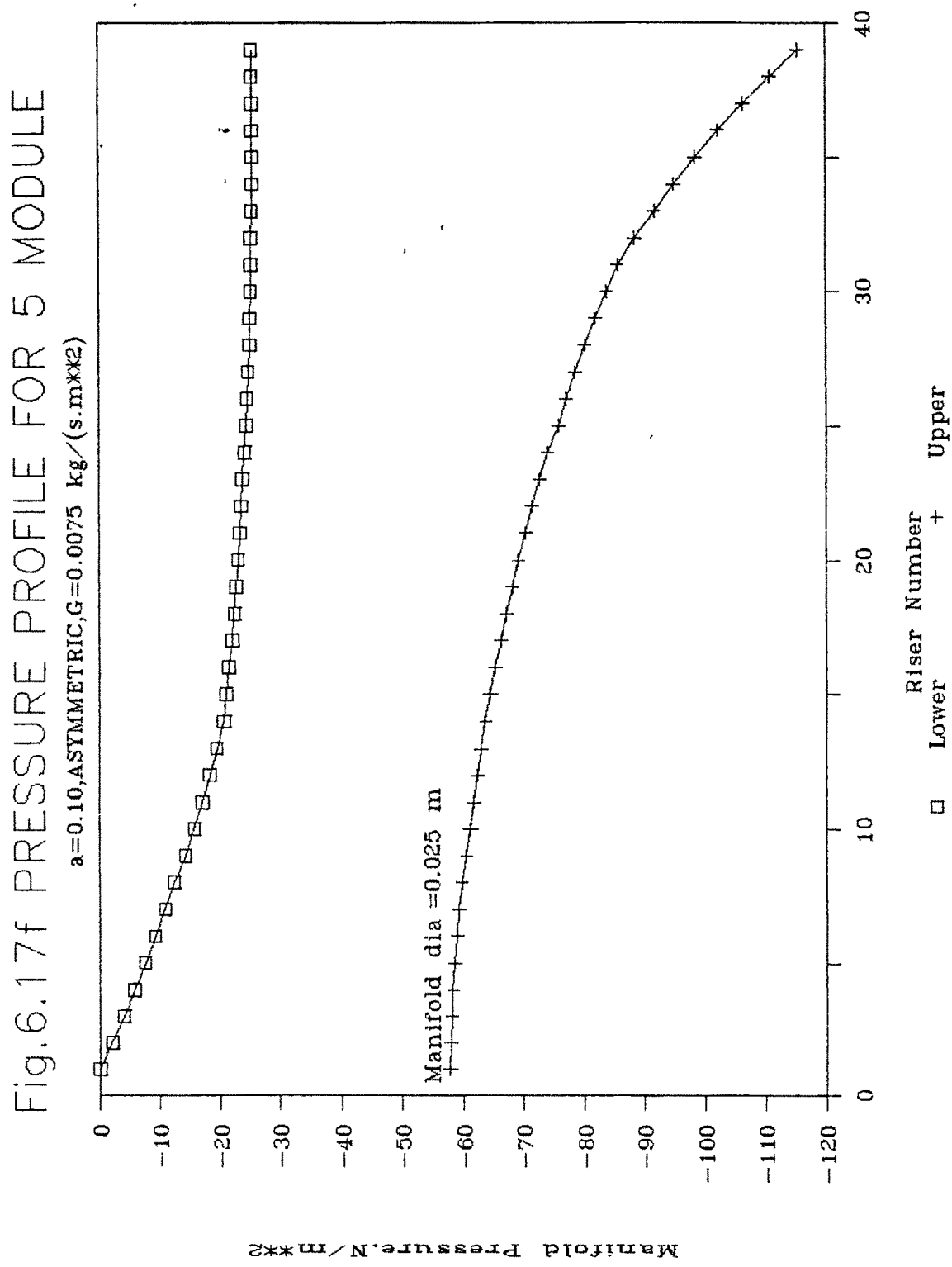
Fig.6.17f PRESSURE PROFILE FOR 5 MODULE
a=0.10,ASYMMETRIC,G=0.0075 kg/(s.m**2)
Manifold dia =0.025 m
Manifold Pressure,N/m**2
0
-10
-20
-30
-40
-50
-60
-70
-80
-90
-100
-110
-120
0
10
20
30
40
Riser Number
□ Lower
+ Upper

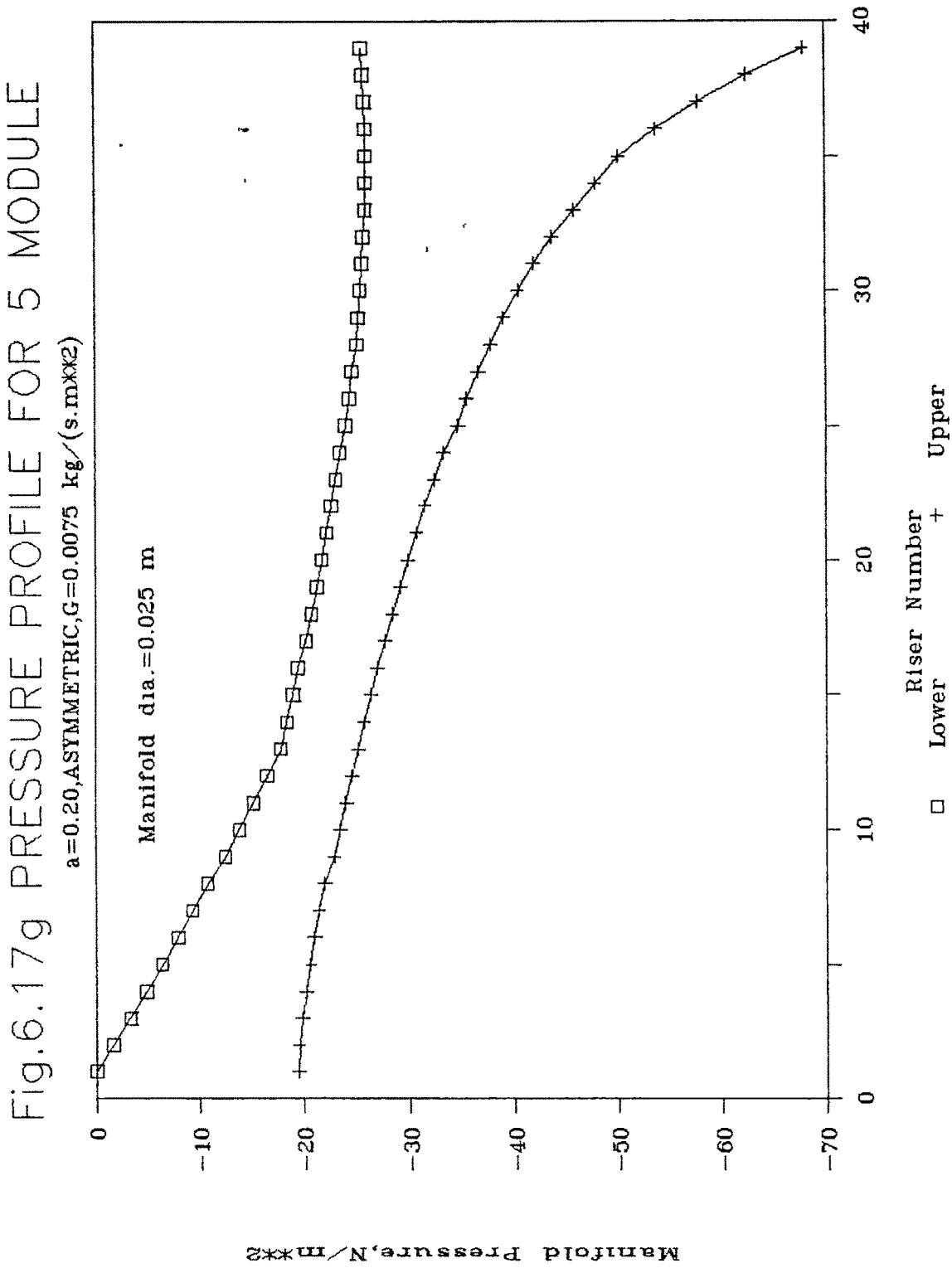
Fig.6.17g PRESSURE PROFILE FOR 5 MODULE
a=0.20,ASYMMETRIC,G=0.0075 kg/(s.m**2)
Manifold dia.=0.025 m
Manifold Pressure,N/m**2
0
-10
-20
-30
-40
-50
-60
-70
0
10
20
30
40
Riser Number
□ Lower
+ Upper

Fig.6.18a FLOW PROFILE FOR 5 MODULE

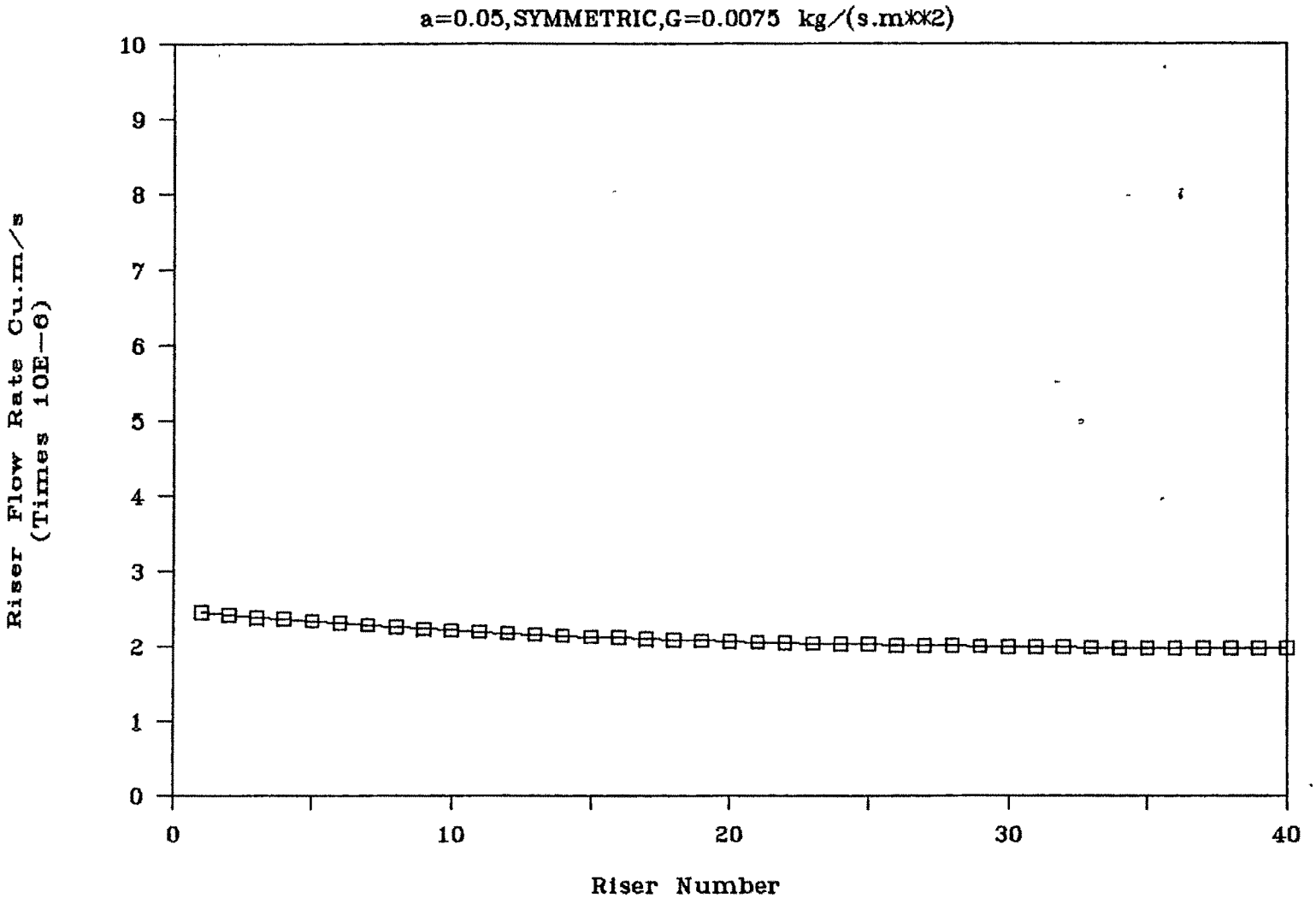

Fig.6.18b FLOW PROFILE FOR 5 MODULE

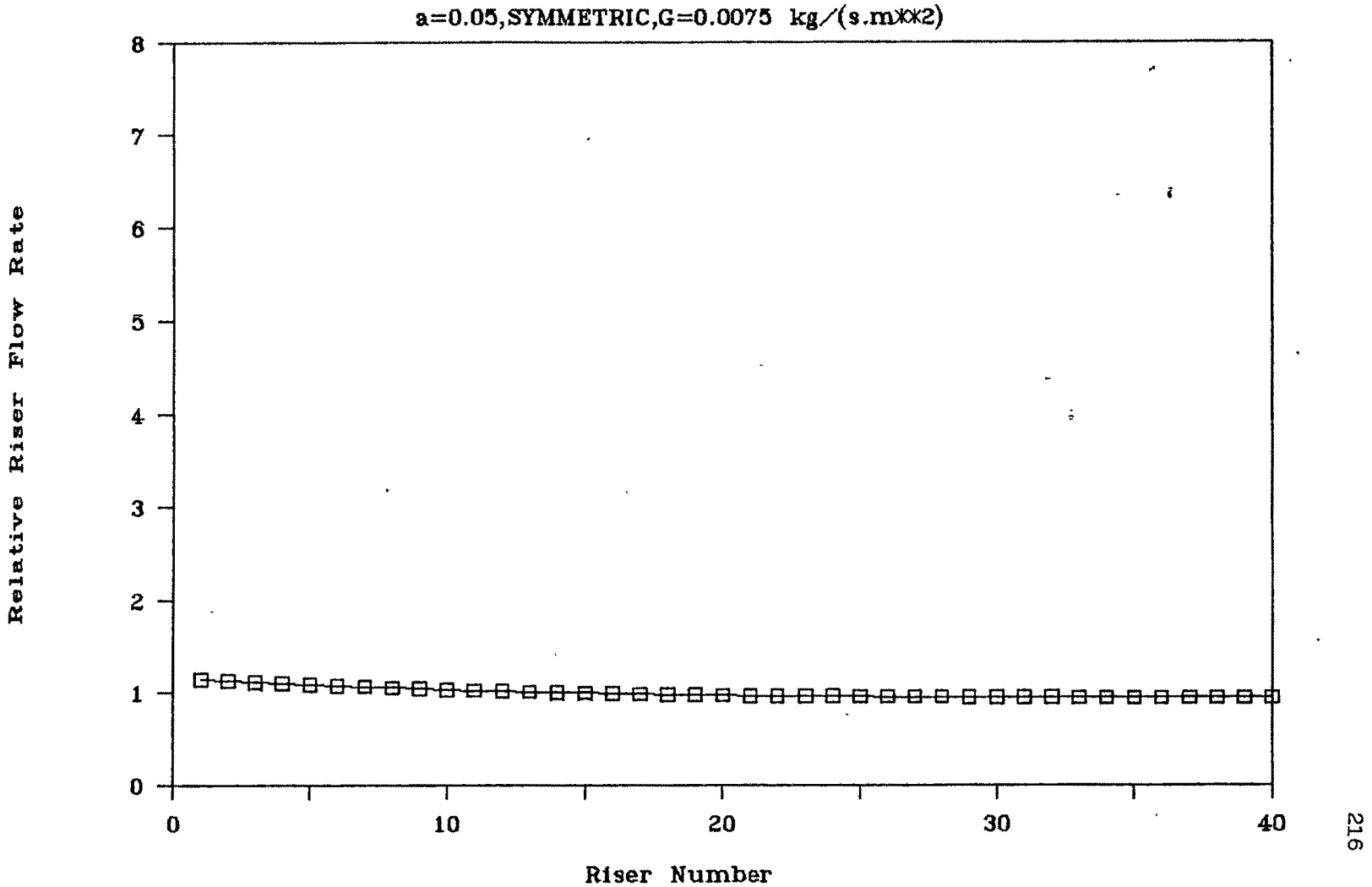

Fig.6.19a FLOW PROFILE FOR 5 MODULE

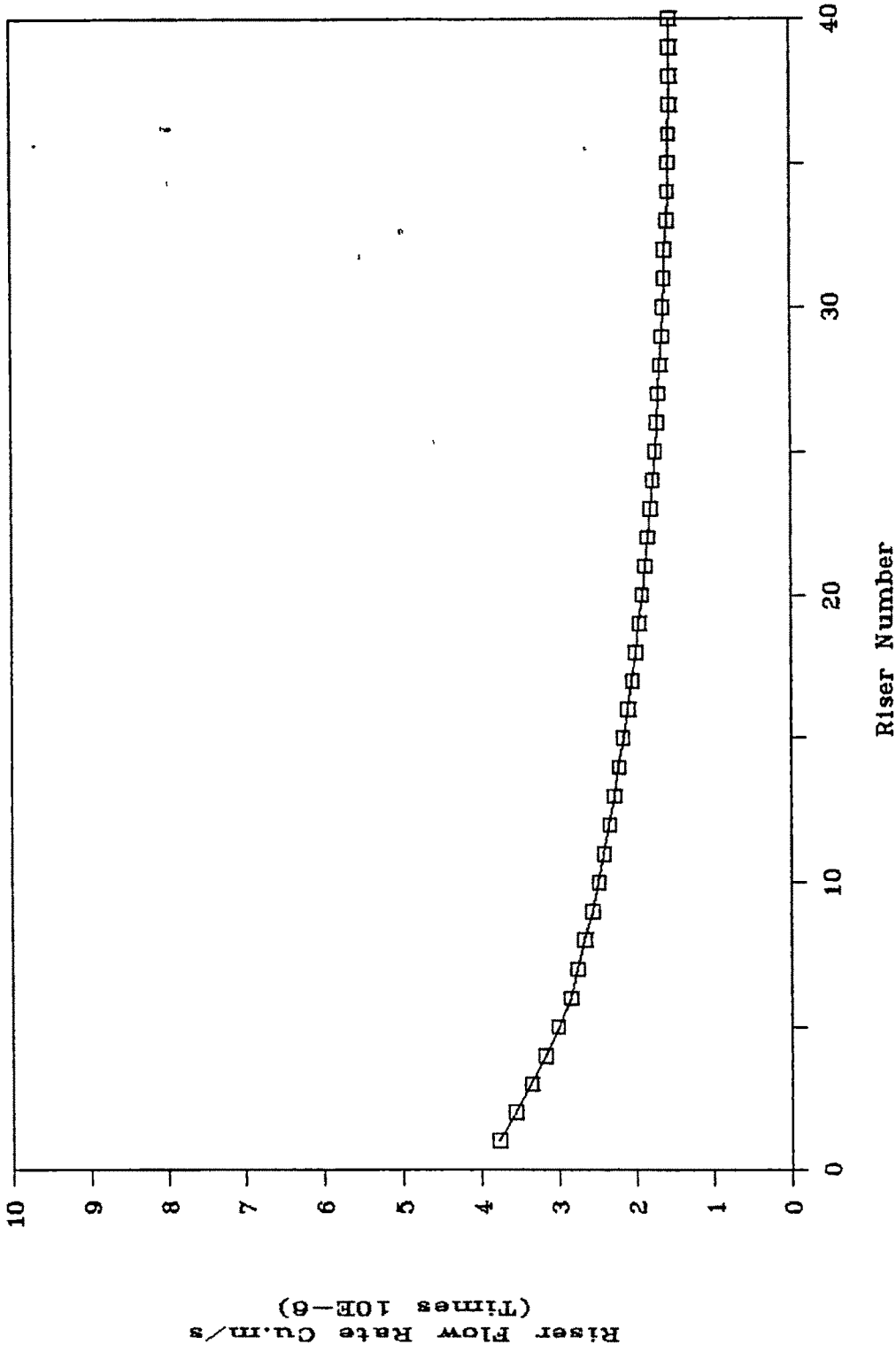

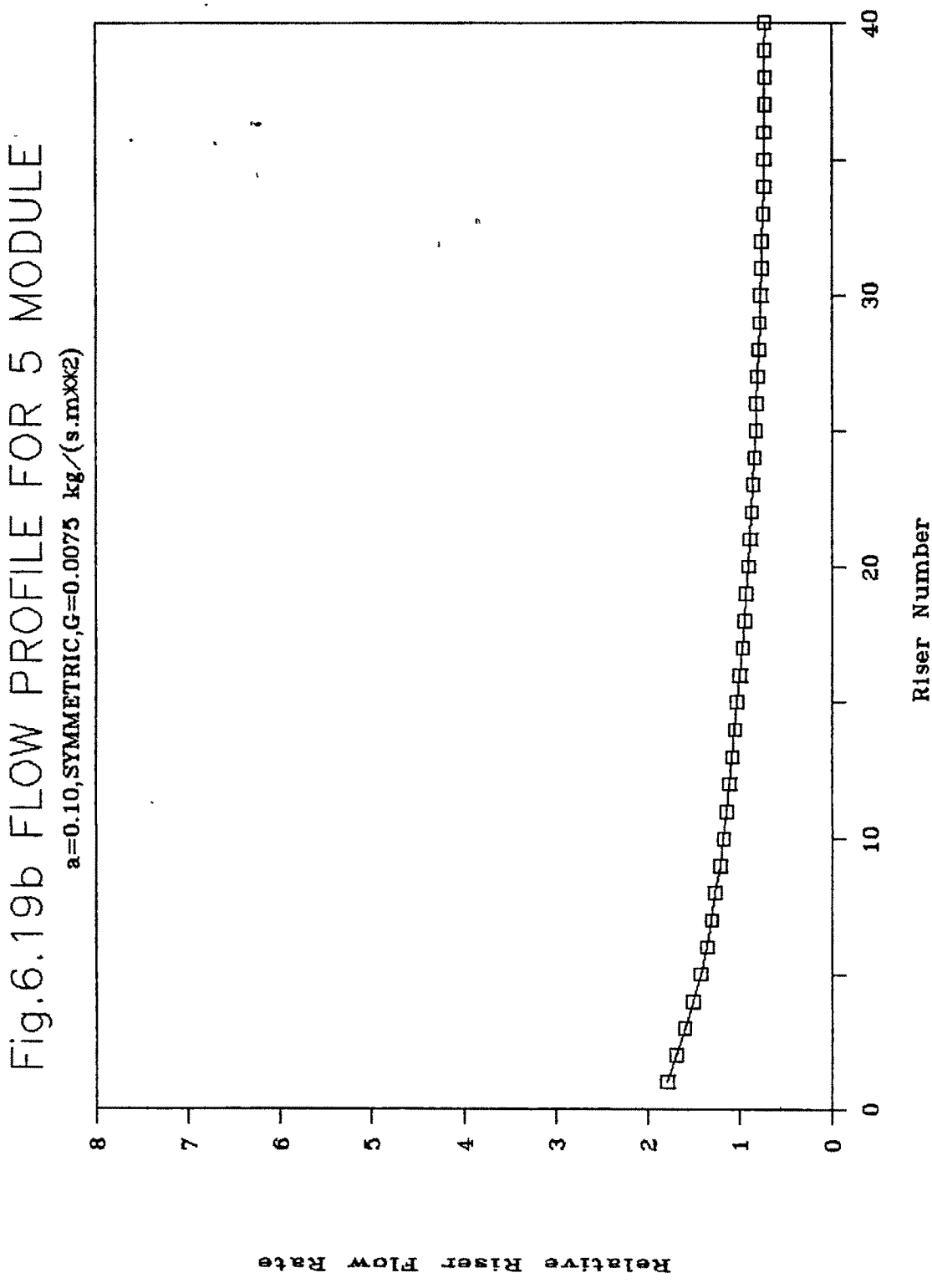
Fig.6.19b FLOW PROFILE FOR 5 MODULE
a=0.10,SYMMETRIC,G=0.0075 kg/(s.m**2)
Relative Riser Flow Rate
Riser Number
0
1
2
3
4
5
6
7
8
0
10
20
30
40

Fig.6.20a FLOW PROFILE FOR 5 MODULE

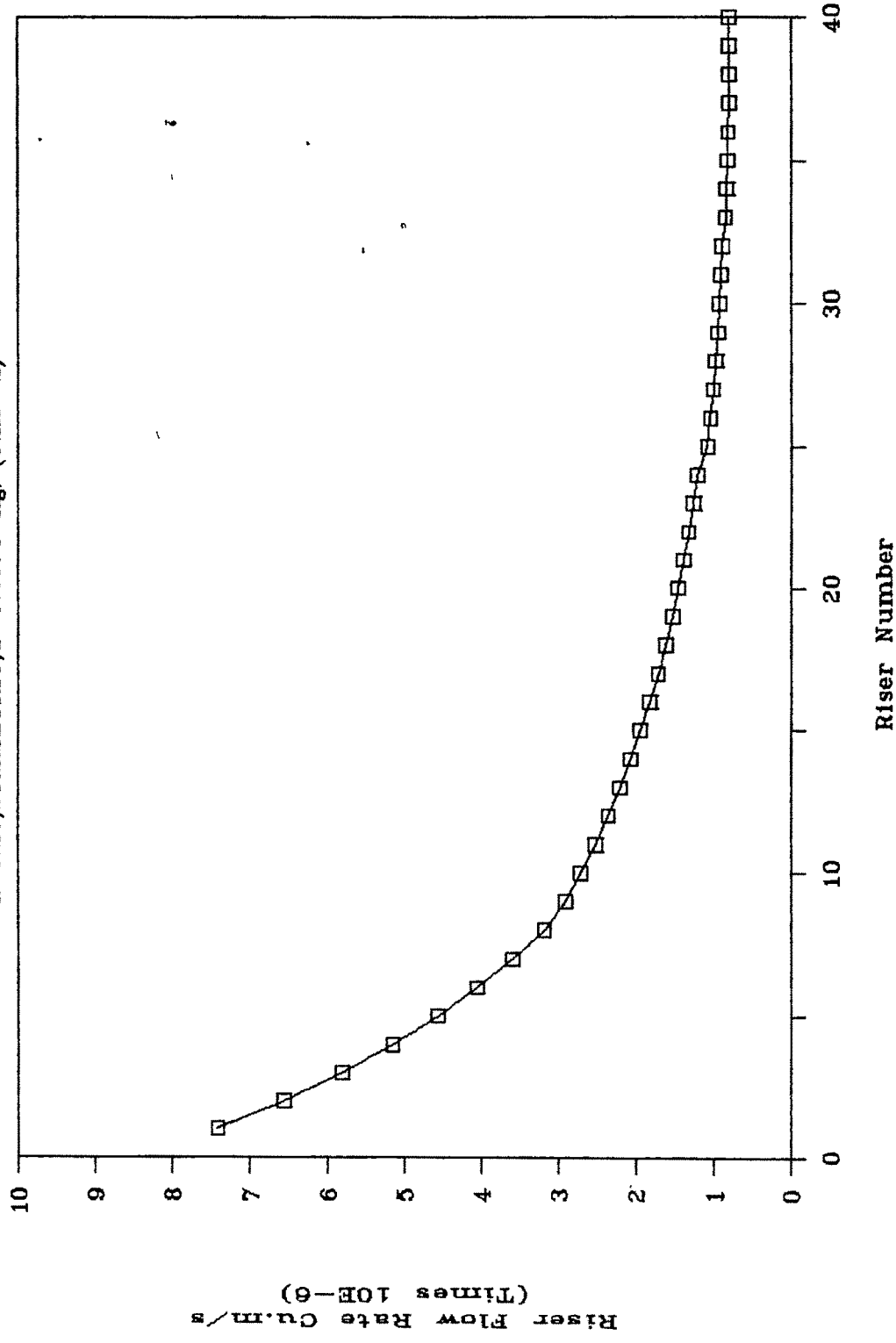

Fig.6.20b FLOW PROFILE FOR 5 MODULE

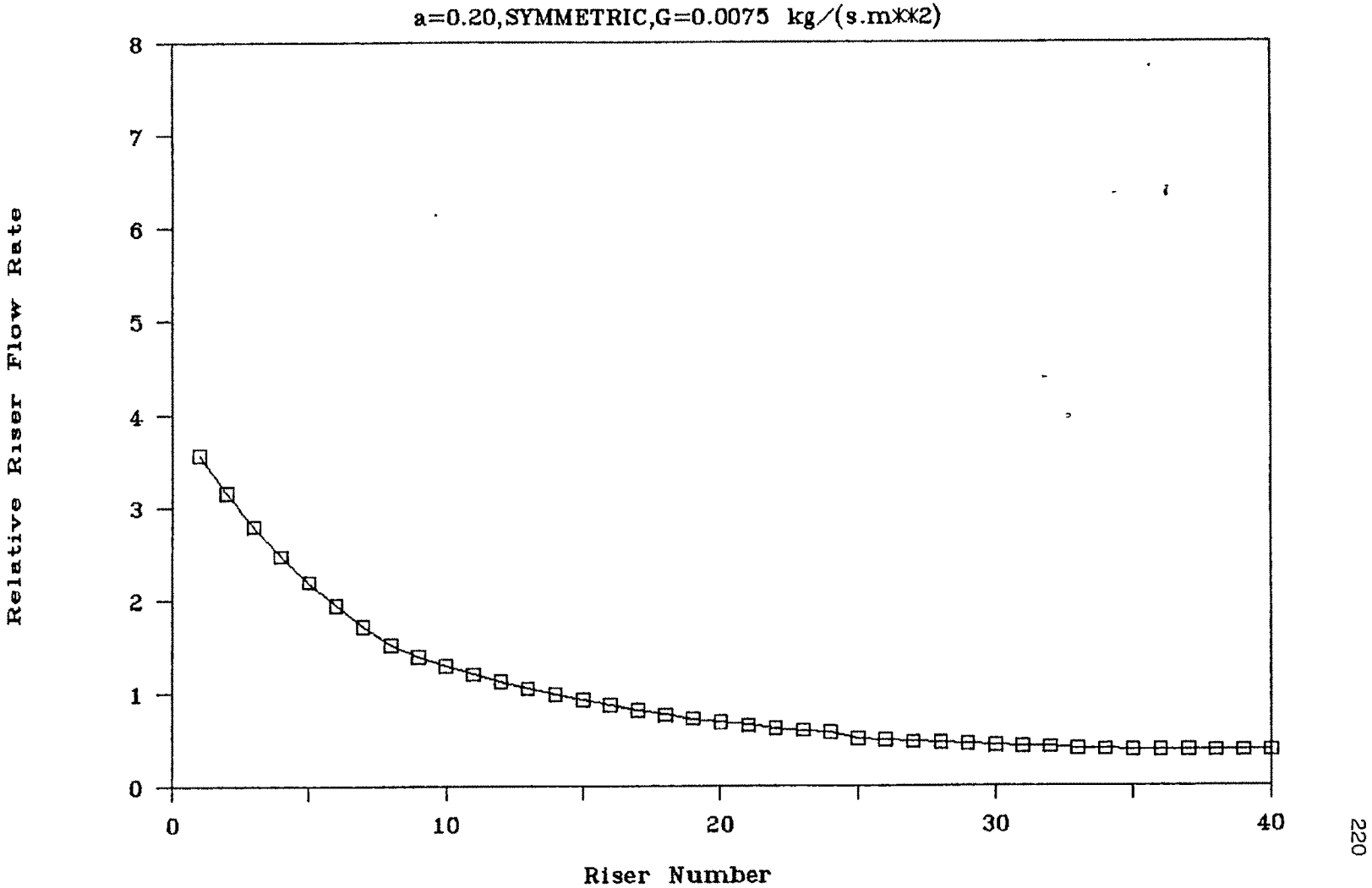

Fig.6.21a FLOW PROFILE FOR 5 MODULE

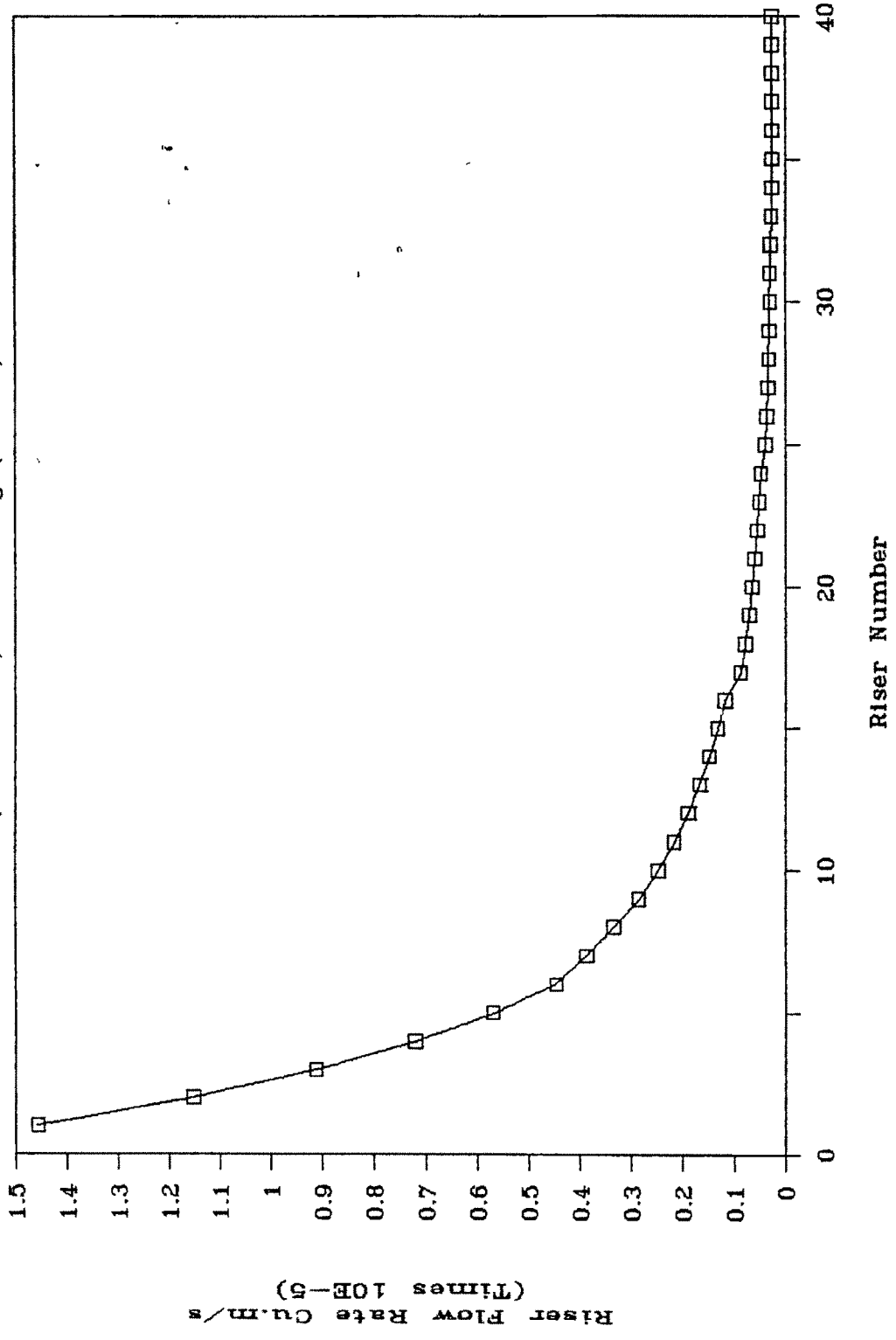

Fig.6.21b FLOW PROFILE FOR 5 MODULE

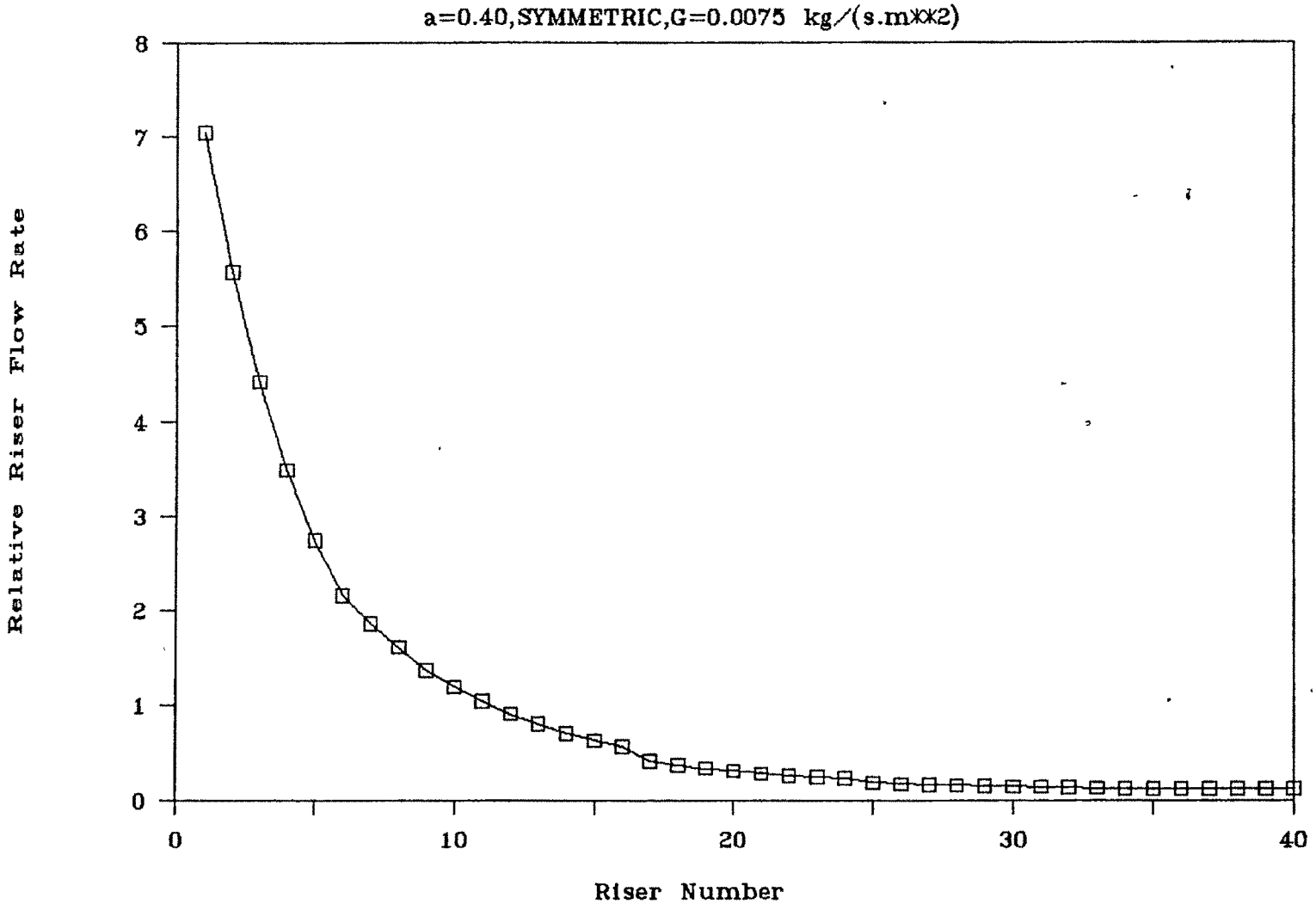

Fig.6.22 COMPARATIVE FLOW FOR 5 MODULES

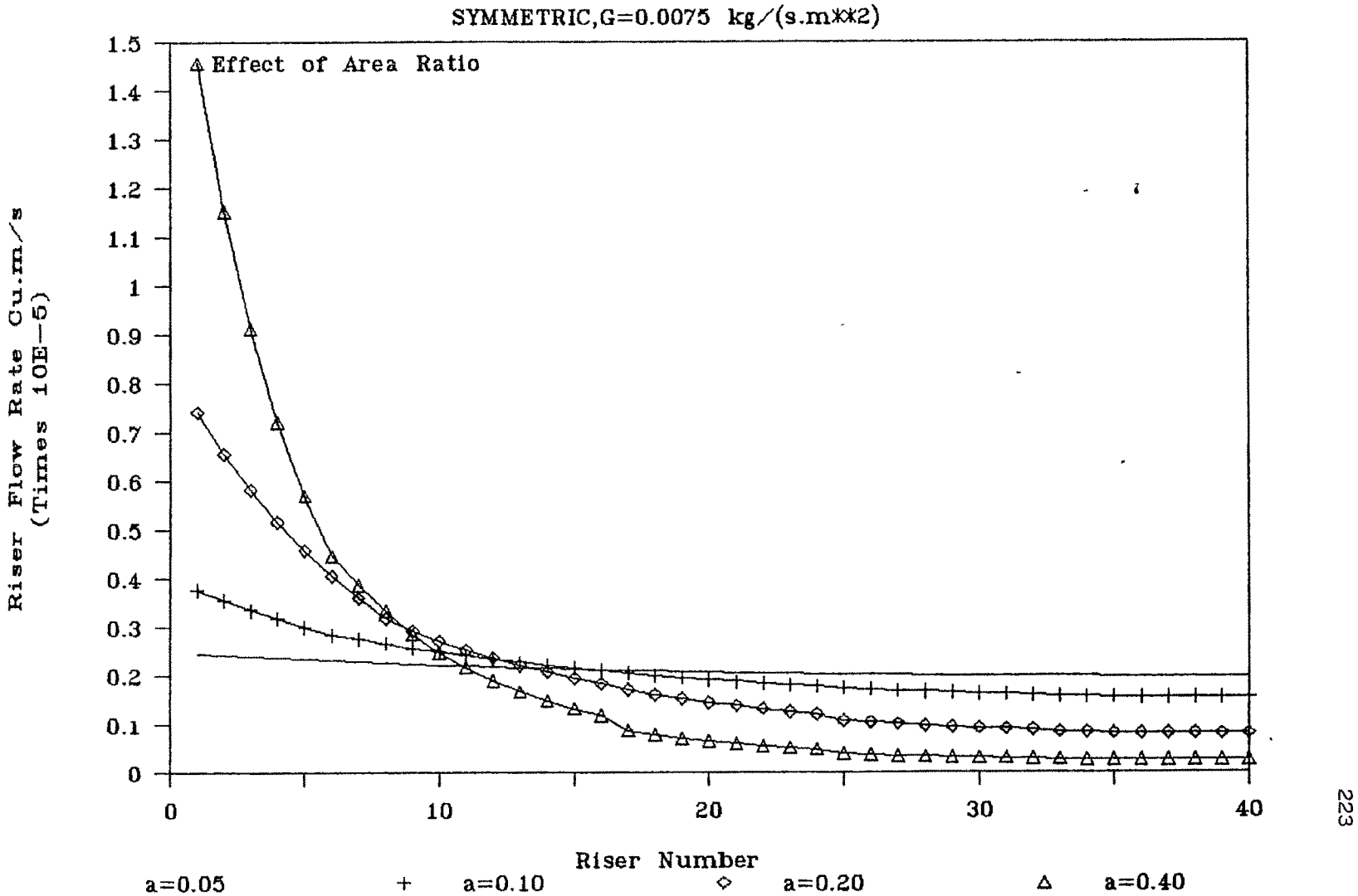

Fig.6.23a FLOW PROFILE FOR 5 MODULE

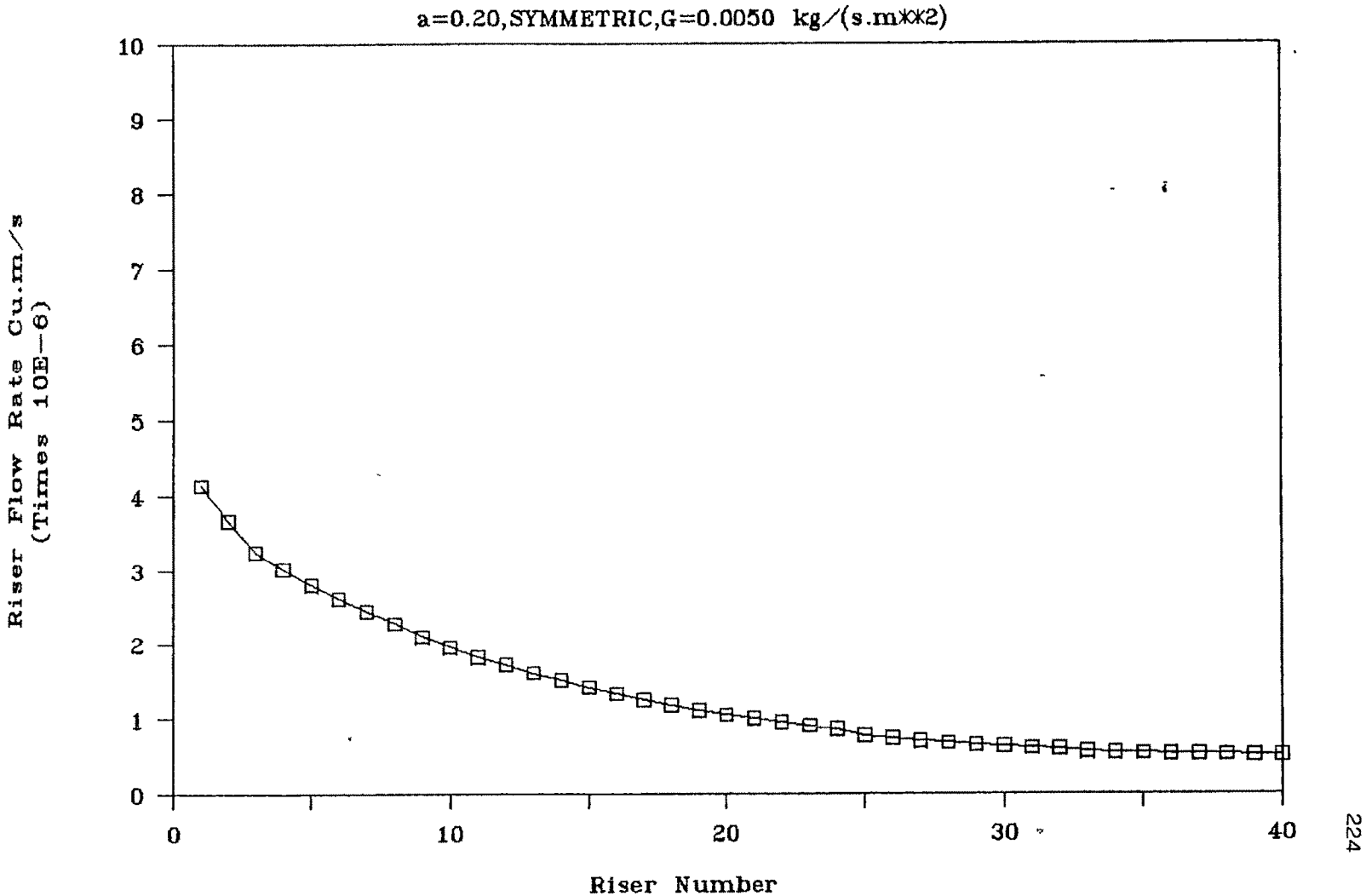

Fig.6.23b FLOW PROFILE FOR 5 MODULE

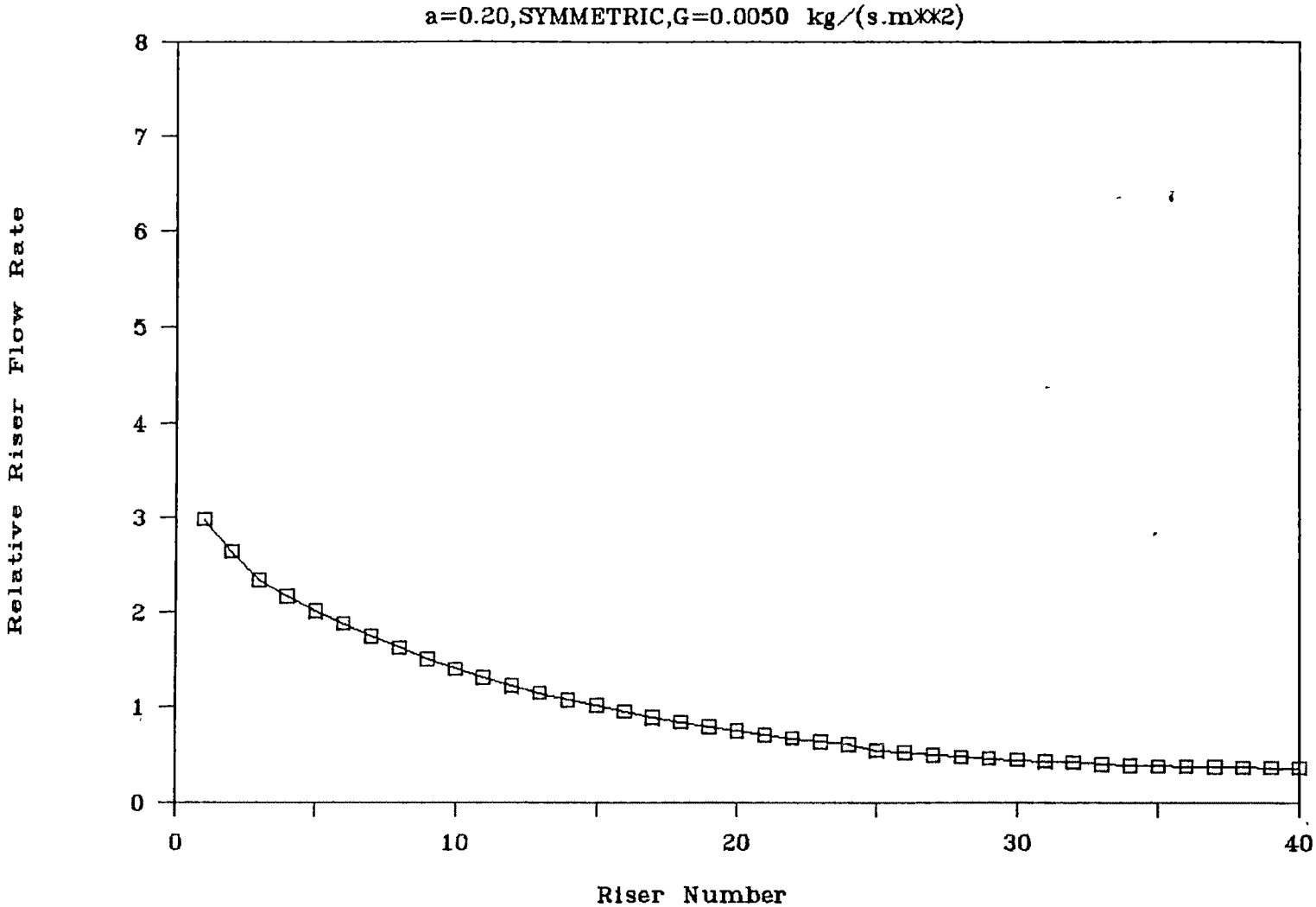

Fig.6.23c PRESSURE PROFILE FOR 5 MODULE

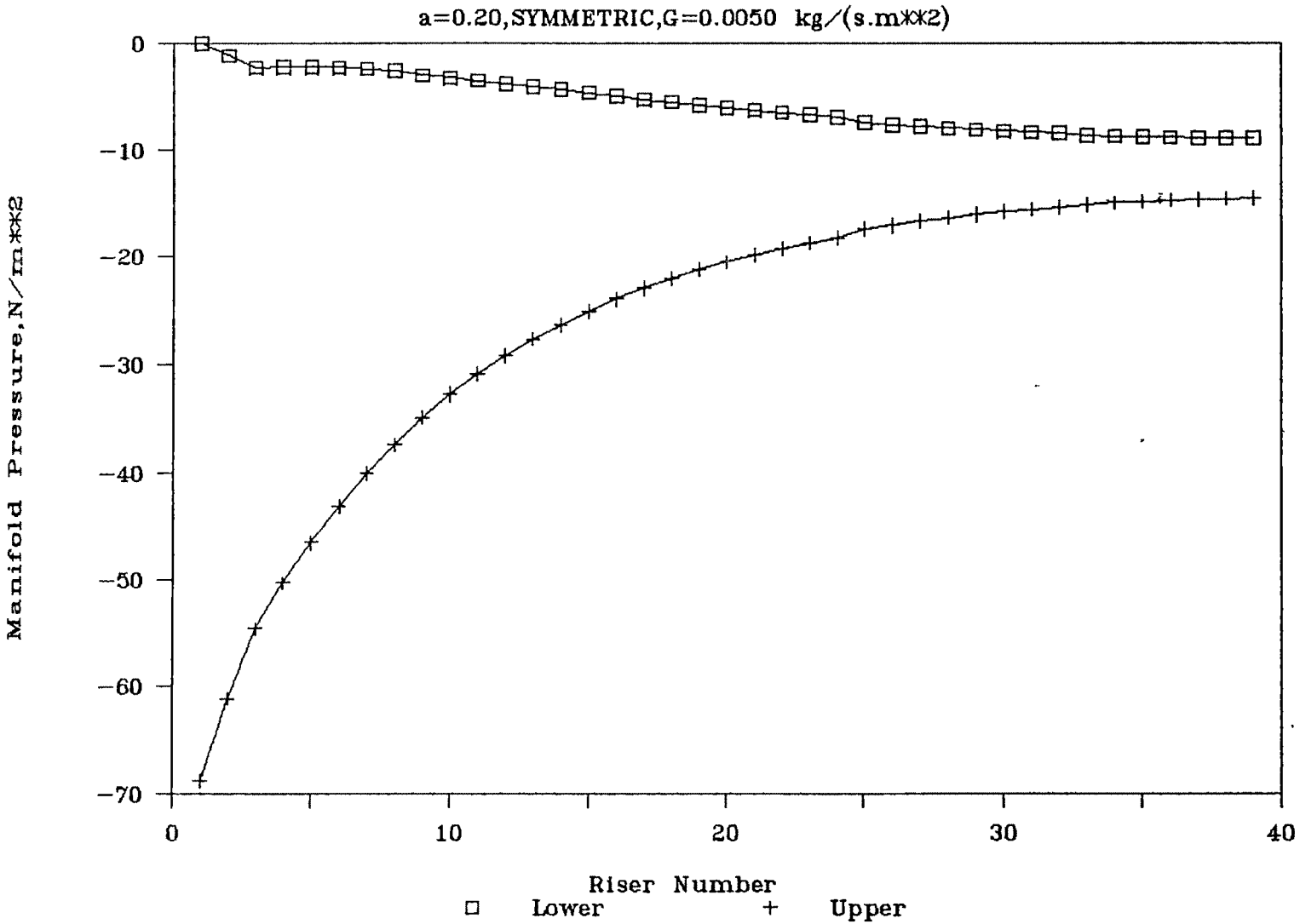

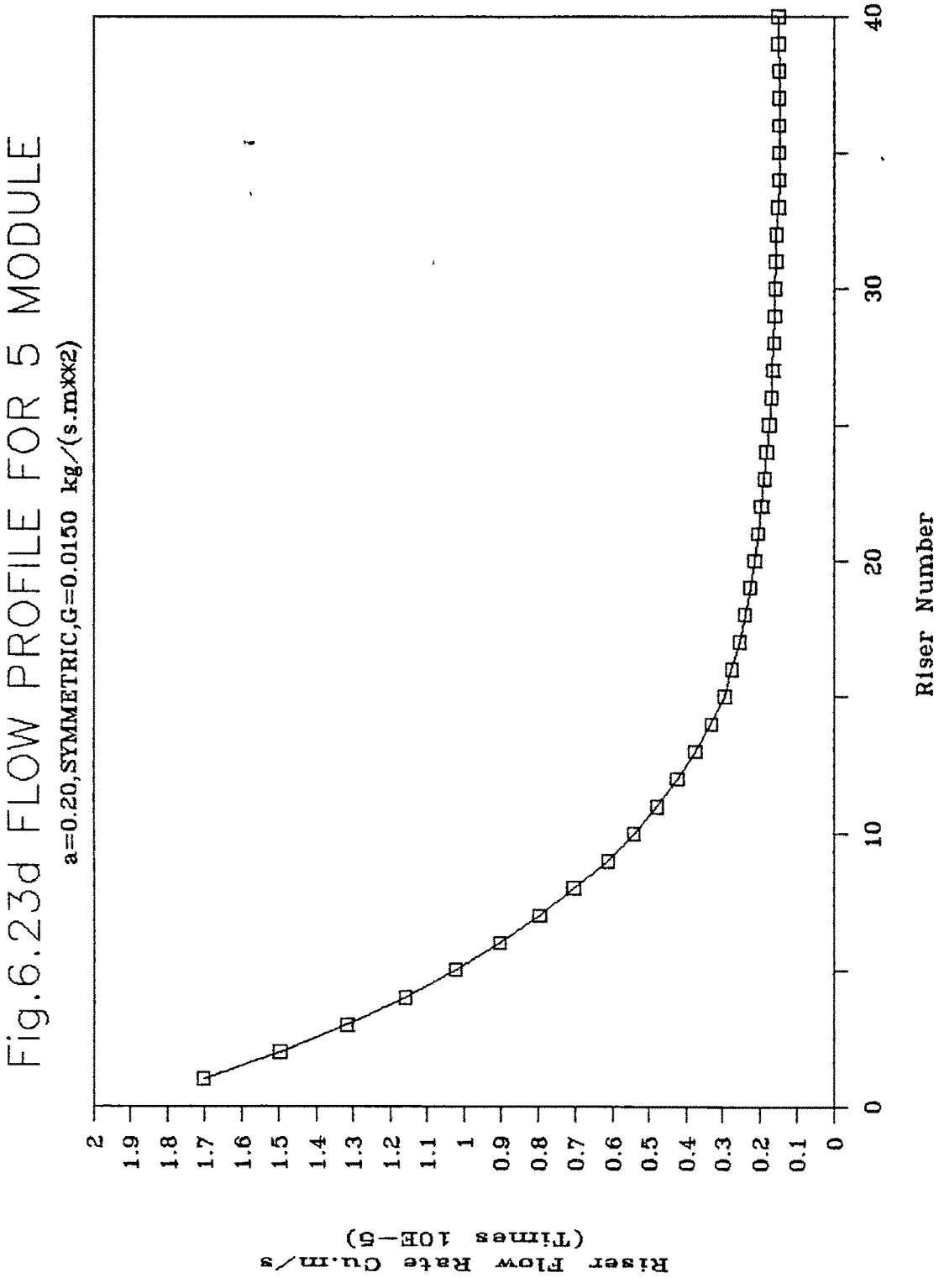
Fig.6.23d FLOW PROFILE FOR 5 MODULE
a=0.20,SYMMETRIC,G=0.0150 kg/(s.mXX2)
Riser Flow Rate Cu.m/s
(Times 10E-5)
Riser Number
0
0.1
0.2
0.3
0.4
0.5
0.6
0.7
0.8
0.9
1
1.1
1.2
1.3
1.4
1.5
1.6
1.7
1.8
1.9
2
0
10
20
30
40

Fig.6.23e FLOW PROFILE FOR 5 MODULE

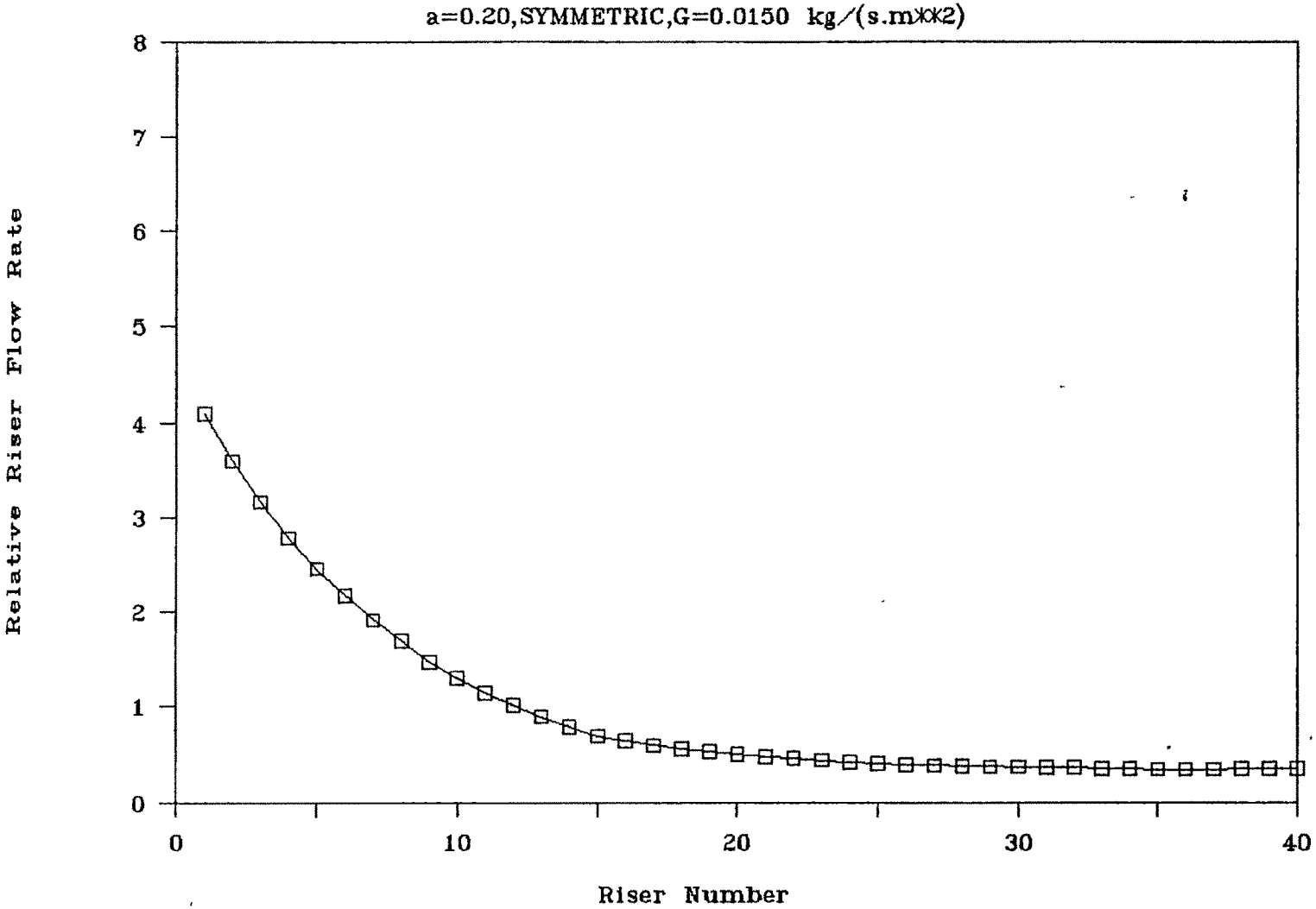

Fig.6.23f PRESSURE PROFILE FOR 5 MODULE

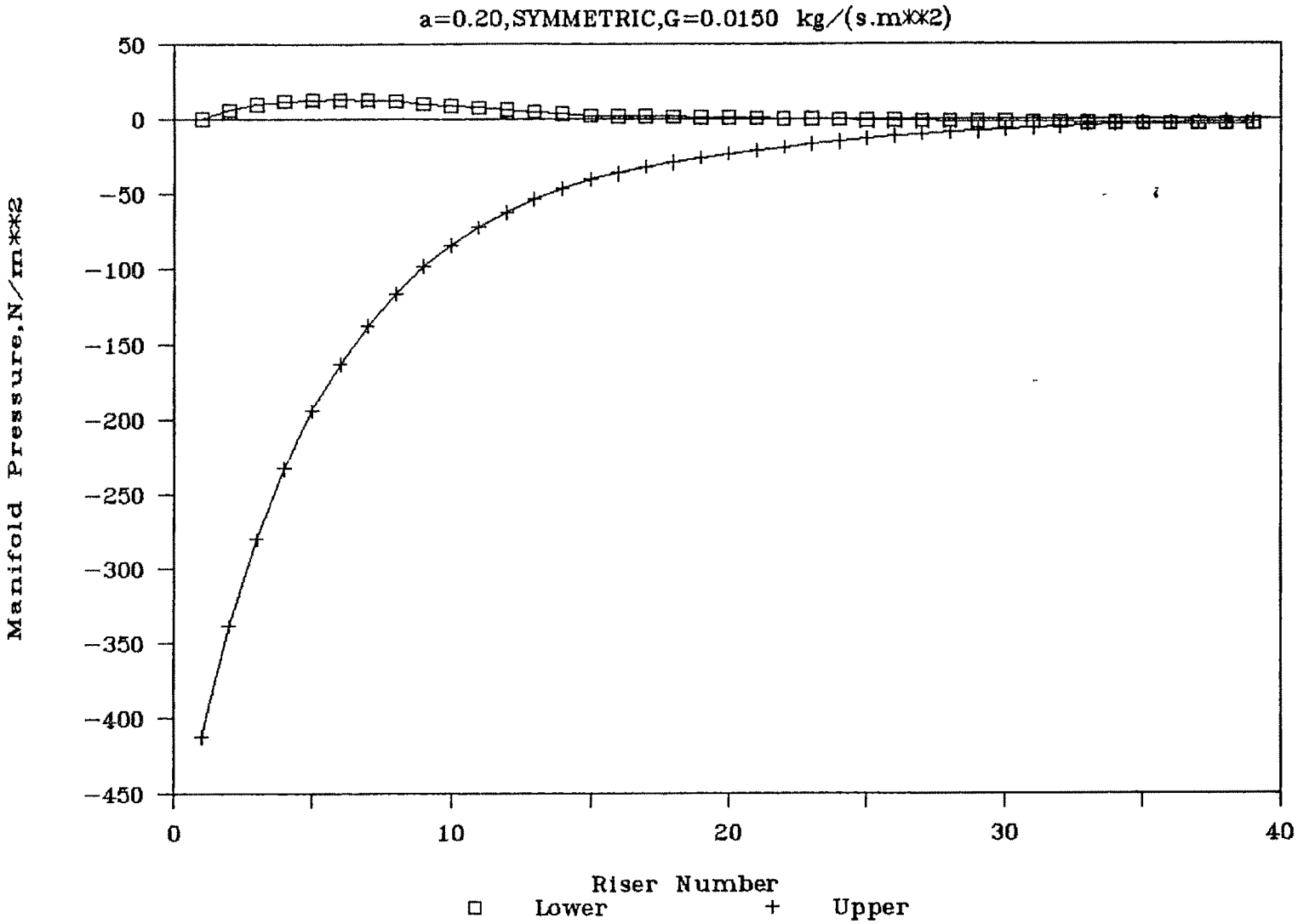

Fig.6.23g COMPARATIVE FLOW FOR 5 MODULE

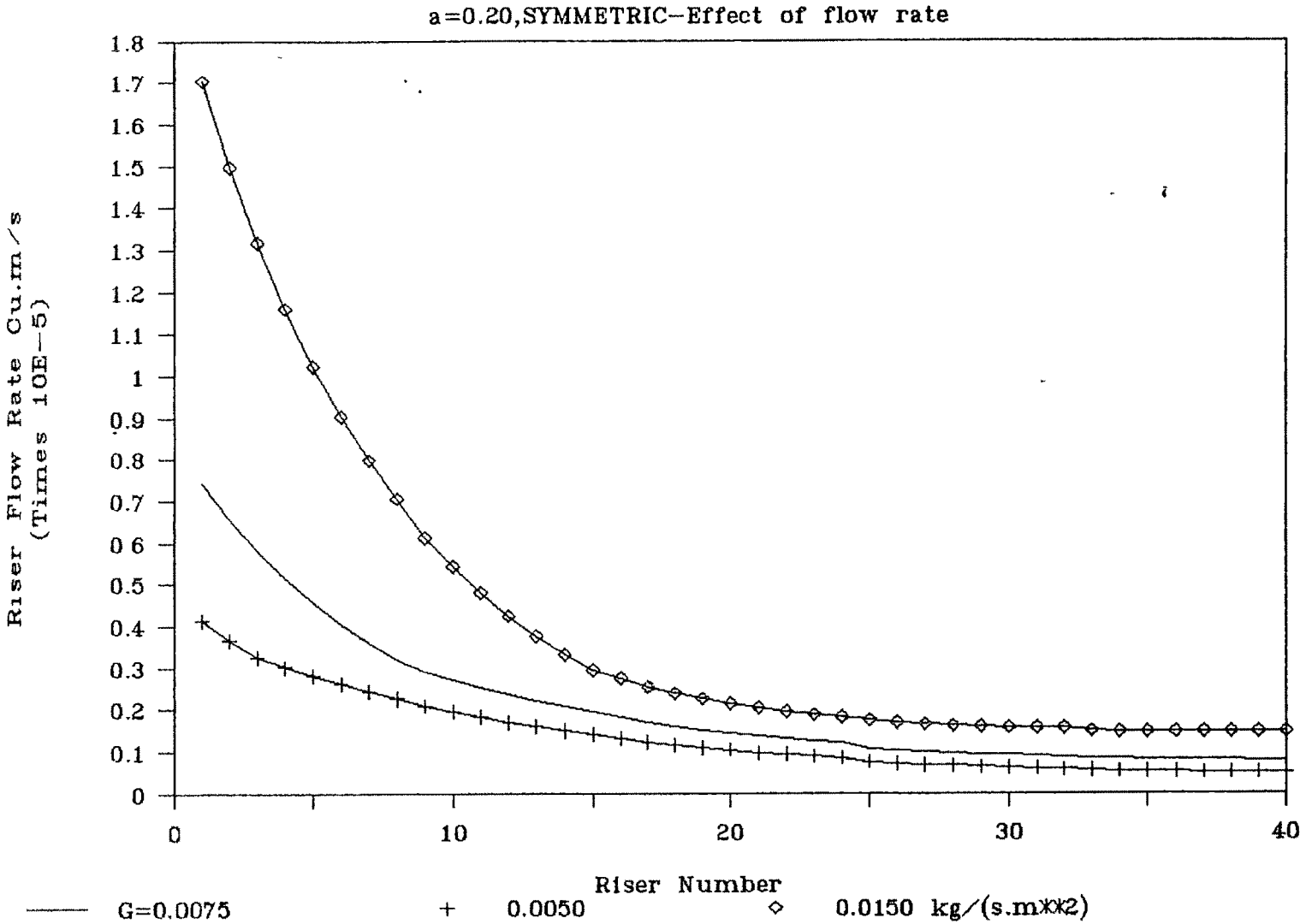

Fig.6.24a PRESSURE PROFILE FOR 5 MODULE

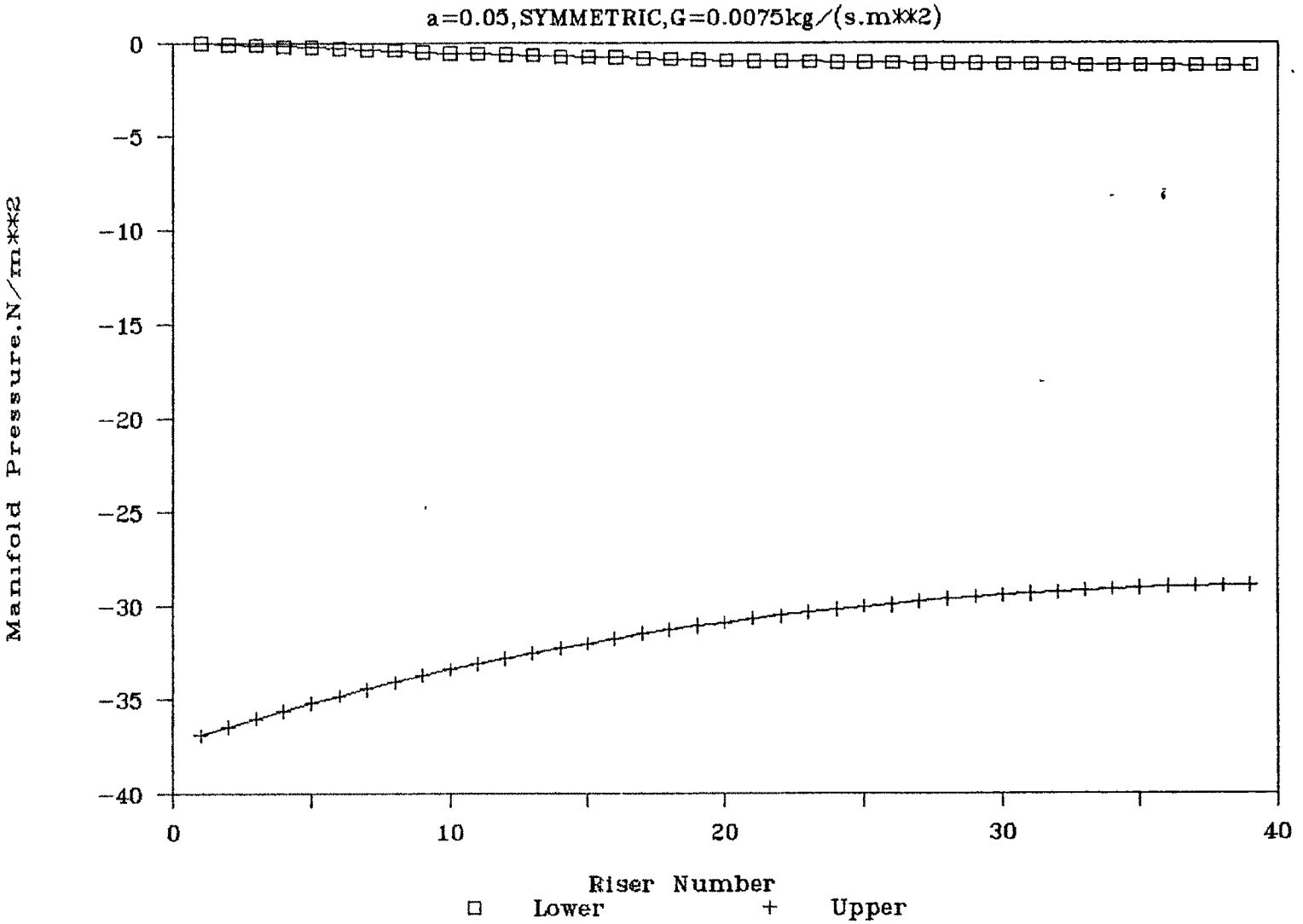

Fig.6.24b PRESSURE PROFILE FOR 5 MODULE

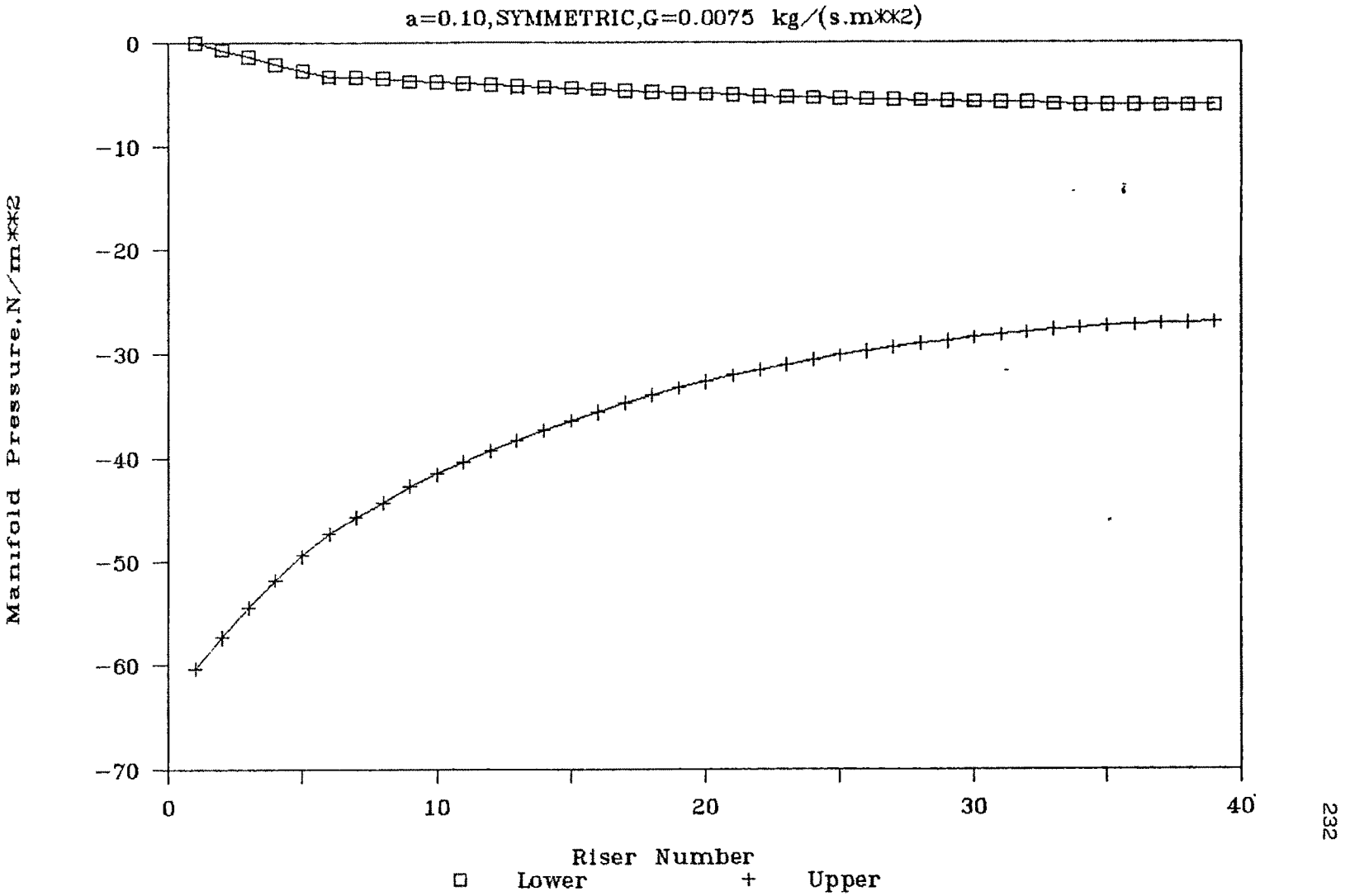

Fig.6.24c PRESSURE PROFILE FOR 5 MODULE

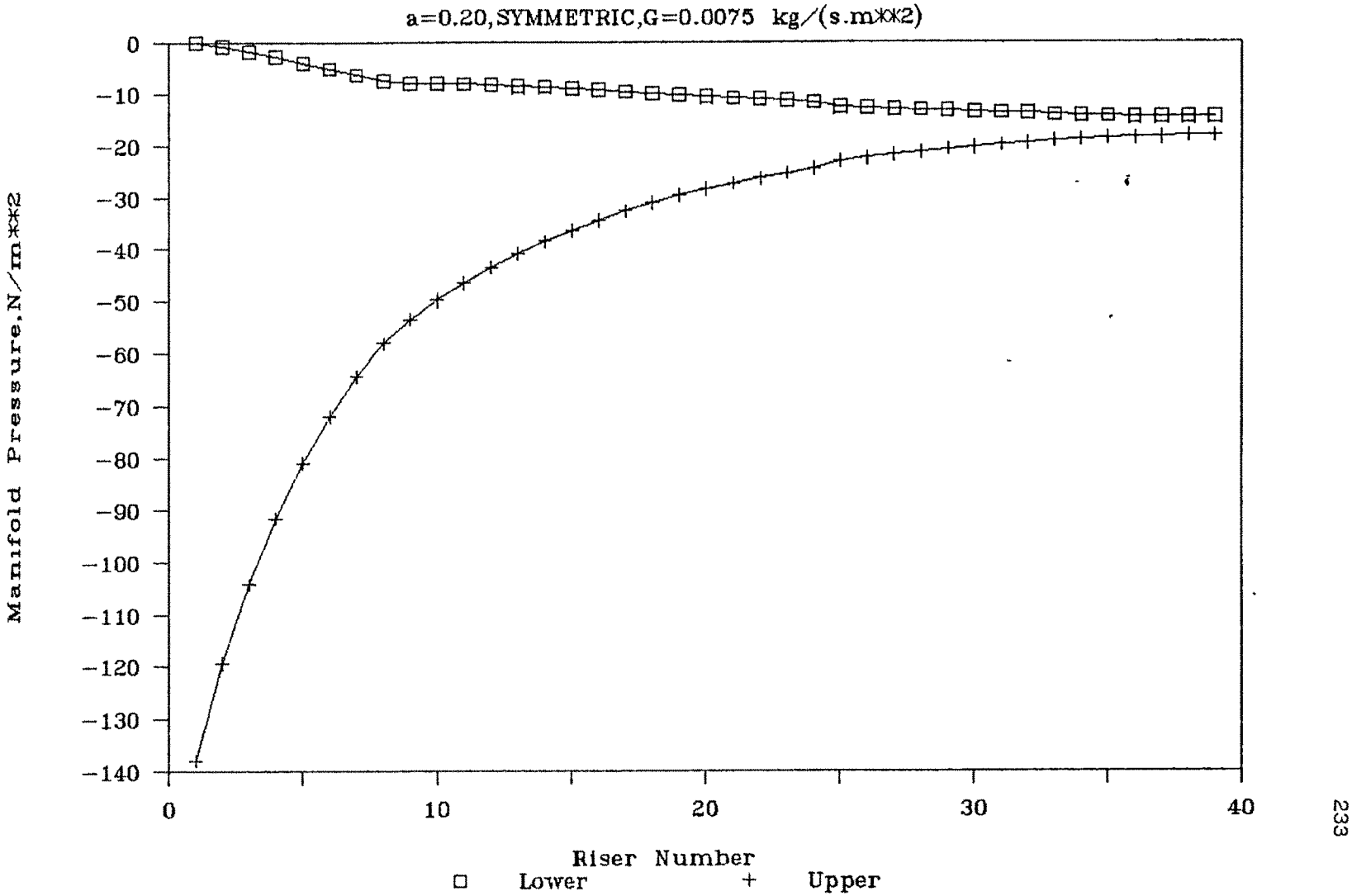

6.2.3 Effect of Collector and Riser Spacing

Effect of Collector Spacing

The 5-module collector array behaviour shown employ a collector pipe inlet/outlet of 0.055 such that the spacing of extreme risers between adjacent collectors is 0.110 identical to the collector riser spacing. In an actual installation, the collector spacing could be higher to allow easier erection depending upon the design of the collector interconnection. To estimate the effects on the flow distribution, a collector spacing of 0.30 m is chosen, which is probably the maximum normally used in practise.

The results for 5-module array with an area ratio of 0.20 is shown in Fig. 6.25. It is observed that the effect on the flow distribution is small. The pressure profile is shown in Fig. 6.26. The sudden change in pressure at the collector interconnection is due to longer pipe.

For lower area ratio, as higher manifold diameter is used, the effect of the collector spacing will be insignificant.

The above results are for interconnecting pipe diameter same as that of the manifold. If lower diameter is chosen, then depending upon the pipe size the effect on the flow distribution could be significant [Soin(1983)]. Normally, however, similar pipe sizes are used.

Effect of Riser Spacing

Riser spacing in a solar collector is decided based on the type of collector and the materials used, especially the thermal conductivity and the emissivity of the absorber. The spacing is optimally determined to provide a cost effective collector. For higher thermal conducting absorber material, such as copper, and selective coating, the optimum spacing is about 100 - 120 mm. For non-selective collector or lower thermal conductivity absorber e.g. steel, spacing is normally lower. It would be of interest to determine the effect of riser spacing on the flow distribution.

Keeping the geometry as that of the baseline collector, reduced riser spacing of 0.070 m is chosen resulting in 12 risers per collector. Such spacing is normally used for integrated steel tube-in-sheet collector, e.g. Soin (1983).

The results for 5-module with an area ratio of 0.05 are shown in Figs. 6.27-28. The array pressure drop is lower due to higher number of risers. The non-uniformity factor is 0.004, which is twice that of the baseline collector (see Table 6.11 for a = 0.05).

The results for an area ratio of 0.20 are shown in Figs. 6.29-30. As in the case of lower area ratio of 0.05, the flow maldistribution has increased marginally. The non-uniformity factor is 0.545 in comparison to 0.350 of baseline collector.

It may be concluded that the effect of collector spacing within the range investigated is small other factors remaining identical. Reduced riser spacing on the other hand increases flow maldistribution.

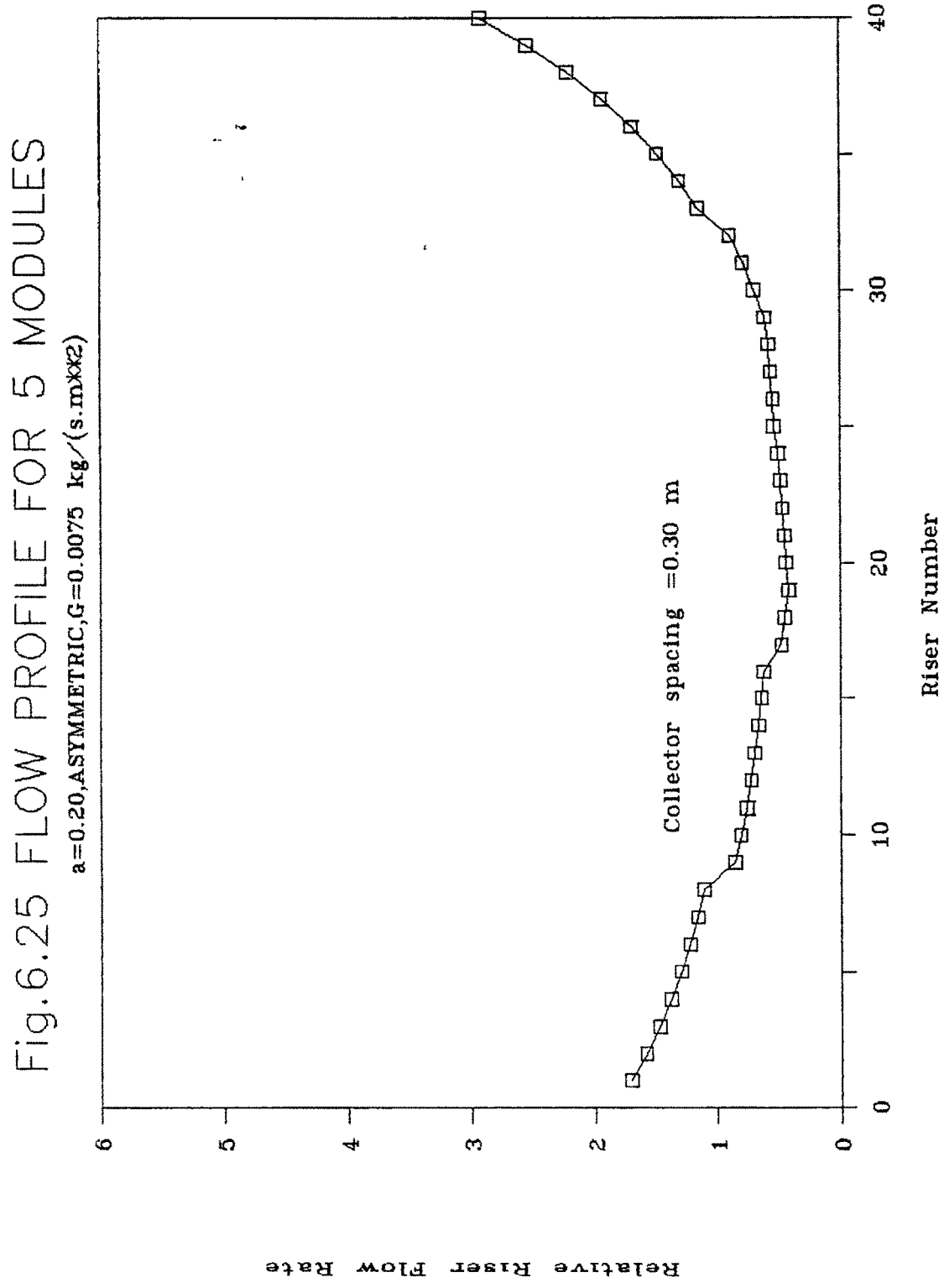
Fig.6.25 FLOW PROFILE FOR 5 MODULES
a=0.20,ASYMMETRIC,G=0.0075 kg/(s.m**2)
Collector spacing =0.30 m
Relative Riser Flow Rate
Riser Number
0
1
2
3
4
5
6
0
10
20
30
40

Fig.6.26 PRESSURE PROFILE FOR 5 MODULES

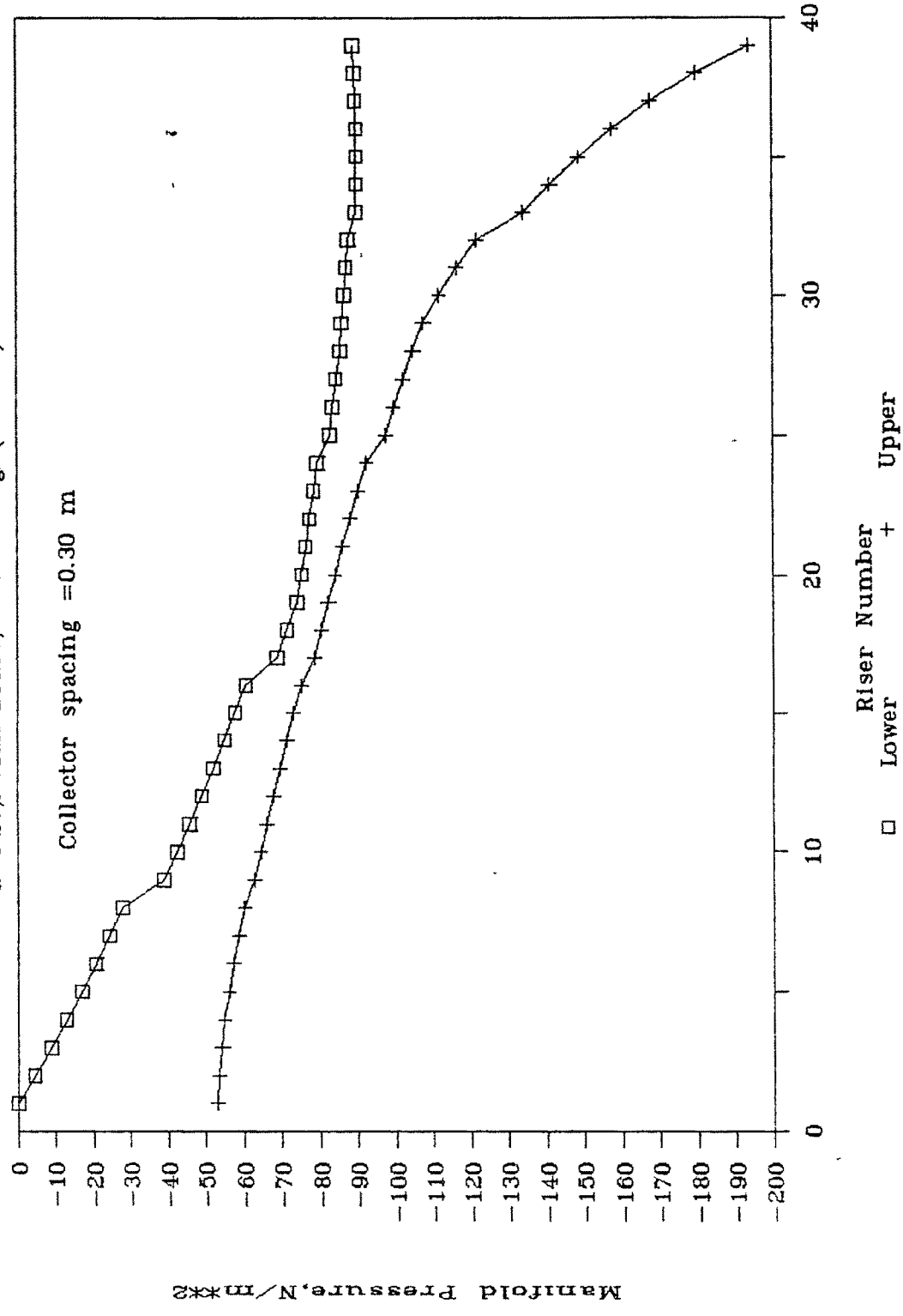

Fig.6.27 RISER PROFILE FOR 5 MODULES

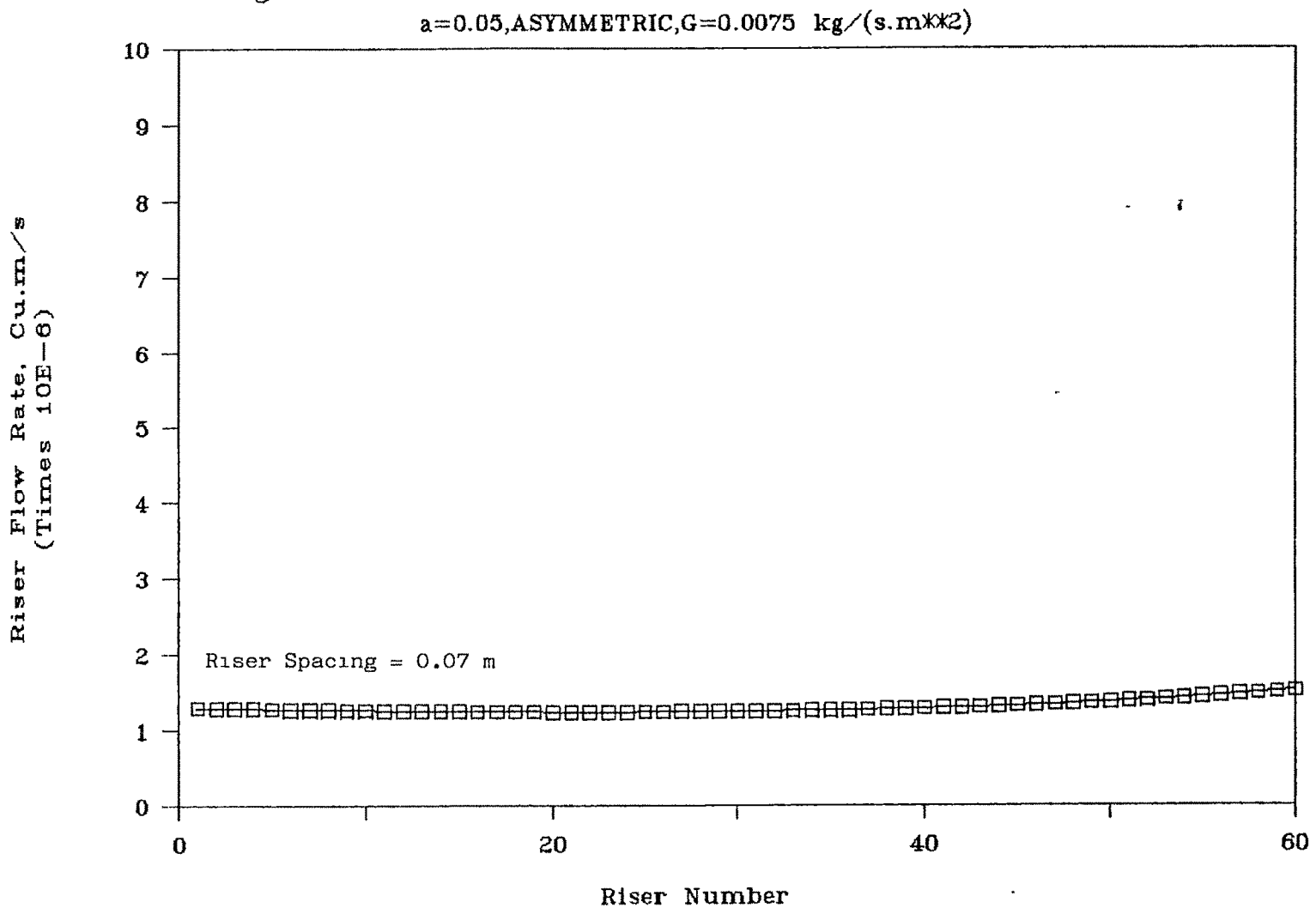

Fig.6.28 PRESSURE PROFILE FOR 5 MODULE

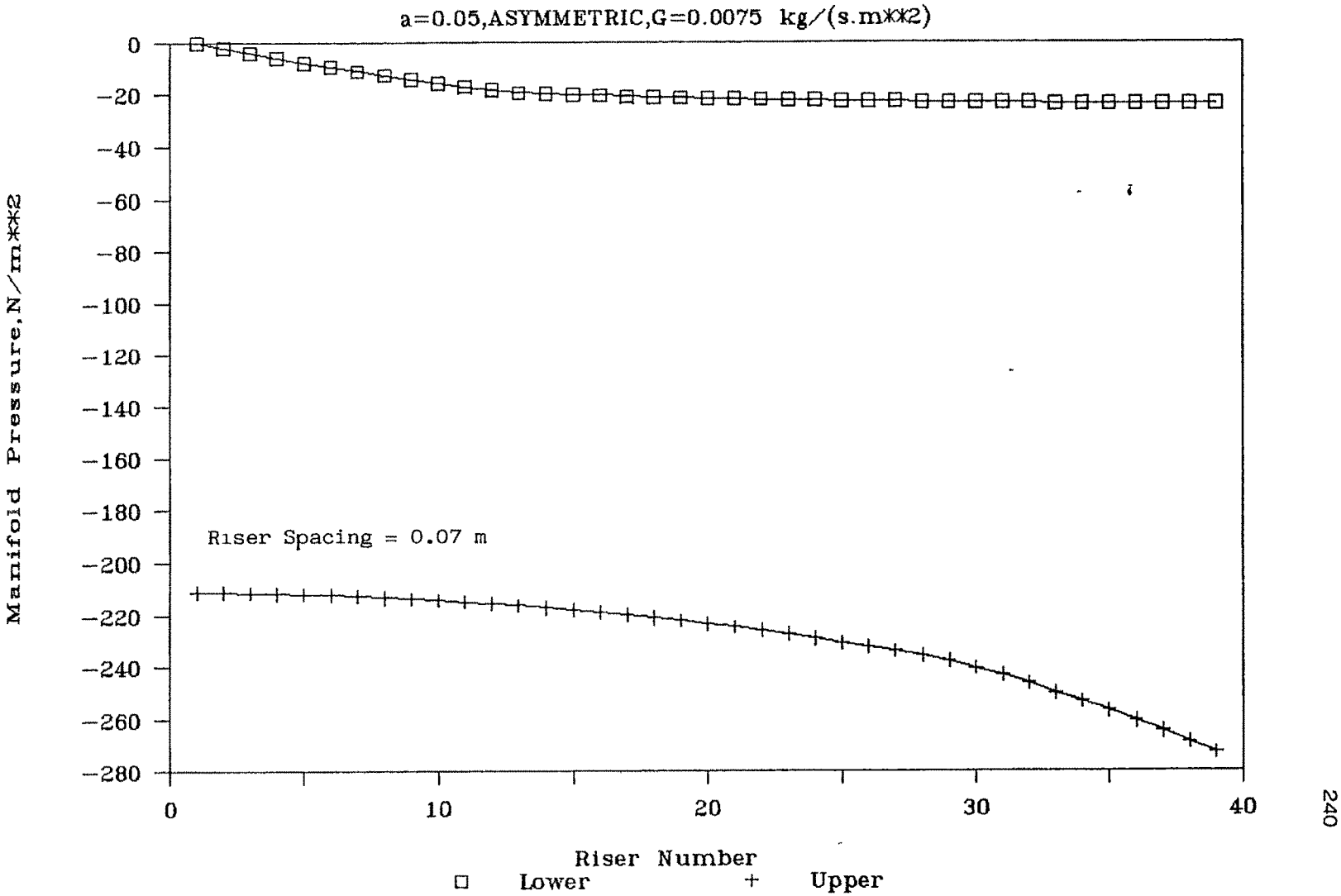

Fig.6.29 FLOW PROFILE FOR 5 MODULES

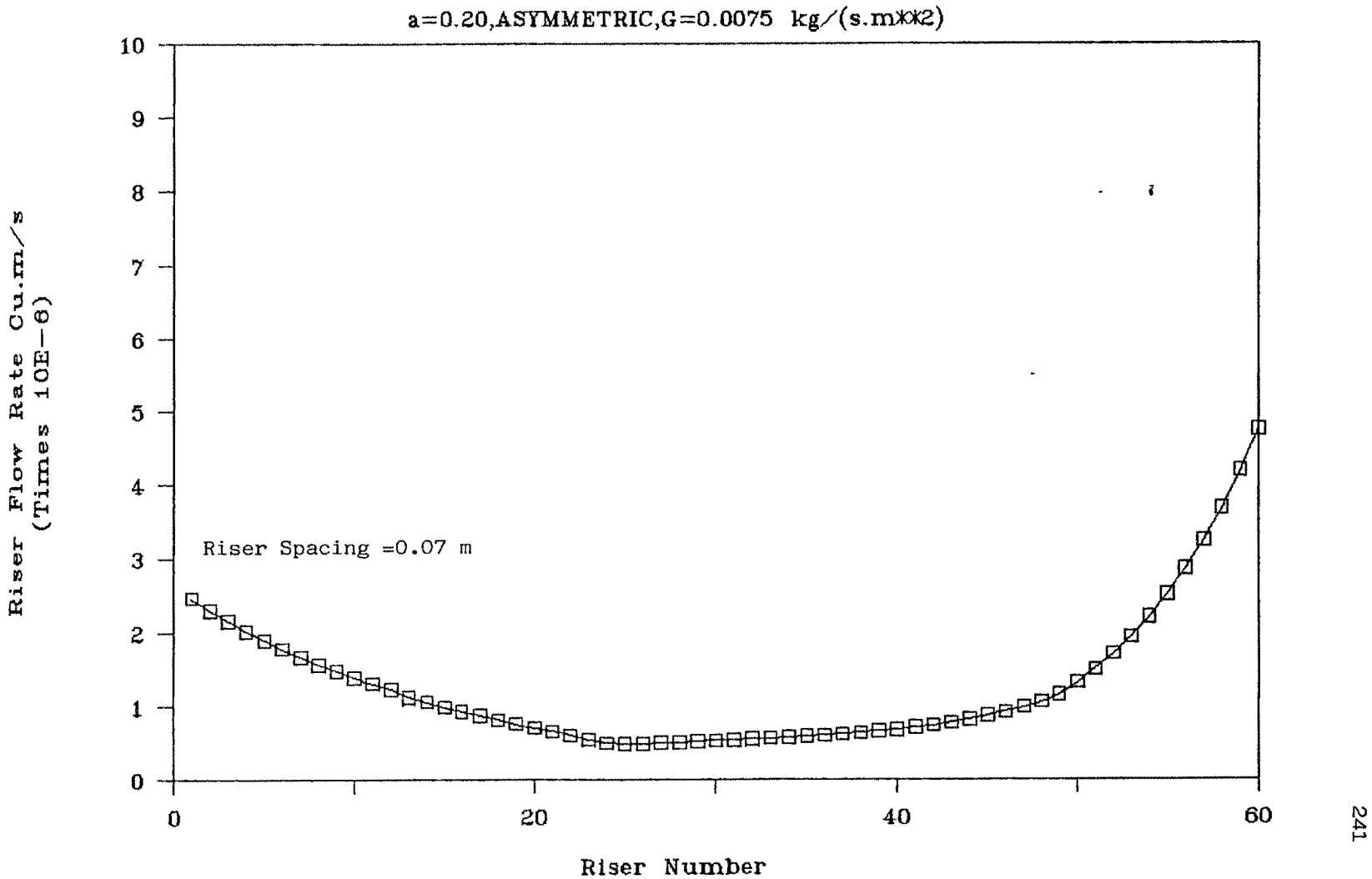

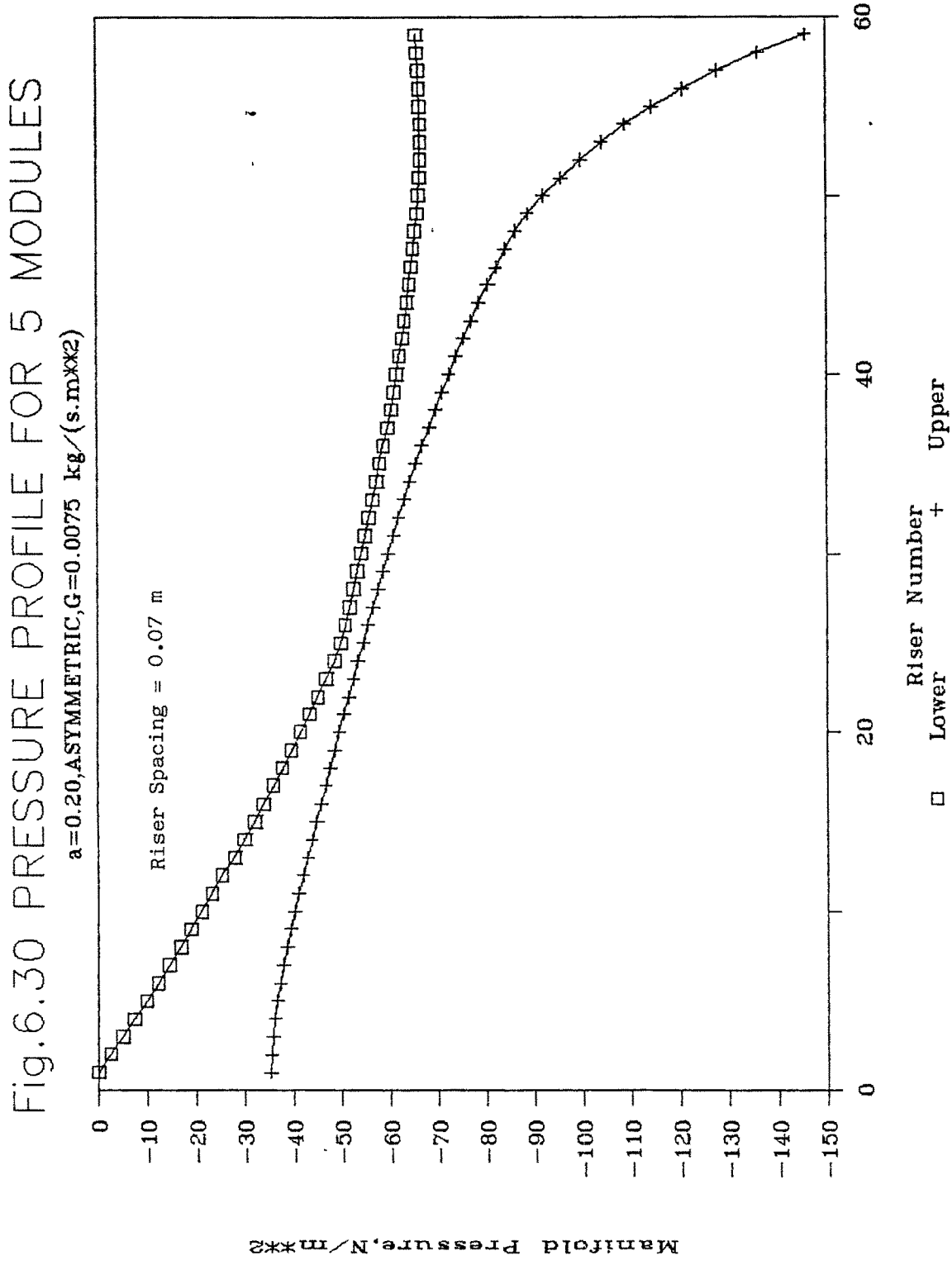
Fig.6.30 PRESSURE PROFILE FOR 5 MODULES
a=0.20,ASYMMETRIC,G=0.0075 kg/(s.m**2)
Riser Spacing = 0.07 m
Manifold Pressure,N/m**2
0
-10
-20
-30
-40
-50
-60
-70
-80
-90
-100
-110
-120
-130
-140
-150
0
20
40
60
Riser Number
□ Lower
+ Upper

6.3 Comparison of Asymmetric and Symmetric flow for 5-module solar collector array.

The results for 5-module collector array are given in Table 6.11 for asymmetric flow and Table 6.12 for symmetric one. The tables show the pressure drop in the array, the non-uniformity factors and correspondingly the effect on the collector array efficiency. ceffs denotes the collector array efficiency.

Table 6.11 Pressure drop, non-uniformity factor and collector efficiency for 5-module collector array, Asymmetric, G = 0.0075 kg $s^{-1}m^{-2}$. Riser diameter = 9 mm.

	Pressure drop, N m^{-2}	NUF	ceffs	
Area ratio			Selective	Non-selective
0.05	37.5	0.002	1.00	1.00
0.10	67.5	0.037	0.99	0.99
0.20	201.0	0.350	0.98	0.97
0.40	783.0	1.470	0.92	0.85

NUF = Non Uniformity Factor

Table 6.12 Pressure drop, non-uniformity factor, collector efficiency for 5-module collector array, Symmetric, G = 0.0075 kg $s^{-1}m^{-2}$. Riser diameter = 9 mm.

Area ratio	Pressure drop, N m^{-2}	NUF	ceffs	
			Selective	Non-selective
0.05	37.5	0.004	1.00	1.00
0.10	62.5	0.083	0.99	0.99
0.20	150.0	0.650	0.96	0.93
0.40	410.0	2.420	0.87	0.76

NUF = Non Uniformity Factor

Table 6.13 Pressure drop for 5-module collector array, Asymmetric and Symmetric, G = 0.0075 kg $s^{-1}m^{-2}$. Manifold diameter = 25 mm.

Area ratio	Pressure Drop, N m^{-2}		
	Asymmetric (i)	(ii)	Symmetric (i)
0.05	278	276	275
0.10	119	120	113
0.20	63	76	47
0.40	48	--	28

(i)-Soin(1983); (ii)-present collector geometry

The collector properties given in Table 6.10 are for selective collector, that is absorber coating of low emissivity (0.10). It would be interesting to estimate the collector array efficiency for a non-selective collector having absorptivity of 0.95 and high emissivity of 0.90. Tables 6.11 and 6.12 report the values for both types of collector.

It is observed from Tables 6.11 and 6.12 that :

a) The array pressure drop in asymmetric flow is practically equal to that in the symmetric one for lower area ratios. This, incidentally, is when flow is nearly uniform. For higher area ratios pressure drop in symmetric flow is lower than that of asymmetric flow. The reason for lower pressure drop in symmetric flow is that most of the flow is diverted in the first few risers. Having lower pressure drop, the flow configuration would require lower pumping power. This is, however, at the cost of reduced collector array efficiency.

b) The non uniformity factor is higher in symmetric flow. The corresponding collector array efficiency is thus lower compared to that for asymmetric flow. This is contrary to the observations made for a single collector.

c) The reduction in collector array efficiency is very small for low area ratio. For a selective collector area ratio of upto 0.20 can be used for asymmetric flow, while for symmetric-flow area ratio upto 0.10 only can be used. The reduction in collector efficiency is significant for symmetric flow for area ratio greater than 0.20, and is as high as 13 % for area ratio of 0.40. For non-selective collector the collector array efficiency is not affected for area ratio upto 0.10 both for asymmetric and symmetric flows. For area ratio of 0.20 and higher the collector array efficiency is low. The reduction in efficiency is significant for area ratio of 0.40 in asymmetric mode at 15 %, while for symmetric it is 24 %.

To summarise:

Uniform flow distribution is obtained by having a low area ratio both in asymmetric and symmetric flow configurations. The most important collector parameter is the area ratio. Essentially, the riser pressure drop should be significantly higher than that across the manifold. This is possible either by having low pressure drop manifold or high pressure drop riser.

Flow maldistribution increases with flow rate. For a given design i.e. no. of collectors in parallel, collector geometry and flow rate, lower flow rates can be used with more uniform flow distribution.

Upper manifold plays a more important role in symmetric flow compared to that in asymmetric flow. Keeping the upper manifold diameter greater than the lower one helps in improving the flow distribution. This was observed also by McPhedran (1983), who had demonstrated that the flow distribution improves with the upper header having bigger diameter than the lower one.

Collector array efficiency is computed for the predicted flow distribution in the collector array. For low area ratios typically 0.05 - 0.10, both symmetric and asymmetric flow configurations can be used with collector array efficiency reduction within 1 %. It is shown that symmetric flow configuration can also be used, contrary to general belief, if proper area ratio is chosen.

6.4 Methods of Balancing

From the discussions in the previous section and literature survey in Chapter 2, the following major techniques can be adopted to balance flow in a collector array to obtain nearly uniform flow distribution :

a. collector with low area ratio, both for symmetric and asymmetric flow configurations.

b. collector having upper manifold diameter greater than the lower one

c. for asymmetric flow, using orifice inserts as suggested by Lydon (1979).

In case of orifice inserts, the calibrated orifice inserts are placed at pre-determined positions in the array. The major advantage with this method is that an array can be extended beyond the optimal level by putting appropriate inserts (may or may not be identical) at the required places. The additional pressure drop is marginal. The cost of inserts is also low. The only disadvantages are:

- a particular solution is applicable for chosen no. of collectors in parallel and flow rate

- improper placement at site can result in worse flow distribution

- it is not so easy to balance collector array with identical orifices, in which case different orifices have to be employed and more careful placement is needed.

- this method is applicable only for asymmetric flow.

Keeping upper manifold greater than the lower one is a simple method. This can be used to extend an optimal design when lower area ratio may be needed. The disadvantage is that two different diameters of manifold is required.

In the author's opinion the simplest and yet an effective solution is the area ratio method. In this case a collector design is chosen with an area ratio which can give a low flow maldistribution for 10 - 15 collectors in parallel. Normally, keeping in view the site constraints a designer has to opt for series-parallel connection. Thus a designer may select 10 collectors in parallel and a number of such arrays in series. In such a solution, the collector upper and lower manifolds will be of the same diameter. The only selection required is the diameters of the riser and manifold to give the required area ratio.

It was illustrated in the previous section that for a chosen area ratio a designer can either fix the same riser diameter and select the manifold diameter or vice versa.The 'area ratio' method of balancing thus offers a flexibility and at the same time offer an advantage that firstly, the manifold diameters are the same and secondly, the same collector can be used upto 10 to 15 numbers in parallel.

To illustrate this method, flow distribution for 10 collectors in parallel with an area ratio of 0.05 and the collector geometry of Table 6.10 was obtained. The results are given in Figs. 6.31 - 6.33. The riser flow rates can be seen to be within +/- 20 % of the uniform flow rate, except in the last collector (see Fig. 6.32). The manifold pressure is shown in Fig. 6.33. It can be observed that the pressure drop across the upper manifold is comparable to the average pressure drop across the risers. Table 6.14 gives the non-uniformity factors and the collector efficiencies. It is seen that the reduction in collector efficiency is only 1 %.

The flow distribution with an area ratio of 0.10 is also illustrated in Figs.6.34-6.36. It can be seen that the flow maldistribution has increased. The results are given in Table 6.14.

It can be observed that the reduction in efficiency is 2 % for selective collector and 4 % for non-selective one.

Table 6.14 Performance of 10 module collector array, G = 0.0075 kg $s^{-1}m^{-2}$

Area ratio	Pressure Drop, Nm^{-2}	NUF	Collector Array Efficiency,%	
			Selective	Non-selective
Asymmetric				
0.05	83	0.05	0.99	0.99
0.10	260	0.38	0.98	0.96
Symmetric				
0.05	78	0.17	0.99	0.98

In the previous section symmetric flow configuration was recommended for 5-module collector array having area ratio equal to or less than 0.10. The flow distribution for 10-module with an area ratio of 0.05 is also obtained. The results are presented in Figs. 6.37-6.39. It is observed that in the first three collectors the

flow rate is higher than uniform, typical of symmetric flow behaviour, while the flow in the remaining collectors are at 75 % of uniform flow. The collector array efficiency drop is negligible for selective collector.

The results for symmetric flow implies that this configuration with low area ratio of 0.05 can be used upto 10 modules in parallel. The riser flow rates, barring the first few, are practically equal at 75 % of uniform flow rate. This, incidentally, equals the lower limit recommended for solar water heating systems i.e. 0.0050 kgs-1m-2 [Soin(1982)]. The symmetric configuration offers an advantage of utilising less array piping as discussed in Chapter 1.

To extend the number of collectors the area ratio should be reduced or the collector flow rate may be reduced, say, between 0.0050 and 0.0075 $kgs^{-1}m^{-2}$. Alternatively, as suggested earlier two array can be placed in series.

It may be noted that to attain similar flow distribution the collector flow rate ($kgs^{-1}m^{-2}$) should be halved since the total flow (kg/s) will double for the design flow rate ($kgs^{-1}m^{-2}$) when two parallel arrays are placed in series. However, the temperature rise will double which will reduce the collector efficiency. Thus, the lower limit of 0.0050 $kgs^{-1}m^{-2}$ may be used.

Therefore, nearly uniform flow distribution can be obtained by any of the following alternatives beyond 10 collectors in parallel optimally designed for collector flow rate of 0.0075 $kgs^{-1}m^{-2}$ in asymmetric flow :

- reduce area ratio below 0.05, either by reducing the riser diameter or increasing the manifold diameter.

- place two collector arrays in series, with flow rate reduced upto 0.0050 $kgs^{-1}m^{-2}$.

It would be interesting if a universal collector parameter can be obtained related to a prescribed reduction in the collector array efficiency. It may be recalled that Bajura and Jones (1976) recommended that to obtain uniform flow the porosity of the manifold should be less than unity. Pigford (1983) also gave a similar value, but added that flow uniformity is governed by the pipe pressure drop. The later is true since thumbrules are applicable only for a particular situation.

For the present case, recalling that area ratios of 0.10 and 0.05 were recommended for 5- and 10-module array employing the baseline collector (riser diameter = 9 mm) and flow rate of 0.0075 $kgs^{-1}m^{-2}$. The corresponding porosities are $40(9^2/28.5^2)=3.99$ and $80(9^2/40.25^2)=4.00$. For fixed manifold diameter of 25 mm, the porosity for 5-module array with area ratio 0f 0.10 is $40(7.92/252)=4.00$.

Thus, for the baseline collector and flow rate, a single value of porosity is applicable for upto 10 collectors in parallel to ensure that the reduction in the collector array efficiency is within 1 %.

Fig.6.31 FLOW PROFILE FOR 10 MODULE

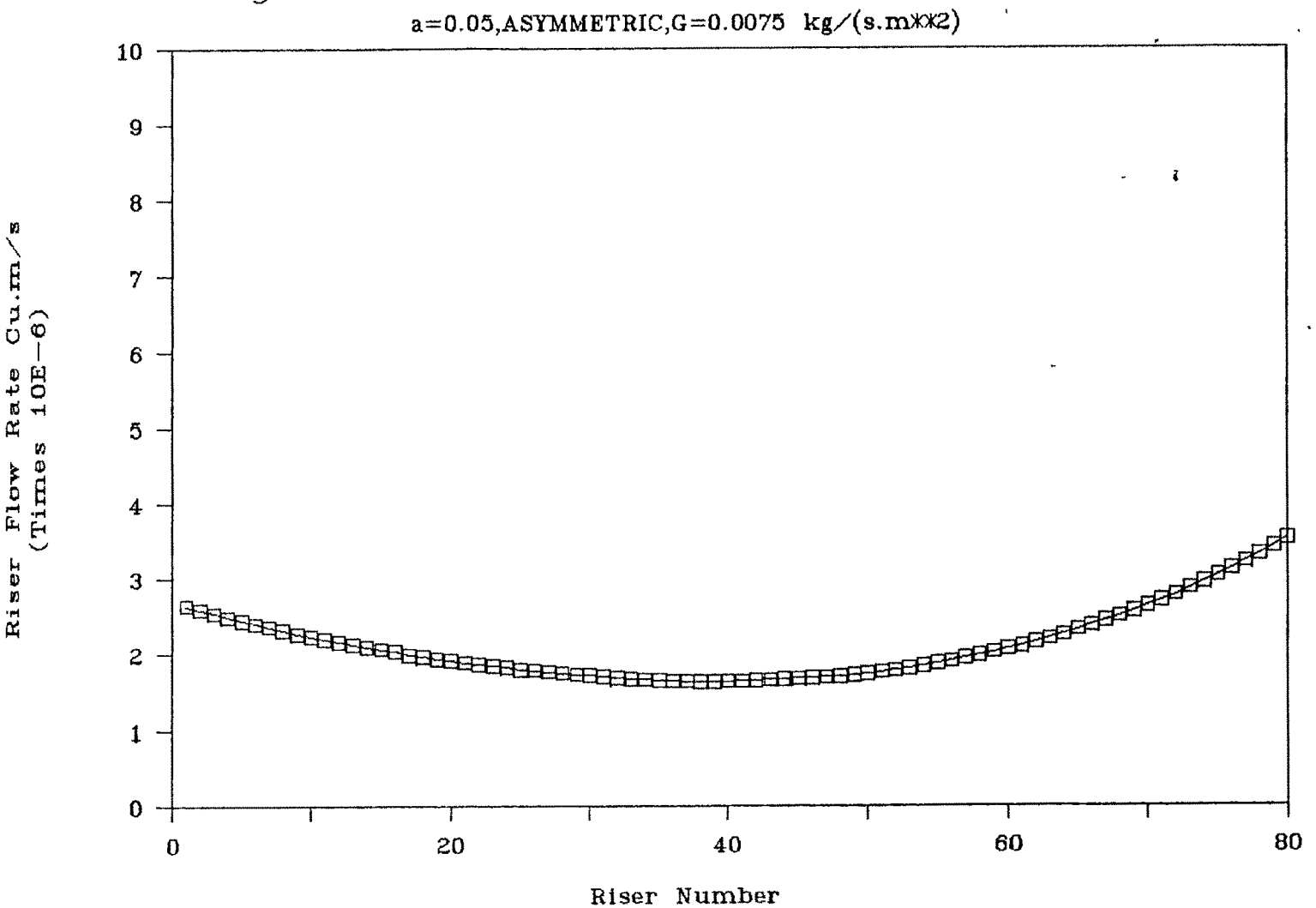

Fig.6.32 FLOW PROFILE FOR 10 MODULES

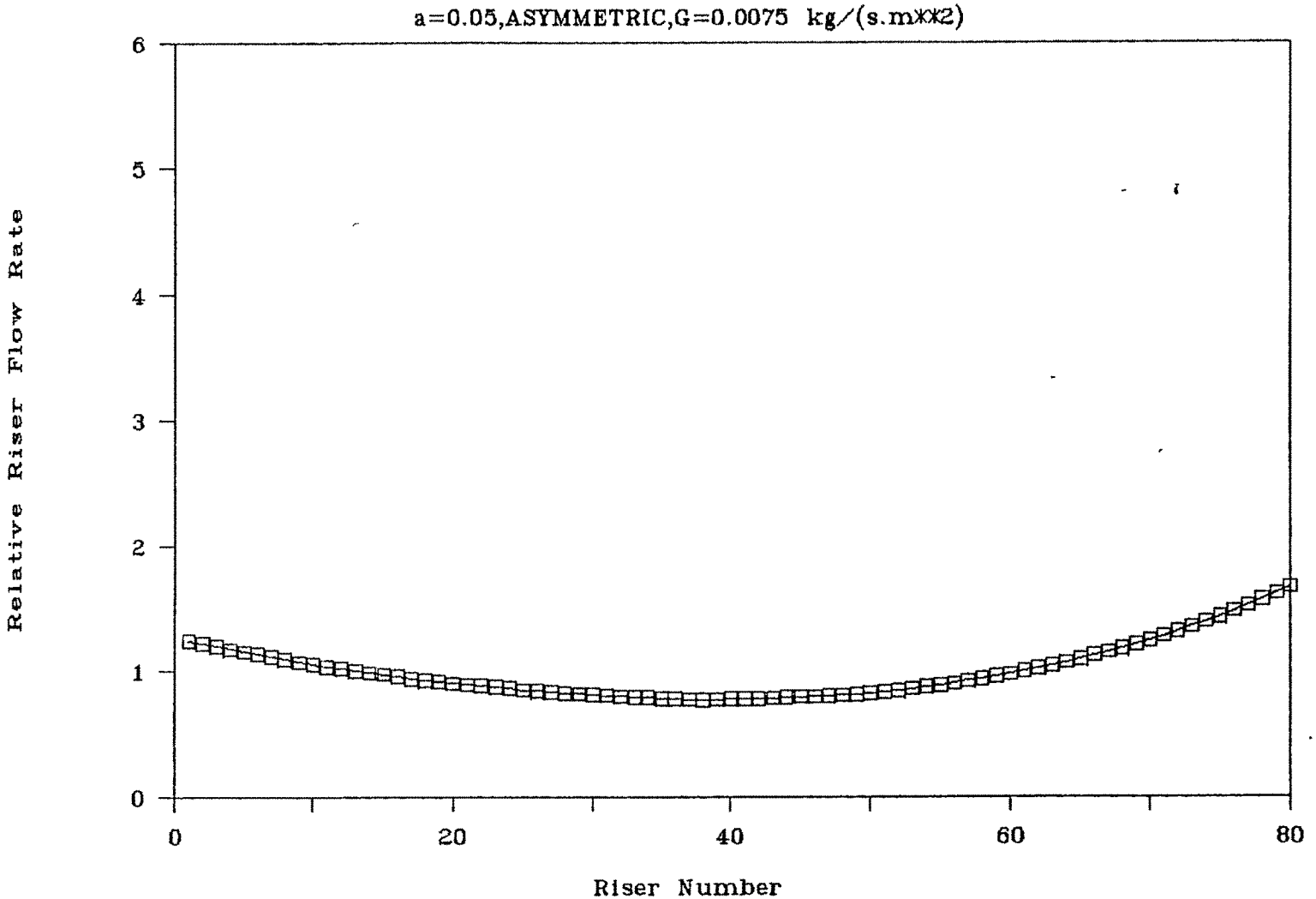

Fig.6.33 PRESSURE PROFILE FOR 10 MODULE

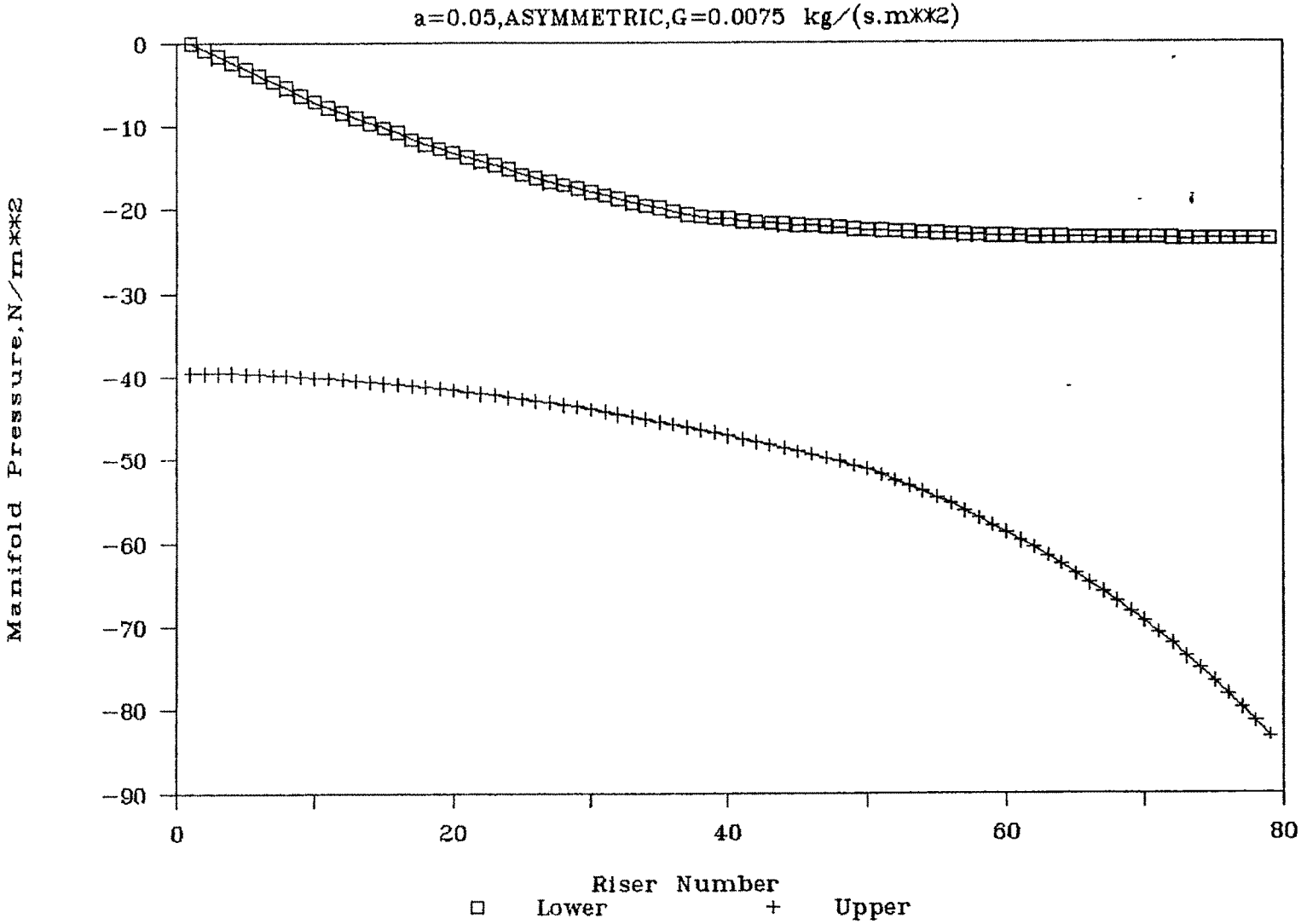

Fig.6.34 FLOW PROFILE FOR 10 MODULES

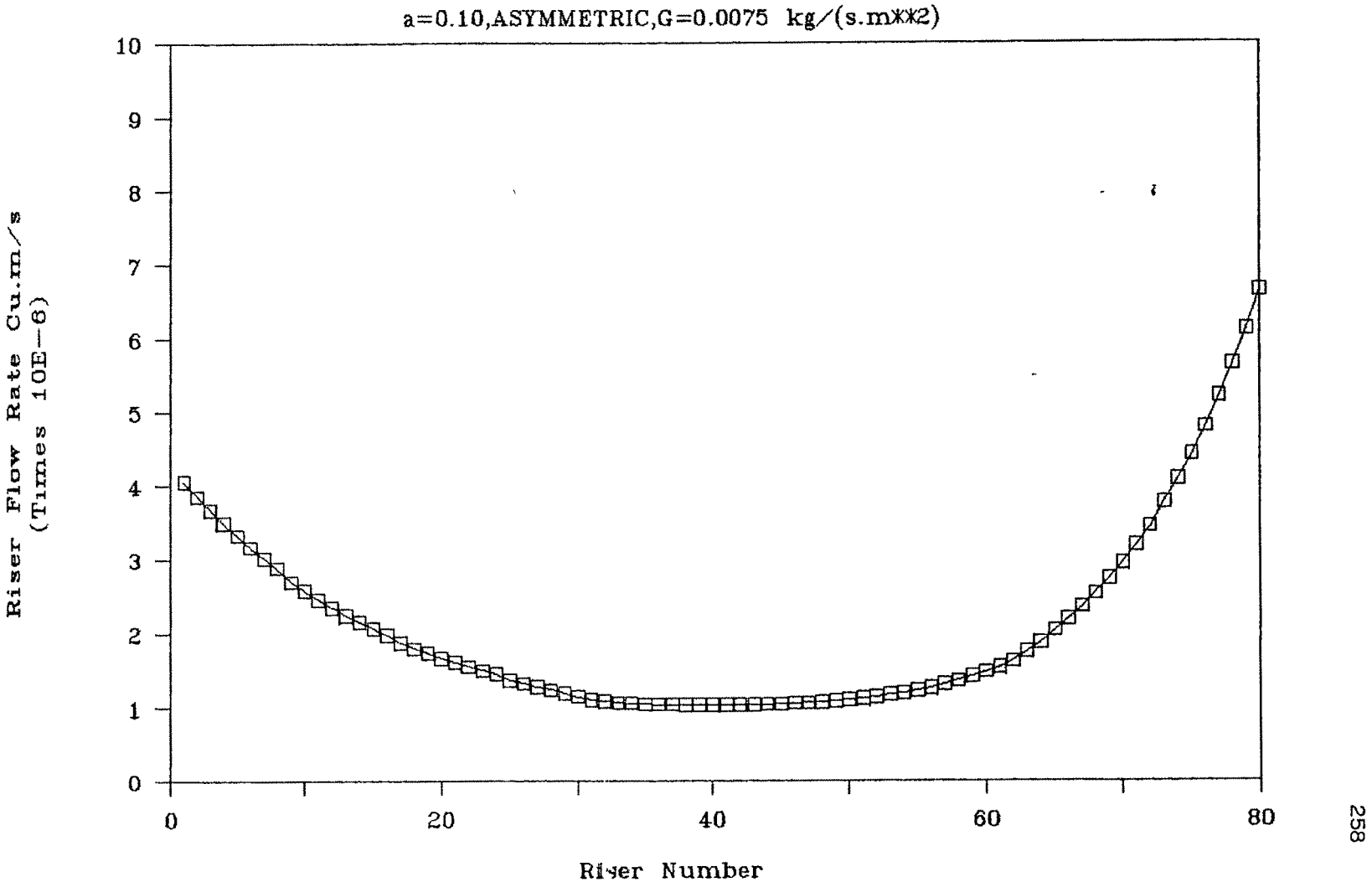

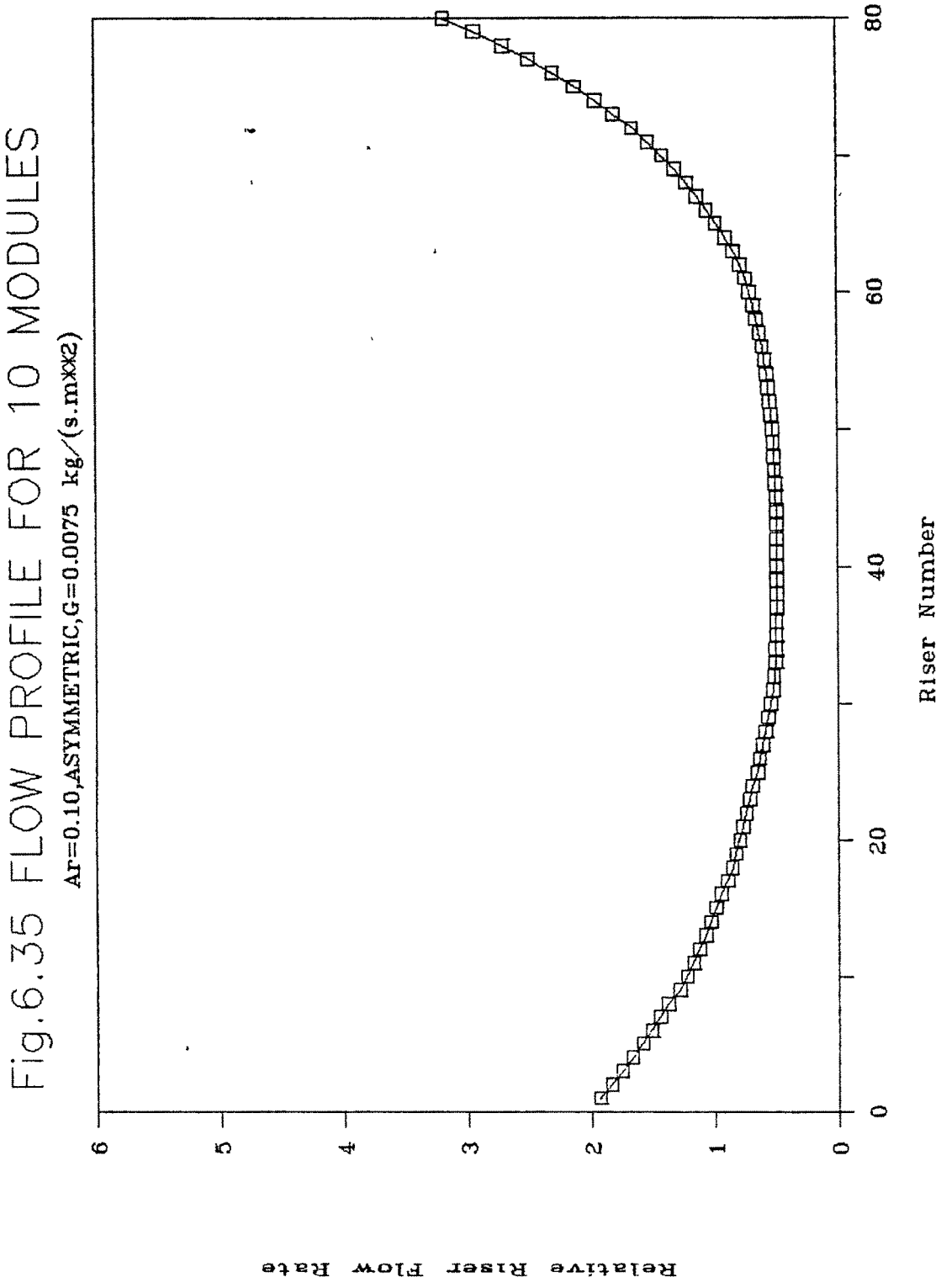
Fig.6.35 FLOW PROFILE FOR 10 MODULES
Ar=0.10,ASYMMETRIC,G=0.0075 kg/(s.mxx2)
Relative Riser Flow Rate
Riser Number
0
1
2
3
4
5
6
0
20
40
60
80

Fig.6.36 PRESSURE PROFILE FOR 10 MODULE

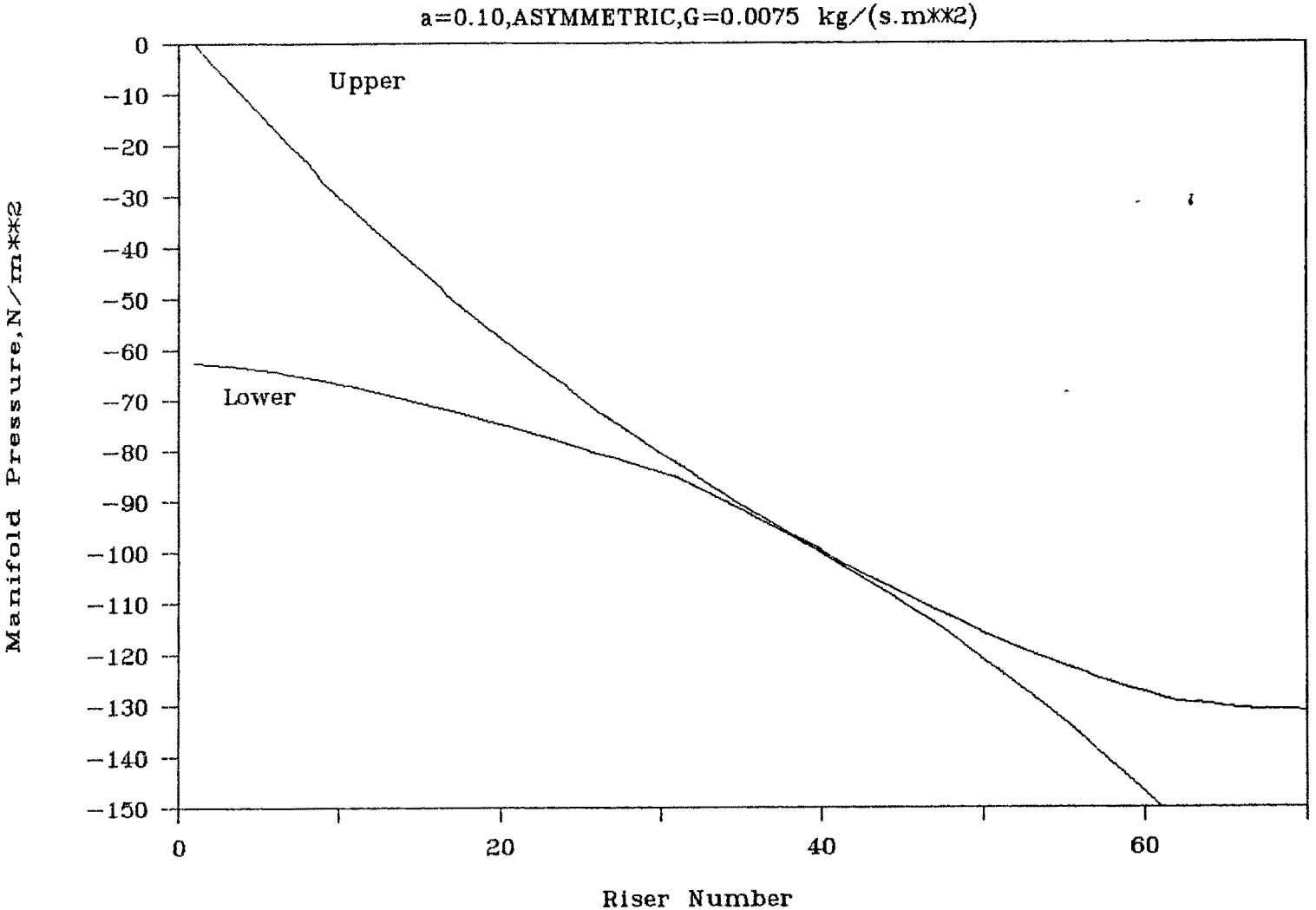

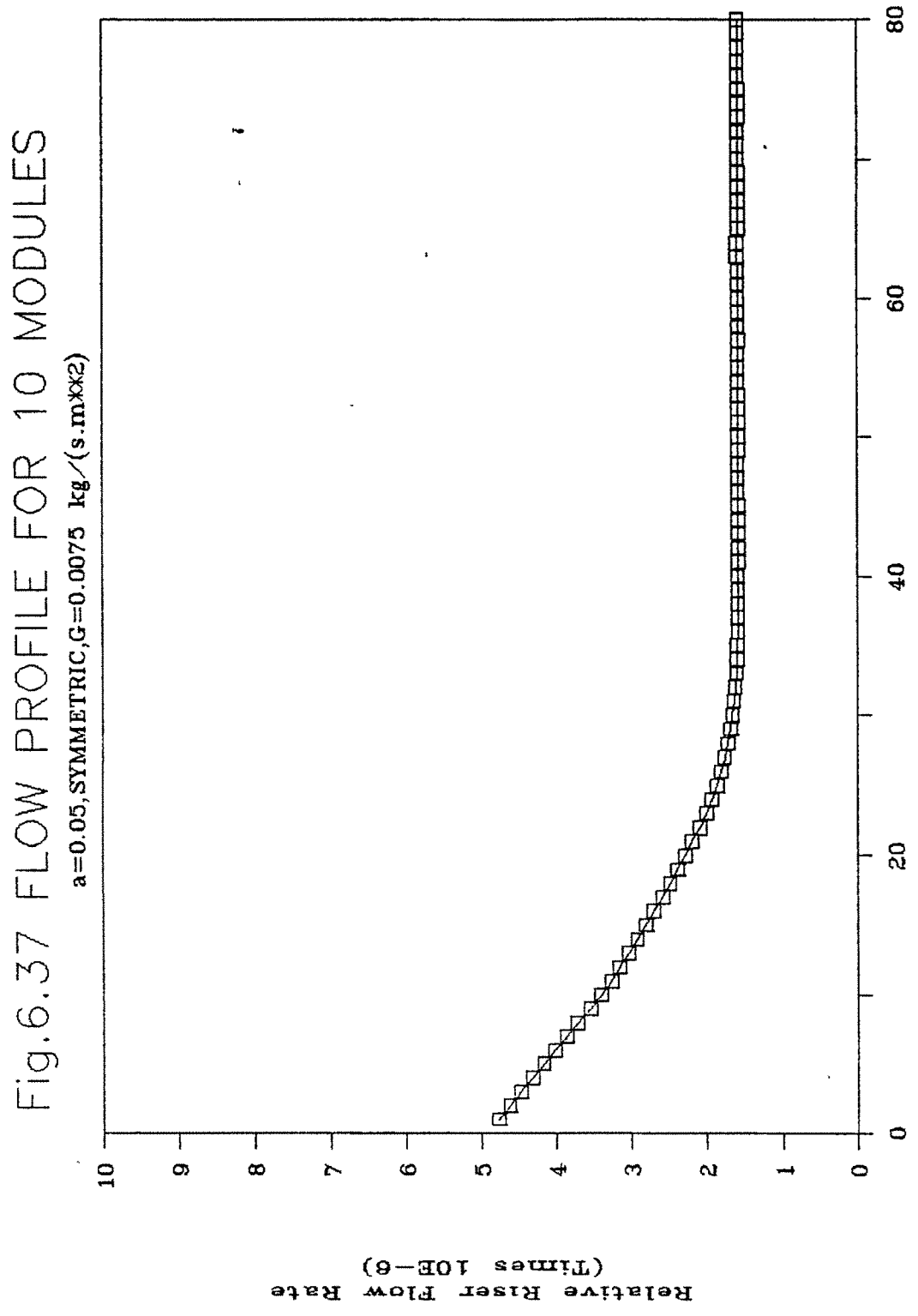
Fig.6.37 FLOW PROFILE FOR 10 MODULES
a=0.05,SYMMETRIC,G=0.0075 kg/(s.mxx2)
Relative Riser Flow Rate
(Times 10E-6)
10
9
8
7
6
5
4
3
2
1
0
0
20
40
60
80
Riser Number

Fig.6.38 FLOW PROFILE FOR 10 MODULES

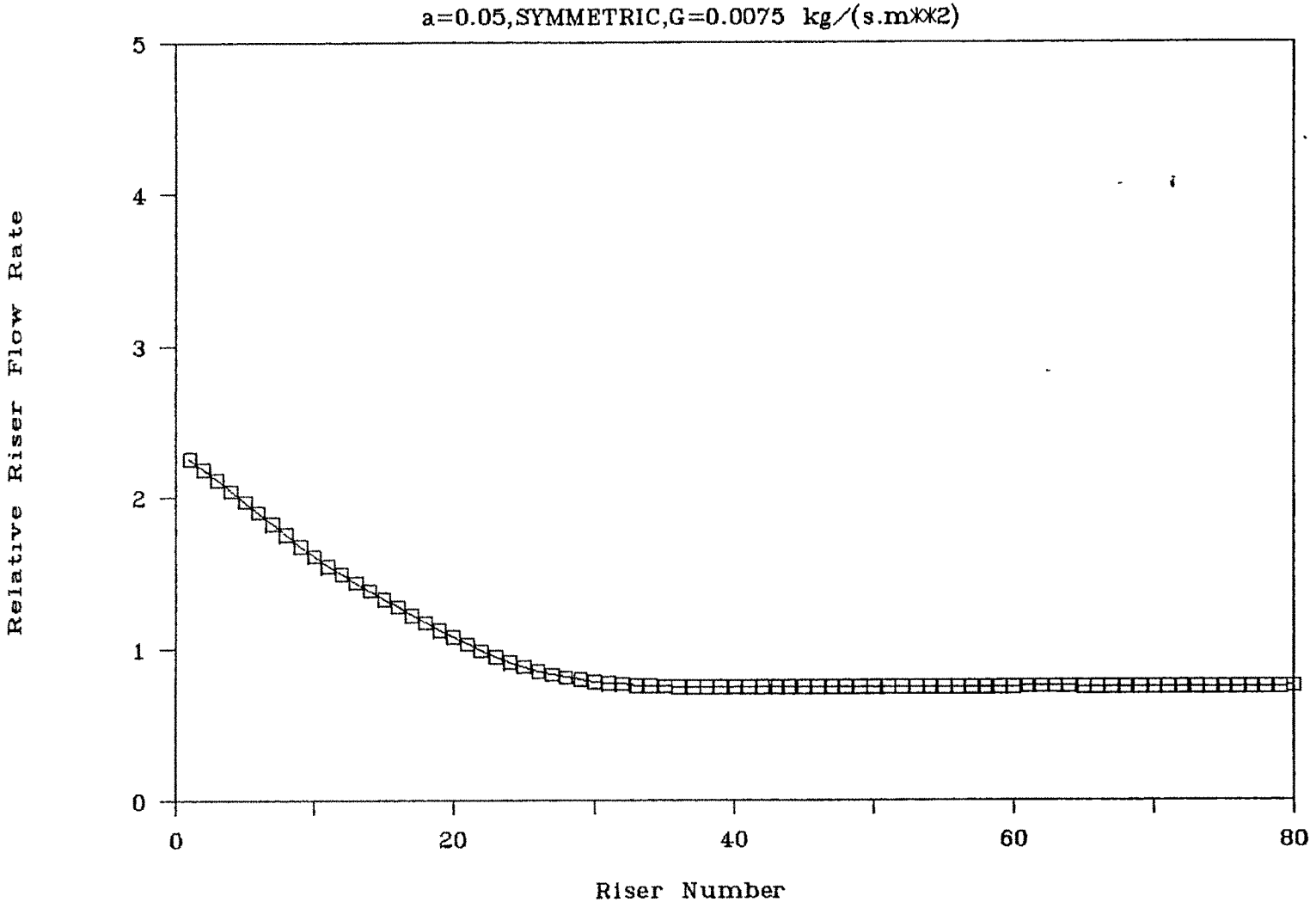

Fig.6.39 PRESSURE PROFILE FOR 10 MODULE